Ministry of Higher Education
and Scientific Research
University of Babylon
College of Engineering
Chemical Engineering Department

Demulsification of Synthetic Petroleum Wastewater Using Electrocoagulation/Electroflotation Technique

A Thesis

Submitted to the College of Engineering University of Babylon
in a Partial Fulfillment of the Requirement for the Degree
of Master of science in Electrochemical Engineering

By

Aqeel Talib Kadhim

(B.Sc. in chemical Engineering 1991)

Supervised by

Asst. Prof. Alaa Nour Ghanim Al-Mosawi

February 2022

Rajab 1443

بسم الله الرحمن الرحيم

يُؤْتِي الْحِكْمَةَ مَن يَشَاءُ ۚ وَمَن يُؤْتَ الْحِكْمَةَ فَقَدْ أُوتِيَ خَيْرًا كَثِيرًا ۗ وَمَا يَذَّكَّرُ إِلَّا أُولُو الْأَلْبَابِ

صدق الله العلي العظيم

البقرة ﴿269﴾

عن أبي عبد الله عليه السلام قال: قال **رسول الله صلى الله عليه وآله:**

"من سلك طريقا يطلب فيه علما سلك الله به طريقا إلى الجنة وإن الملائكة لتضع أجنحتها لطالب العلم رضا به وإنه يستغفر لطالب العلم من في السماء ومن في الأرض حتى الحوت في البحر، وفضل العالم على العابد كفضل القمر على سائر النجوم ليلة البدر، وإن العلماء ورثة الأنبياء إن الأنبياء لم يورثوا دينارا ولا درهما ولكن ورثوا العلم فمن أخذ منه أخذ بحظ وافر"

الكافي - الشيخ الكليني - ج ١ - باب ثواب العالم والمتعلم- الصفحة ٣٤

CERTIFICATE OF EXAMINERS

We certify, as an examining committee, that we have read this thesis entitled " **Demulsification of Synthetic Petroleum Wastewater Using Electrocoagulation/Electroflotation Technique** ", examined the student "**Aqeel Talib Kadhim"** in its content and found that the thesis meets the standard for the degree of Master of Science in Electrochemical Engineering.

Signature:

Name: **Asst. Prof Alaa Noor Ghanim**
(Supervisor)

Date: / / 2022

Signature:

Name: **Asst. Prof. Dr. Shaker Salih Baha**r
(Chairman)

Date: / / 2022

Signature:

Name: **Asst. Prof. Dr. Sarmad Talib Najim**
(Member)

Date: / / 2022

Signature:

Name: **Asst. Prof. Dr. Hameed Hussein Alwan**
(Member)

Date: / / 2022

Approved by the Head of the Chemical Engineering Department

Signature:

Name: **Asst. Prof. Dr. Hameed Hussein Alwan**
(Head Department)

Date: / / 2022

Approved by the Dean of the College of Engineering

Signature:

Name**: Prof. Dr. Hatam Hadi Obaid Al-Taei**
(Acting Dean)

Date: / / 2022

SUPERVISOR CERTIFICATION

I certify that the preparation of this thesis entitled "**Demulsification of Synthetic Petroleum Wastewater Using Electrocoagulation/Electroflotation Technique**" has been prepared by "***Aqeel Talib Kadhim***" under my supervision at the Department Electrochemical Engineering, College of Engineering, University of Babylon, as a partial fulfillment of the requirements for the degree of Master of Science in Electrochemical Engineering.

Signature:

Name: **Asst. Prof. Alaa Nour Ghanim Al-Mosawi**

(Supervisor)

Date: / / 2022

Signature:

Name:**Asst. Prof. Dr. Hameed Hussein Alwan**

(Head of Department)

Date: / / 2022

DEDICATION

To the one who led mankind’s hearts and minds to the harbor of safety, the first teacher of mankind, Muhammad, may God’s prayers and peace be upon him and his family,

To my parents' soul,

To whom was my shadow when I was overwhelmed by fatigue, my faithful wife, To the hope of tomorrow, dear children,

To my brothers and sisters,

To the brothers with whom the field of work brought me together. Dear colleagues, To the righteous martyrs, especially the martyr Abu Mahdi Al-Mohandas,

To every hand and heart that walked with me the path of achievement to be,

To everyone who knows me literally,

I offer you gifts with love, elevation and dignity.

ACKNOWLEDGMENT

In the name of God, the most gracious, the most merciful.

First of all, I would like to thank my God who gave me strength and patience to complete this research.

I would like to thank everyone who helped me during my work, especially the supervisor. **Asst. Prof. Alaa Nour Ghanim Al-Mosawi** for his guidance, advice and constant encouragement in preparing this message in addition to the extra time granted from his busy schedule.

I would also like to express my thanks to the Head and Associates of the Chemical Engineering Department. **Asst. Prof. Dr. Hameed Hussein Alwan** for the continuous support throughout the preparation period for this work.

Most importantly, I would like to thank my wife and My daughter and sons for their endless support and sincere prayers.

I would like to thank my brothers, sisters and all my friends who have supported me in this work and everyone who prayed for me.

My sincere gratitude to Mrs. Angham Sami for her assistance

Thanks to everyone who helped complete this study.

ABSTRACT

This research deals with the demulsification of oily wastewater effluents of petroleum refineries using hybrid electrocoagulation/electroflotation (EC/EF) techniques. A dynamic flowsystem was constructed using an improved design of a compact electrochemical reactor made of (Perspex glass) containing two parallel vertical sheets as electrodes. A galvanostatic transient technique for two types of electrodes, Al-Al and Al-C felt were used to achieve the hybrid (EC/EF) treatment in one reactor. Emulsified synthetic wastewater was prepared by mixing crude oil (0.1,0.2 and 0.3gram) per liter deionized water and 0.05g/L sodium dodecyl was added as an emulsion stabilizing agent and sodium chloride at a concentration of 1.5 g/L to increase the electrical conductivity. Electrocoagulation produces Al^{3+} ions by corroding sacrificial anodes, releasing active coagulant precursors into the solution. Furthermore, the release of finely dispersed H_2 gas bubbles at the cathode causes flocs to lift to the upper surface of the solution. All experiments were carried out in continuous operation for two hours with a variety of operating conditions, including initial O/W concentration, current density, volumetric flow rate, and cathode type. Results revealed that for an initial O/W emulsion of 100 ppm and 30 mA/cm^2 current density with different solution flow rate of 2,4 and 6 L/hr the COD removal efficiency was 96.93, 89.07 and 84.11 % for Al-Al electrodes and 99.8, 98 and 83.73% for Al-Carbon felt, respectively. These parameters reduced the turbidity of the wastewater. The specific electrical energy consumption (SEEC) and the current efficiency (CE) for the demulsification experiments were also studied. The total operating cost(TOc) of the process was estimated at 1.5255 and 0.65383 US$/$m^3$ of treated oily wastewater for the Al electrodes and Al-Carbon-felt electrodes, respectively.

List of symbols and Abbreviations		
Symbols	Description	Unit
$\sum CE$	Summation of Applying unit price of chemicals and the cost of laboratory test used per m^3 of wastewater	$
A	Active Surface of Electrode	cm^2
A_E	Unit Price of Electricity	$/kWh
B_{Al}	Unit Price of Aluminum Metal used as Electrode for EC/EF	$/kg for Al
C	Concentration	g/L
C_i	Unit Price of Chemicals	$/kg
C_o	Initial Emulsion Concentration	ppm
e^-	Electron	
Ec	Electrical Conductivity	µ seminice
E_i	The Cost of Laboratory Test used Per m^3 of Wastewater	kg
E_x	Energy Consumption/m^3 of Solution (SEEC) For EC/EF	kWh
E_y	Electrode Consumption Per $m^3$of Solution	kg
F	Faraday Constant	96 485.332 **s A / mol**
I	Current Intensity	A
i	Current Density	mA/cm^2

O/W	Oil in water (emulsion)	ppm
t	Time	Min
t	Temperature	^{o}C
TOc	Total Operational cost	US$/$m^3$
V	Applied Voltage	Volt
W1	Weight before treat	G

Abbreviations	
Abbreviations	Item
Al	Aluminum
AOPs	Advanced Oxidation Processes
BDD	Boron Doped Diamond Anode
BOD	Biological Oxygen Demand
BTT	Bipolar Trickle Tower
CE	Current Efficiency
CFD	Computational Fluid Dynamics
C-felt	Carbon-felt
COD	Chemical Oxygen Demand
DAF	Dissolved Air Flotation
DC	Direct Current
EC	Electrocoagulation

EC/EF	Hybrid Electrocoagulation Electroflotation
ECEFMM	Electrocoagulation and electroflotation enhanced membrane module
ECF	Electrocoagulation/flotation
ED	Electrodeposition
EF	Electroflotation
EO	Electrooxadation
HRT	Hydraulic Residence Time
IAF	Induced Air Flotation
ICDD	International Center for Diffraction Data
Mbpd	million barrels per day
M-GO	Magnetic Graphene Oxide
MIAF	Modified Induced Air Flotation
O/W	Oil in Water
PAC	Powdered Activated Carbon
PAZSC	Poly-Zinc Silicate Chloride
PCWW	Petrochemical Wastewater
PEF	Photo-Electro-Fenton
PEO	Photo-Plectro-Oxidation
pH	Negative Logarithm of a Hydrogen Ions Concentrationin Solution

PRW	Petroleum Refinery Wastewater
PVDF	Poly Vinylidene Fluoride
RSM	Response Surface Methodology
SDS	Sodium Dodecyl Sulphate
SEEC	Specific Electric Energy Consumption
TDS	Total Dissolved Solid
TPH	Total Petroleum Hydrocarbons
TS	Total Solid
TSS	Total Suspended Solids
XRD	X-ray Diffraction

List of Tables

1
2 3

1 CHAPTER one

INTRODUCTION

Aqeel Talib

Chapter One
Introduction

1.1 Background

Wastewater pollutants associated with crude oil storage, desalting, and fractionation are primarily free oil, emulsified oil, and suspended solids. Water and suspended solids in crude oil are separated during storage. The water layer forms the bottom sludge beneath the oil layer. Emulsified oil at the oil-water interface is frequently lost to the sewers when the water layer is removed. This waste has a high chemical oxygen demand (COD) and a biochemical oxygen demand (BOD). Wastewater from crude oil fractionation usually comes from one of three sources. The first source is water drawn from overhead accumulators before recirculation or hydrocarbon transfer to other fractionators. Thedischarge from oil sampling lines is the second waste source. This should be separable, but it may form emulsions in the sewer. In addition, the very stable oil emulsions formed in the barometric condensers used to create the reduced pressures in the vacuum distillation units are a third waste source [Yu et al,2017].

Water and energy are significant challenges for the 21st century because of pollution from point and non-point sources, water quality has become a crucial problem for Third-World Countries [Chaturvedi,2013].

Oily wastewater is a two-phase dispersive system with oil as the dispersed phase and water as the continuous phase [Eskandarloo et al., 2018]. Dispersions of oil droplets in water, namely emulsions, are known asstable oil-in-water (O/W) solutions [Sun et al., 2009]. The presence of surfactants improves emulsion stability, increasing the difficultly of oil droplet removal. Surfactant forms a film and avoids the coalescence of oil droplets. The emulsion stability depends on the surfactant concentration [Maiti et al.,2011]

Electrocoagulation is an electrochemical technology of treating polluted water whereby sacrificial anodes dissolve due to an applied

potential, thus producing active coagulant precursors. Electrocoagulation is a complicated process with many mechanisms operating synergistically to remove the pollutants in wastewaters [An et al.,2017]

The Al^{3+} ions generated immediately hydrolyze to produce corresponding hydroxides and/or poly hydroxides inadequate pH. A^{2+} hydroxides and polyhydroxides from the electrochemical dissolution were reported to have a stronger affinity to capture the pollutants in the wastewater, causing more coagulation than those from the conventional Al coagulants. Additionally, the gas bubbles that evolve due to the water electrolysis can cause flotation of the pollutants and the coagulated materials. Therefore, electroflotation may also play an essential part in an electrocoagulation cell. [Wang et al.,2009]

The formation of an inhibiting. layer on the Al electrode surface prevents Al dissolution and electron transfer, limiting Al^{3+} to the solution. As a result, the EC system is usually designed to operate in a condition of high voltage, usually higher than 10 V, to break down the inhibiting layer. The energy consumption is thus high and the electrodes are likely to be destroyed when using a high voltage for the long-term operation [Ghernaout et al.,2011].

Several technologies have been used for pollutant removal from wastewater; such technologies include coagulation-flocculation, Fenton process, Chemical sedimentation [Zhang et al., 2018], and adsorption. However, these methods are very restricted because applying high concentrations of chemicals during wastewater treatment may cause secondary pollution [Do & Chen, 1994]. Compared with other methods, EC is an environment-friendly and efficient technology for wastewater treatment [Moreno-Casillas et al., 2007]. EC involves the generation of coagulants in situ through the electrolytic oxidation of aluminum or iron sacrificial anodes [Mollah et al., 2004]. Coagulants produced in the EC contribute to the removal of pollutants via adsorption or precipitation [Changmai et al., 2019]

Electrocoagulation/electroflotation (EC/EF) has been reported to successfully treat wastewater of different kinds, containing oil [Chen, 2000], fluoride [Hu, 2003], arsenic [Kumar et al,2004], dyes [Chen et al,2003], suspended particles [Larue et al,2003], surfactant, chromium ions [Gao et al,2005], phosphate [İrdemez et al,2006].

1.2 Oily Wastewater Demulsification Methods

The most commonly exploited demulsification techniques (i.e., chemical, biological, membrane, electrical, and microwave irradiation) of oilfield and synthetic emulsions, considering the emulsion-stabilizing and destabilizing effects concerning the dominant parameters plus the emulsion composition. Further, the variations occur in the interfacial properties of emulsions by the demulsification process. The most efficient demulsification approach can attain desirable separation efficiency while complying with the environmental regulations and imposing the least economic burden on the petroleum industry [Zolfaghari et al.,2016].

The standard electrical demulsification approach for oil-in-water emulsions involves “electrocoagulation” in DC fields. Electrochemical reactions help alter the pH and thus destabilize the oil droplets [Zheng et al.,2018].

Briefly, the methods for demulsification can be summarized by the following techniques.

1.2.1 Chemical Demulsification.

This involves the flocculation and/or alteration of the characteristics of the interfacial films using chemicals to cause coalescence. It is the common method for treating w/o and o/w emulsion where the breaking process is facilitated by the chemical additives [Nour et al.,2007]. Several factors, like the type of oil and its viscosity, the size distribution of the water phase, and the presence of solids, can affect the performance of a demulsifier [Mikula & Munoz,2000]. Another study by [Liu et al.,2017] used magnetic graphene oxide (M-GO) to separate o/w emulsion. The results showed the

capability of M-GO to facilitate the separation of the o/w emulsions within a short period of time. The M-GO was recycled 6–7 times and still achieved 99.98% demulsification efficiency at the optimum concentration (0.04-0.25) wt.% [Abed et al.,2019].

1.2.2 Biological Demulsification

Studied α-amylase and its effect as a bio demulsifier (Demulsifier concentration, 0-6000 mg/L) on the de-emulsification rate and viscosity of amphiphilic polymer solution. The concentration of α-amylase, salinity, and the temperature were altered during the experiments. The results show α-amylase to be a good bio demulsifier as it can improve the rate of de-emulsification of such emulsions [Jiang et al., 2018].

1.2.3 Mechanical Demulsification

The mechanical demulsification process involves using mechanical forces to break down the physical barrier/difference in the water and oil phase densities to achieve separation. Among the tools that can be used to achieve mechanical separation during crude oil, demulsification include cyclones, centrifugal separators, gravity settling tanks, etc. [Auflem,2002 & Jiang,2010].

1.2.4 Thermal Demulsification

Thermal demulsification involves using heat to promote emulsion breakdown in an oil field or refinery. The commonly used method is the conventional hot plate to generate the required temperature on the lab scale. The rigidity of the interface, which promotes the coalescence of droplets when they collide, may be affected by high temperatures. Furthermore, a higher temperature can increase the rate of collision between the droplets and cause a reduction in the stability of the emulsion. One effect of heating is that light compounds that help increase the density of crude oil could be lost, thereby affecting gravity settling [Stokowski,2005, Kokal& Al-Juraid,1998]. Heat treatment is often used in conjunction with chemicals to enhance the efficiency of the process since the viscosity of emulsions can be

tremendously reduced by temperature [Issaka et al.,2015].

1.2.5 Microwave Demulsification

The first microwave irradiation-assisted demulsification process was reported by [Wolf 1986]. Microwave heating has been reported to be superior to the traditional heating schemes in the breakdown of emulsions due to its less energy consumption and faster separation rate [Evdokimov&Losev,2014]. The microwave heating technique can be applied as a standalone demulsification process in the petroleum sector to minimize chemical demulsifiers [Nour et al.,2010].

1.2.6 Electrical Demulsification

Electrical demulsification involves the deformation of droplets and the generation of an attraction force between drops (thus leading to coalescence) by applying an electric field. The application of the electric field makes it easier for small water droplets to fuse into larger ones quickly. The droplets deform in the electric field as they migrate to each other. Coalescence occurs more quickly as the droplets are elongated and deformed [Less et al., 2008]. Electrical demulsification is considered a better option than chemical and thermal demulsification; however, adapting this method to the different emulsion properties is not adequately understood. So, some of the previous studies that used the electrical technique as a demulsifier for emulsions will be reviewed [Lundgaard et al.,2005]

1.2.7 Ultrasonic Demulsification

Sonication provides a cheap, simple, and harmless separation of crude oils from water droplets via demulsification. The ultrasonic separation method of an oil-in-water emulsion by simultaneous application of electrolysis can be used to remove up to 100% of the grease from the studied oily wastewater, studied the role of pH, conductivity, temperature, ultrasound intensity and duration, electrolysis voltage, current, and duration, in the study treatment. Conductivity was the most significant factor [Stack et al.,2005].

1.3 The Aim of the Present Study

The present work aims to study the application of electrochemical techniques to the oily wastewater prepared in the laboratory. It investigates parameters affecting the demulsification of the oil from the O/W emulsion of the water by EC/EF in a continuous flow. The process was examined under different parameter of (flowrate, current density, initial crude-oil concentration, electrode materials and time). During the operation time for each variable the study was reinforced by the effect of the above parameters on pH, turbidity, total suspended matter, total dissolved matter, and thus total solid matter (pollutants).

The EC/EF process with the above-changing parameters with a continuous supply of potential voltage to achieve the required current, the de-emulsification process was studied by calculating the following points:

1) Determining the removal and concentration for the COD from the experiment work with variable time.
2) Computing the specific electrical energy consumption.
3) Current efficiency (yield of the electrodissolution).
4) Variation of pH, Ec (electroconductivity) with time.
5) Variation of TDS, TSS, TS, Turbidity with time. It investigates parameters affecting the demulsification of the oil from the O/W emulsion of the water by EC/EF in a continuous flow. The process was examined under different flow rate values, current density, initial crude-oil concentration. During the operation time for each variable, also the study was reinforced by the effect of the above parameters on pH, turbidity, total suspended matter, total dissolved matter, and thus total solid matter (pollutants).

2

CHAPTER two

THEORETICAL CONCEPT AND LITERATURE REVIEW

Aqeel Talib

Chapter Two
Theoretical Concept and Literature Review

2.1 Introduction

Oil industries face a great challenge in removing oily wastewater pollutant without causing environmental damage. Oil pollution in the air, water and soil can be toxic and dangerous to humans. oily wastewater has caused serious problems during its treatment. In general, as this pollution appears clearly in two forms, oil and emulsified oil. For a pure environment, scientists have worked on many different processes to demulsify oily wastewater pollutants for reuse in different fields, one such process is hybrid electrocoagulation/electroflotation [Han., 2019].

2.2 Petroleum Refinery Wastewater and Its Characterization

Significant volumes of wastewater are generated in the process of refining crude oil because of consumes large amounts of water. Consequently, 0.4–1.6 times the amount of crude oil processed is the volume of petroleum refinery wastewater (PRW) generated during processing. Thus, at least a total of 33.6 Mbpd of effluent is generated globally based on the current yield of 84 million barrels per day (Mbpd) of crude oil [Diya'uddeen et al., 2011]. Wastewater is a primary source of aquatic environmental pollution, and these effluents are composed of oil and grease, along with many other toxic organic compounds. The PRW is one of the wastes originating from industries primarily engaged in refining crude oil and manufacturing fuels, lubricants, and petrochemical intermediates [Diya'uddeen et al., 2011].

According to U.S. Environmental Protection Agency (US EPA, 1982), 50% of the wastewater generated in the refineries is almost fromused raw water because refining processes use large volumes of water in the cooling, hydrotreating, distillation, desalting, etc. [Sobreira et al.,2011]. Refinery wastewater content of different inhibitory, biodegradable, inorganic and

toxic organic pollutants including aromatic hydrocarbons, alkanes (C_{10}-C_{21}), nitrogen compounds, polyaromatic hydrocarbons, sulfur compounds, carboxylic acids, greases, carbonates, different metal ethers, aldehydes and ketones etc. Because of the large variety of compounds in the PRW, chemical oxygen demand, biochemical oxygen demand, or total organic carbon concentration parameters are used to estimate the organic fraction [Rauckyte et al., 2010].

The discharge allowable limits in Iraq were shown below in table (2.1) according to discharge water quality Iraqi Environmental Standards [W3QR-50-M074, Rev. No.: 03Oct 2011].

Table (2.1) Discharge allowable limits according to Iraqi Environmental Standard[W3QR-50-M074, Rev. No.: 03Oct 2011].

Parameter	**Primary water source (river, stream)**
Temperature	<35 °C
Total suspended Solids (TSS)	60 ppm
pH	6-9.5
Biological Oxygen Demand (BOD)	<40ppm
Chemical Oxygen Demand (COD)	<100ppm
Cyanide	0.05ppm
Fluor	0.5ppm
Free Chlorine	Trace
Phenols	0.01-0.05ppm
Sulphate	If the proportion of wastewater tosource water is 1:1000 or less
Zinc (Zn)	0.2ppm
Chrome (Cr)	0.1ppm
Aluminum (Al)	0.5ppm
Barium (Ba)	0.4ppm
Boron (Bo)	1ppm
Cobalt (Co)	0.5ppm
Iron (Fe)	2ppm
Manganese (Mg)	0.5ppm
Silver (Ag)	0.05ppm
Total Petroleum Hydrocarbons (TPH)	Ten mg/L if the proportion of wastewater to receiving water is lessthan 1:1000

2.3 Principle of Hybrid Electrocoagulation/Electroflotation

2.3.1 Theory of Electrocoagulation

The electrocoagulation process operates based on the principle that the cations produced electrolytically from iron and/or aluminum anodes are shown in Figure (2.1), which is responsible for the increase in the coagulation of contaminants from an aqueous medium. Electrophoretic motion concentrates negatively charged particles in the anode region and positively charged particles in the cathode region. [Mollah etal.,2004]. Consumable metal anodes are continuously used to produce polyvalent metal cations in the anode region. These cations neutralize the negative charge of the particles moved towards the anodes by the production of polyvalent cations from theoxidation of the sacrificial anodes Al and the electrolysis gases like hydrogen evolved at the cathode and oxygen evolved at the anode, as seen in Eq. (2-1)[Chaturvedi,2013].

$$2H_2O + 2e^- \rightarrow H_2\uparrow + 2OH^- \qquad E^o = 0.37V \qquad (2\text{-}1)$$

This process involves three successive stages:

(i) Formation of coagulants by electrolytic oxidation of the sacrificialelectrode.
(ii) Destabilization of the contaminants, particulate suspension and breaking of emulsions.
(iii) Aggregation of the destabilized phase to form flocks [Chaturvedi,2013].

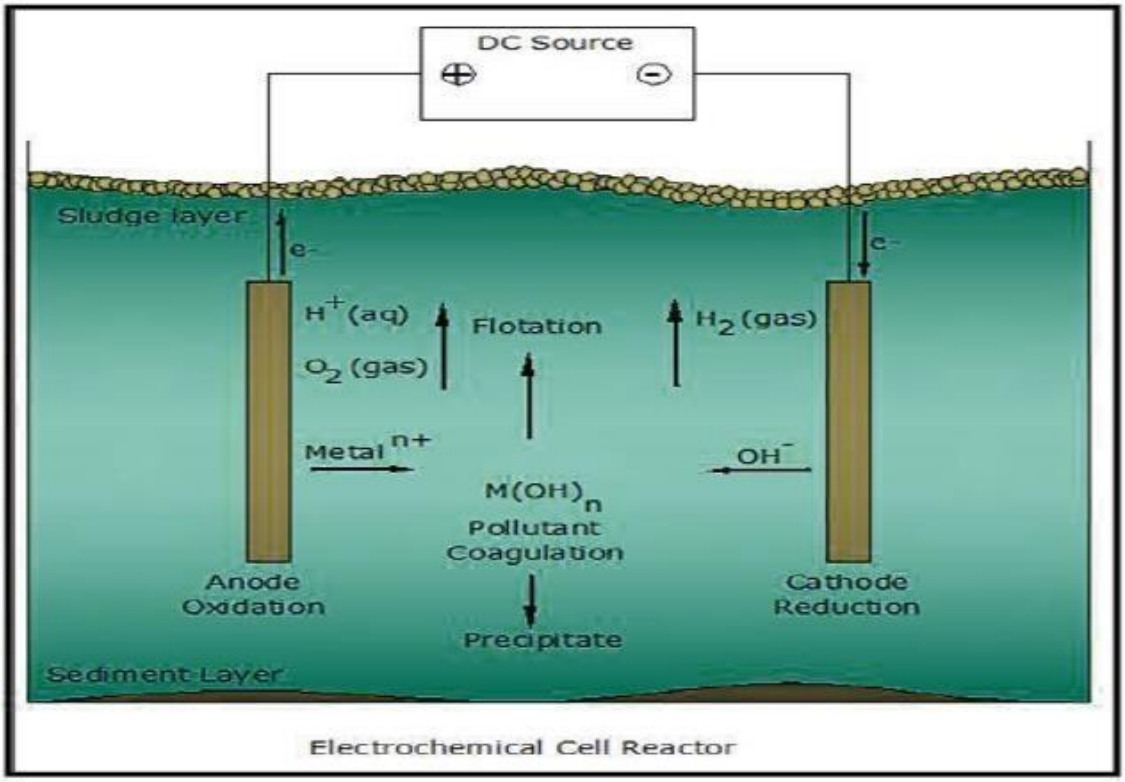

Figure (2.1) Schematic diagram of two-electrode electrocoagulation cell [Mollah etal.,2004]

2.3.2 Theory of electroflotation

Flotation is a unit operation for separating a solid phase from the liquid phase by introducing gas bubbles that adhere to one phase causing a decrease in the apparent density of that phase such that it will rise and float. In dissolved air flotation (DAF), the gas used is air. In contrast, the gas used in electroflotation consists of hydrogen and oxygen produced by water electrolysis [Wang et al.,2010].

In flotation, small bubbles released from the solution attach themselves to suspended particles. The bubble–solid mixture rises to the solution's surface, where it concentrates and is removed. In electroflotation, an electric version of flotation, bubbles are generated predominately by the electrolysis of water. Hydrogen and oxygen bubbles are generated to perform the binding function [Yang,2007]. As shown in Figure (2.2), the complexity of an adequate theoretical treatment of the actual act of flotation, namely, the capture of mineral particles by bubbles, lies in the necessity of considering the hydrodynamic processes of the approach of the

particles and the rising bubbles simultaneously. The chemical reactions occurring at the electrodes to produce these gases are illustrated by Eq. (2.2) at the anode electrode and Eq.(2.1) at the cathode below [Wang et al.,2010].

$$2H_2O \rightarrow 4H^+ + O_2\uparrow + 4e^- \qquad E^o = 1.23V \quad (2\text{-}2)$$

$$2H_2O + 2e^- \rightarrow H_2\uparrow + 2OH^- \qquad E^o = 0.37V \quad (2\text{-}1)$$

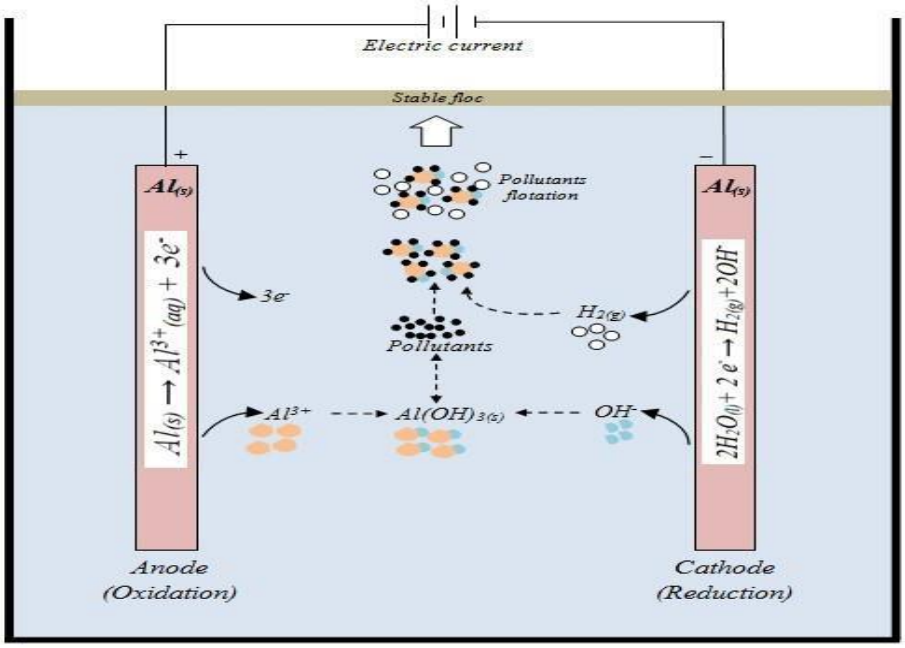

Figure (2.2) The Principle of Electroflotation. [Ammar et al.,2018]

2.3.3 Combined Electroflotation with Electrocoagulation

The combination of electrocoagulation and electroflotation is considered a physical means for wastewater treatment. It is understood as an electrolytic treatment where a sacrificial anode (iron or aluminium) dissolves and produces coagulant agents (AL^{3+} or Fe^{2+}). At the same time, the cathode yields hydrogen that is responsible for the electroflotation process [Majlesi et al.,2016].Therefore, wastewater treatment occurs through coagulation, adsorption, precipitation, and flotation. The main advantages of this combination are less sludge formation, compact equipment, rapid treatment, energy efficiency, safety, and selectivity [Essadki et al.,2009].

Sustaining a relatively neutral pH during the process. However, the need for proper dimensioning and proposal of standard equipment design has

hindered the industrial application of this method. Furthermore, due to the wide variety of parameters potentially controlled in ECEF treatment, such as current density, anode material, electrolyte concentration, pH, and reactor dimensions, the system can be continuously improved to reach optimum treatment conditions [Essadki et al.,2009].

Considering the electrolytic oxidation of the anode responsible for the coagulant generation, low consumption of alkali reagents is seen due to the limited variations in pH, and the process is suitable for portable water treatment units, as previously described [Santos et al.,2018].

2.3.4 Hybrid EC/EF Theory

The EC/EF process is a non-specific hybrid hydro-electrochemical treatment that uses the electrolysis of metal (aluminium in our case) to reduce contamination. It consists of the in situ dissolution of metal cations from the anode and H2 produced at the cathode from reducing water by applying a constant direct current or voltage between the carcass anode and the cathode. After spontaneous hydrolysis, these cations play the role of electrocoagulation, precipitation, adsorbent, and/or electrostatic attractant to enhance contaminant reduction. EC/EF is associated with many decontamination mechanisms, including those of chemical coagulation such as charge neutralization, double-layer compaction of colloidal particles, and sweeping coagulation due to the precipitation of metal hydroxides, adsorption on sediments, but also those resulting from electrochemical treatment, such as Electrooxadation or electroreduction in electrodes, a redox reaction in bulk with electrolyte species. Besides promoting mixing, the separation of sludge caused by flotation is preferred.

At the cathode

$$2H_2O + 2e^- \rightarrow H_2\uparrow + 2OH^- \qquad E^o = 0.37V \qquad (2\text{-}1)$$

At the anode electrode the following reaction appear:

$2H_2O \rightarrow 4H^+ + O_2\uparrow + 4e^-$ $E^o = 1.23V$ (2-2)

$Al \rightarrow Al^{3+} + 3e^-$ $E^o = -1.6V$ (2-3)

Solution reaction

$Al^{3+} + 3OH^- \rightarrow Al(OH)_3$ (2-4)

Electrolysis of anode metal, production of H_2 gas produced by water reduction occurs at the cathode, which positively affects the hydrodynamic system by enhancing mixing and favouring flotation-induced sludge separation. [Hakizimana et al.,2017].

2.3.5 The Characterization of EC/EF Process

Electrocoagulation-Electroflotation (EC/EF) process is characterized by easy operation, reduced sludge production, and no need to handle chemicals. It has been applied efficiently to various water treatment processes [Jiménez et al.,2016]. As shown in Figure (2.3), EC/EF includes the generation of coagulants via the electro-dissolution of a sacrificial anode, which usually consists of iron or aluminum. [An et al., 2017].

Metal ion generation occurs at the anode, and hydrogen gas is released from the cathode. The basic principle of electrocoagulation originated from electrolysis. Michael Faraday first formulated the principle of electrolysis [Emamjomeh & Sivakumar, 2009].

The basic principle of electrocoagulation was originated from electrolysis. Michael Faraday first formulated the principle of electrolysis [Chen et al., 2005]. It occurs as a direct electric current passes through the electrolyte, producing chemical reactions at the electrodes. The electrochemical process in aqueous systems has been explained by [Lin et al.,1998]. The electrocoagulation and electroflotation processes are beneficial for treating oily wastewater

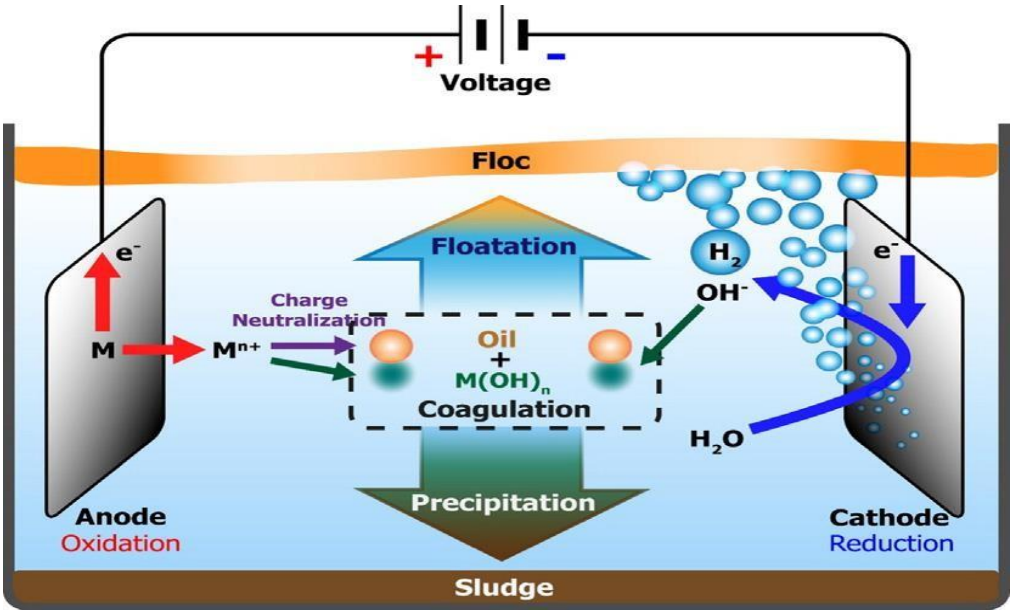

Figure (2.3) The Principle of Electrocoagulation- Electroflotation [An et al., 2017]

2.3.6 Emulsion Destabilization

Related the demulsifying efficiency of a copolymer to its spontaneous curvature, described the demulsification process, as shown in Figure (2.4). In W/O emulsion systems, the oil layer between the two water droplets has to break to allow the coalescence of water drops, i.e., a small but significantly curved hole must nucleate into the oil layer [Le Follotec et al, (2010)].

This process is mainly followed by an energy hindrance concerned with the new interface formation. The useful copolymers with a moderate hydrophobic segment may contribute to the hole nucleation, leading to the separation of W/O emulsions. In contrast, O/W emulsion systems adversely function by obstructing the nucleation of a gap in the water layer between two oil droplets and thus favour the emulsion stabilization. In contrast, the bulky central hydrophobic portion of an inefficient triblock copolymer unfavourably hinders the hole formation, prevents coalescence, and consequently, improves the stability of W/O emulsions.[wang et al.,2021].

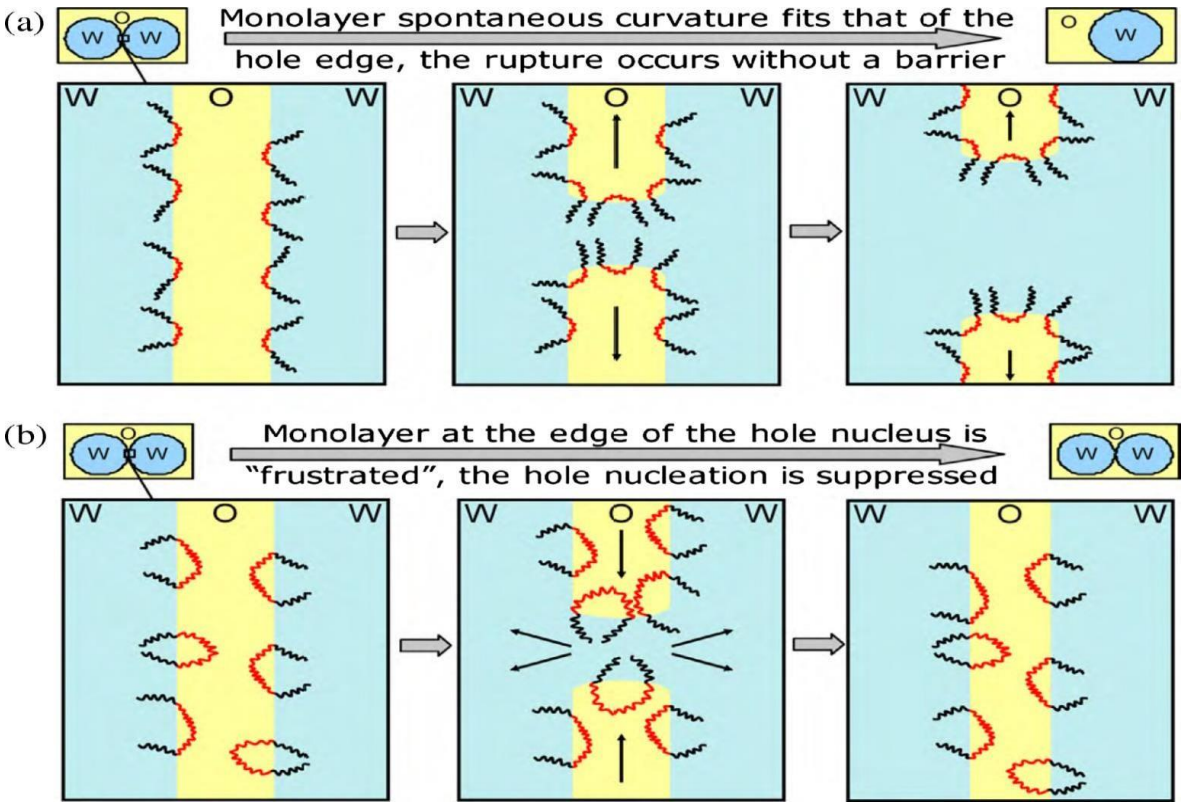

Figure (2.4) (a) Coalescence of two water droplets during emulsion destabilization by efficient molecules, and **(b)** connection without coalescence with inefficient molecules [Le Follotec et al., 2010], [wang et al.,2021]..

2.4 Electrochemical Demulsification Mechanism

The reactions are observed through the hydrogen bubbles that evolve from the cathode and the oxygen bubbles that originate from the anode. However, when the anode is made of metals that have lower oxidation potentials than water, the anode is dissolved to produce metal ions instead of generating oxygen. These ions then react with hydroxyl ions, the by- products of hydrogen generation, to produce metal hydroxides. During electrolysis in wastewater treatment, the sacrificial aluminum anode is oxidized into Al^{3+} ions. As the operation progresses, the ionic strength of the wastewater increases. Figure (2.5a**)** shows how the surfactant stabilizes the oil droplets by forming micelles in aqueous solutions. Figure (2.5b**)** shows that the electro-generated cations with high charges effectively neutralize the surface charges on the surfactant molecules. Simultaneously, hydrogen is formed at the cathode. The net result of the reactions is that the emulsion is destabilized, and the colloidal oil particles begin to merge, as shown in Figure (2.5b**).**

Ultimately, the destabilized oil droplets absorb the highly dispersed aluminum hydroxide colloid formed by the reaction between the electro-generated Al^{3+} and hydroxyl ions. Finally, the oil-rich sludge floats to the top, removed by skimming [Yang,2007].

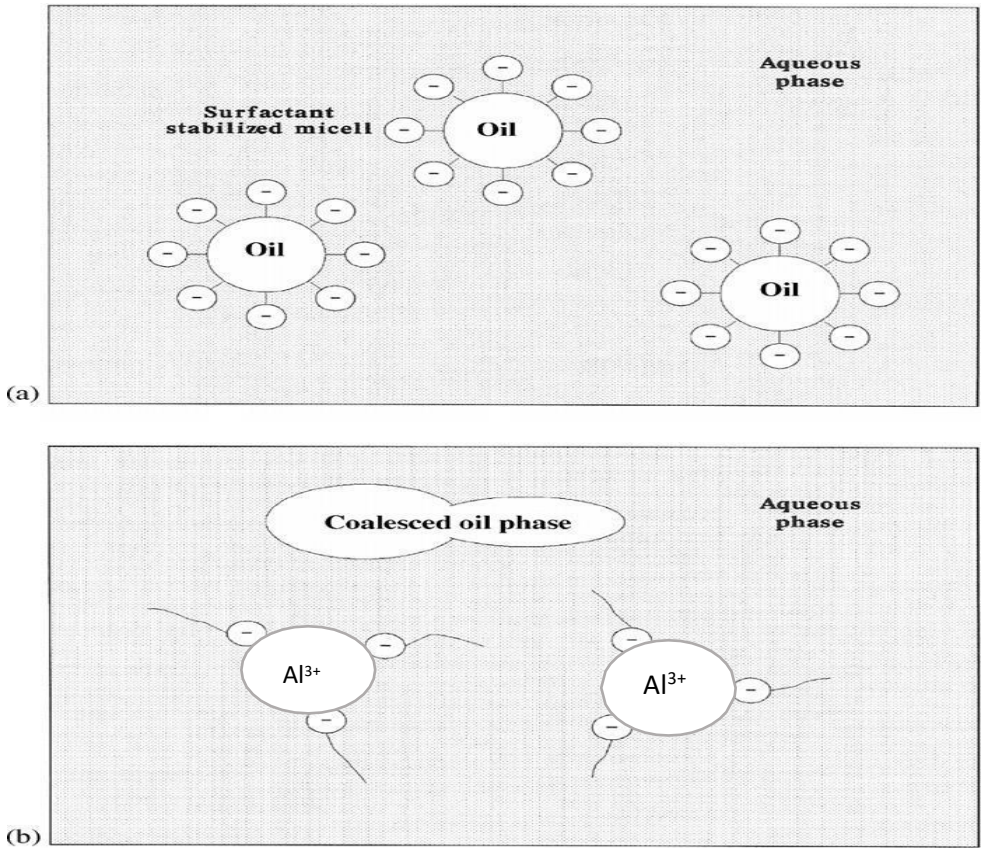

Figure (2.5) The stabilization of an oil-water emulsion by a surfactant **(a)**, and the destabilization of emulsion by cations and the coalescence of oil droplets **(b)**. [Yang,2007].

2.5 Literature Review

1- General Treatment of Oily Wastewater.

2- Electrochemical Treatment of Oily Wastewater.

3- Oily Wastewater Demulsification by Hybrid EC/EF Process.

1- General Treatment of Oily Wastewater

Conventional methods for treating oily wastewater depend on the oil concentration, drop size and physical nature of the oil. The most common methods of treating oily wastewater in general can be summarized as: gravity sedimentation, direct and indirect anodic oxidation, coagulation, flotation, coagulation compound flotation, de-emulsification, membrane

separation, flocculation treatment, chemical precipitation, biological treatment, filtration, and electrochemical methods and hybrids between the above-mentioned possible methods. It's can be classified as primary, secondary, tertiary, b and quartety, as it shown in Fig. (2.6)[Redah, 2016].

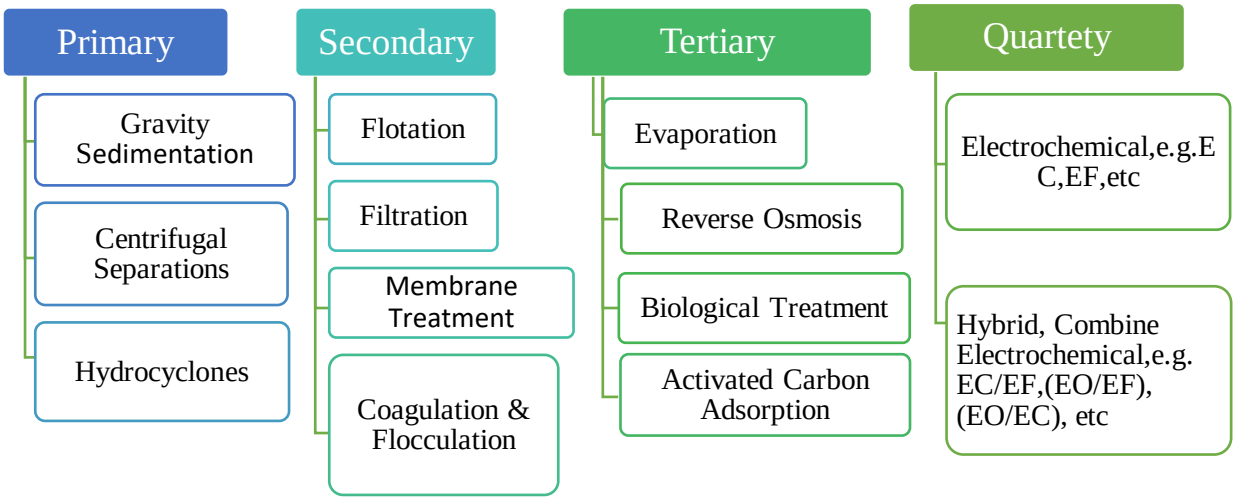

Fig. (2.6) Conventional & advance treatment process of oily wastewater. **(Redah, 2016, Coca et al, 2011)**

Hami et al, 2007, investigated the effect of powdered activated carbon (PAC) on biological oxygen demand (BOD) and chemical oxygen demand (COD) removal by using a dissolved air flotation (DAF) unit to treat refinery wastewater. The treatment was done under the operating parameters (flow rate, recycle ratio, saturation pressure, and the concentration of PAC added) which were studied on the removal efficiency of pollutants in terms of (BOD) and (COD). It was found that for dosages of activated carbon in the range of 50–150 mg/L, the removal efficiencies for BOD increased from 27–70% to 76–94% while those for COD increased from 16–64% to 72–92.5% for inlet values of 45–95 mg/L and 110–200 mg/L for BOD and COD, respectively. Such findings a represent considerable improvement in the performance of the DAF unit.

Abbas, 2011, studied demulsification of oily water by dealing with breaking of oil in the wastewater of refineries. A chemical additives method was used for this purpose accompanied with a flotation method by using

Denver cell. Three types of oils were studied, (kerosene, gasoil, and lubricant). Five types of emulsifiers were compared (Commercial surfactant, sulfate dodecyl sodium (SDS), coconut soap, grape soap and rubber soap) for emulsifying. It was used five chemical additives for demulsifying, (Chimec2439, alum (aluminum sulfate), $CuSO_4$ and starch), they were studies different variable of, pH, temperature, API of dispersed phase and concentration of additives. The best results showed for alum, that recovery of oil percentage increases from80% to 98% with increasing temperature value from 30 °C to 80 °C, decreasing with increase pH value, which is 98% at pH 4, and 23% at pH 11. and increases with increasing API of oil, which formes emulsion; which is increases from 96% at API of 26, and 98% at API of 47.5. It was found that commercial emulsifier gave higher zeta potential (higher stability of emulsion) It was (-200 mV). The emulsion was anion; it was found that zeta potential decreases with decreasing pH of emulsion. Recovery of oil increases with decreasing of zeta potential, and zeta potential decreases with increasing of chemical additives concentration, but was still negative in all manners.

Mohammed et al, 2013, **s**tudied the process of induced flotation through the flotation column (inner diameter 10 cm and height 150 cm), the process of treating oil contaminated water (grease, dispersed oil, emulsified oil or dissolved oil) for the Iraqi North Oil Company. The column operated in a semi-batch mode (batch wastewater, continuous air injection).

Different samples of oily wastewater (30,100,800) ppm were used. Air introduced at different superficial gas velocity, (50 to 250) rpm was used to indicate it effect on the removal efficiency of oil from water, through porous distributor which located at the bottom of column. Different speed of the stirrer, which showed that the removal efficiency was increased with increasing initial oil concentration, it reached up to 76 %. while it became 89% when using stirrer. By dispersed air flotation; The emulsified oil with concentration can be removed high percentage was achieved from 20 to 25

minutes. Induced air flotation (IAF) and modified induced air flotation (MIAF) were applied, the removal efficiency obtained with IAF processes smaller than obtained in MIAF.

Abd et al, 2013, studied the performance of a trickle bed reactor for the decomposition of phenol in refinery wastewater by checking the applicability of 0.5% platinum/alumina commercial catalyst, which is currently used in the desulfurization process in the North Refinery Company-Iraq. The results exhibited that the initial phenol concentration had a negative effect on the removal of phenol and the highest conversion of phenol (98.47%) was obtained above 0.5% Pt/Al_2O_3 in the studied conditions (such as operating pressure of 0.8 MPa, operating temperature of 1200 °C, liquid hourly space velocity (LHSV) 2.5 h^{-1} ,(LHSV) = (Volume of liquid feed at60"F/hr)/volume of reactor or catalyst). It is generally expressed as hr^{-1}, air surface velocity of 0.25 m/s), with an initial phenol concentration of 200 mg/L. The current method has a low residence time, the final products are harmless to the environment and do not produce sludge that requires further treatment.

Liu et al, 2014, studied the application of the isolation of bioflocculant-producing strains in the oily wastewater treatment process. Ten soil samples were screened by the pyridine screening method, and 61strains were isolated of which 27 bacteria strains had high flocculating activity. Three strains, named KL9-1-1, KL9-1-2 and KL9-1-3, whose flocculating rates were more than 90%, were obtained. The bioflocculant KL9-1-3 can effectively deal with oily wastewater, and the corresponding maximum removal rates of oil and COD for oily wastewater were 74.1% and 42.9%, respectively, under the optimum conditions of bioflocculant dosage 0.2 ml/l, pH 10.0, temperature 40°C, and Ca^{2+} as the coagulant. The flocculating rate of KL9-1-3 reached as high as 98.2%.

Hassan et al, 2020, studied the degradation of acidic aqueous solutions of the synthetic diesel oil water emulsion by advanced oxidation

processes (AOPs) using Fenton reagent (Fe^{2+}/H_2O_2). The effect of different process parameters, such as pH, oxidant's dose ($FeSO_4/H_2O_2$) and reaction times on the removal of diesel oil were investigated in terms of COD. It was proved at an optimum concentration of $[H_2O_2] = 11\times10^{-2}$ M and $[Fe^{2+}] = 7.4\times10^{-3}$ M, pH=3.5 the reaction time 60 min reduced COD 65% of diesel oil at 1300 mg O_2/l, so the optimum H_2O_2/Fe^{2+} molar ratio was experimentally determined to be 15. The treatment of this wastewater by Fenton oxidations under optimal conditions were removed 86% of the initial COD and 97 % of total petroleum hydrocarbons (TPH) of the oily wastewater.

Yang et al, 2021, studied the use of electrospun poly vinylidene fluoride (PVDF-SiO_2) nanofibers with a roughness-enhanced surface for oil-water fusion separation. By assembling coarse nanofibers with SiO_2 nanoparticles manufactured through a one-step electrophoresis technique. The underwater hydrophobicity and surface roughness of the PVDF-SiO_2 membrane were enhanced compared to those of the pure PVDF membrane. The fusion separation efficiency has been reached at 98.5% when using the PVDF-SiO_2 nanofibrous membrane in the fusion material to separate the hexadecane emulsion in water. When the initial oil concentration was increased to 2000 mg/L, the fusion separation efficiency was still above 96%. The membrane performed with a high coalescence separation efficiency of 98.6% for hexadecane-in-water emulsion, and the nanofibrous membrane exhibited good separation performances with different flow velocities, initial oil concentrations and types of oil-water systems, which showed high potentials in oily wastewater treatment.

2- Electrochemical Treatment of Oily Wastewater

For more than a century, electrochemical technology has been used as an efficient treatment method. It a cost-effective energy technique that is versatile, easy to automate, uses less space, produces less sludge, and operates at lower temperatures. The last two decades of use in the treatment

of oily wastewater provided excellent solutions to environmental problems because the only used the electron, which is a very clean reagent. Electrochemical treatment has several methods for oily wastewater treatment like Electrocoagulation (EC), Electro-oxidation (EO) Fig. (2.7), Electrofenton, Electrocouguation-floutation (ECF), Electrodeposition (ED), etc [Anglada et al, 2009].

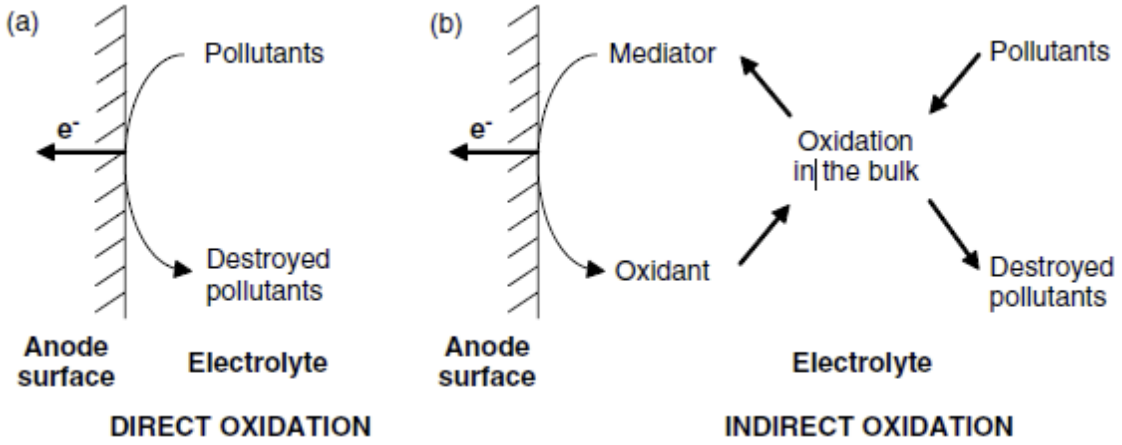

Fig. (2.7). Electrolytic treatment of pollutants (a) direct oxidation and (b) indirect oxidation **Anglada et al, (2009).**

Yavuz at el, 2010, direct and indirect electrochemical oxidation by using boron doped diamond anode (BDD), direct electrochemical oxidation by using ruthenium mixed metal oxide (Ru-MMO) electrode, and electrofenton and electrocoagulation by using iron electrode were investigated for the treatment of petroleum refinery wastewater (PRW). Complete phenol and COD removal can be achieved in almost all electroch -emical methods except electrocoagulation provided that electrolysis time is prolonged. The most efficient method was the electrofenton process followed by the electrochemical oxidation using a BDD anode. A Phenol removal of 98.74% was achieved in 6 min of electrolysis and, COD removal of 75.71% was reached after 9 min of electrolysis in electrofenton. Additionally, 99.53% phenol and 96.04% COD removal were obtained in direct electrochemical oxidation at the current density of 5 mA cm^{-2}. After 40 min of electrolysis, the initial phenol concentration 192.9 mg/L was

reduced to 0.91 mg/L and the initial COD of 590 mg/L decreased to 36.7 mg/L and 23.3 mg/L after 60 min and 75 min of electrolysis, respectively.

Al-Malack et al, 2013, a continuous electrochemical process was investigated for the treatment of synthetic petroleum refinery wastewater. Phenol, crude oil, and kaolin were added in concentrations typical to that found in a refinery wastewater to simulate the soluble, immiscible, and colloidal phases, respectively. Stainless steel electrodes were used in the electrochemical cell, while an immersed Zenon (ZW-1) ultrafiltration membrane module was utilized for solid–liquid separation. The optimum current density was noted to be 30 mA/cm2 with a contact time of 20 min. However, a removal efficiency of 99% was achieved for turbidity while oil was below the minimum detection limit of 1.4mg/L for the EPA method.

Sangal et al, 2013, studied the Parametric and Kinetic Investigation of EC of Soluble Oil Wastewater. Their experimental results on an oil-water emulsion with an initial oil concentration of 9600 mg/l by electrocoagulation are shown in the following. When the pH and initial turbidity of the emulsion were 6.50 and 2960 NTU, respectively. It was also noted that the removal of oil (or turbidity) is very slow at first, and after that, the removal becomes fast, followed by a very slow removal period again. This initial period of slow removal may be called the induction period. The kinetics of removing oil from the emulsion showed the effect of changing the current density on residual turbidity over time is in the range (59.2-179.8 A/m2), it was observed at current density of 138.8 A/m2 which gives the highest turbidity removal in 120.

Rincon & Motta, 2014, the researchers here in presented electrocoagulation (EC) as a method to treat bilge water, using a continuous flow reactor, and a synthetic emulsion as artificial bilge water. With a focus on oily emulsions removal efficiency. The synthetic emulsion contained 5000 mg/L of oil. In order to determine the optimal conditions, experiments

were carried out at different parameters such as combination electrodes, detention time, flow rate, and current density. The experimental results demonstrate that EC is very efficient in removing oil and grease, where the best treatment and cost efficiency was obtained when using a combination of carbon steel and aluminum electrodes, at a detention time of less than one minute, a flow rate of 1 l/min and 0.6 A/cm^2 of current density. The final effluent oil and grease concentration, before filtration, was always less than 10 mg/L.

Gargouri et al, 2014, studied the anodic oxidation of real produced water (PW), generated by the petroleum exploration of the Petrobras plant-Tunisia in an electrolytic batch cell. In order to know the feasibility of electrochemical treatment, the electrolytic process was monitored by COD and the residual TPH. At compared the efficacy of two different electrodes: PbO_2 reinforced on tantalum Ta/PbO_2 and BDD anodes contained, operated at different current densities (30, 50 and 100 mA/cm^2) for the treatment of oily wastewater. Results demonstrated COD removal efficiencies of 85% and 96% after 11 h when using PbO_2 and 96% after 7 h when using BDD. In addition, BDD was more efficient with higher oxidation rate and consumes less energy for removal of petroleum hydrocarbons from the produced water when compared with a PbO_2.

Davarnejad et al, 2015, studies on the treatment of petroleum refinery wastewater by the electro-Fenton process were successfully simulated, by computational fluid dynamics (CFD). The effects of H_2O_2/PRW (ratio of mole of H_2O_2 per PRW volume), H_2O_2/Fe^{2+} molar ratio, current density, pH and reaction time were numerically investigated. Furthermore, the simulated data showed that maximum COD removal in the experimental was around 82.55% at H_2O_2/PRW of 0.04, H_2O_2/Fe^{2+} molar ratio of 2.75, pH of 3.5, current density of 52.5 mA/cm^2 and reaction time of 90 min while the experimental data obtained from the literature showed maximum COD

removal of 77% in the same operating conditions, indicating that the simulation data showed good agreement with the experimental ones.

Safari et al, 2016, investigated removal of COD and diesel from oily wastewater using electrocoagulation. The effects of different parameters, such as pH, time, voltage, supporting electrolyte, electrode material, and diesel initial concentration, on the treatment of this wastewater in a batch EC reactor were investigated. The optimal initial pH for current experiments was 7 and it was nearly constant during the process due to the buffering effect of the EC. The highest removal efficiency for treating oily wastewater using EC was observed at pH 7, 40 min, 10.5 V, NaCl concentration of 0.5 g/L, aluminum as anode and cathode material, and initial diesel concentration of 3500 mg/L. In the optimized conditions, removal rates of 99.1% for the COD and 98.8% for the diesel are achieved. Moreover, the amount of sludge produced and energy consumption were 1995 mg/L and 6.47 kWh/ m^3, respectively.

Fahim,2020, conducted a comparison among the electrochemical processes, Photo-Electro-Fenton (PEF) as well as Photo-Electro-Oxidation (PEO) for treating an effluent resulting from Al-Diwaniya petroleum refinery (phenolic complexes and organic compounds) plant using a lab-scale batch, electrochemical cell, stainless steel cathode and porous graphite anode. Impact of operating parameters such as current density (5-25mA/cm^2), addition of NaCl (0-2g/l), pH (3-9), and time (20-60min) on the removal efficiency of COD. The optimum conditions were found to be an initial value of the pH = 3, current density of 5mA/cm^2, NaCl concentration equal to 2g/l, and duration of 60min, where COD removal efficiency of 95.33% was achieved and energy consumption of 0.729 Kwh/Kg COD was required. Results showed that the PEF is more effective than PEO where COD removal increased from 71.5% in the case of PEO to 92.67 % and 95.33% in the case of PEF with one and two lamps, respectively. Nevertheless, PEF was found to be more economic than PEO (0.729

Kwh/Kg COD in the case of PEF in comparison with 1.2266 Kwh/Kg COD in the case of PEO). As a final conclusion, PEF can be used as an efficient method for the treatment of wastewater generated from Al-Diwaniya petroleum refinery.

3- Oily Wastewater Demulsification by Hybrid EC/EF Process

Many studies have looked into the performance of EC/EF and the parameters that influence it, such as type of the reactors (batch or continuous), flow rate of contaminated oily wastewater emulsions, initial pollutant concentrations, current density, electrode material, distance between electrodes, voltage, PH, temperature, and so on. Experiments or simulations may be used. Some of these studies are as follows: Each study project's goal, assumptions and conclusion.

Dimoglo et al, 2004, with the help of (EF and EC) processes the efficiency of electrolytic applied to the purification of oil refinery wastewater from different contaminants is investigated. In the EF unit, a graphite anode and a stainless-steel mesh as cathode were used. In the EC unit, iron and aluminium were used simultaneously as materials for two blocks of alternating electrodes. At voltage 12 V, current density (*i*) was varied from 5 -15 mA/cm^2, and the residence time varied in the limits of 2–20 min for EF and 1–10 min for EC. The results have shown that EC removes the mentioned contaminants from petrochemical wastewater (PCWW) more effectively than EF. Turbidity removal in the process of PCWW purification was estimated as 83% for EF and 88% for EC. The results of the EF process applied have shown that it is possible to separate suspended particles (oils, greases, oil-fuel products) with a density close to that of water. Application of the EC method makes the treatment of oil refinery wastewater easy for regulation and automation. A constructional optimization of the EF and EC apparatus for the treatment of PCWW, it is feasible to transfer from laboratory-scale models to industrial specimens with the same degree of technological qualities, and this technology is now being developed.

Ge et al, 2004, developed a single continuous reactor for simultaneous electrocoagulation/electroflotation (EC/EF) to a new bipolar EC / EF to treat laundry wastewater, by using the above process and Eight pieces of monopolar titanium and 21 pieces of bipolar aluminum plates with an effective area 50 cm^2 of each one. Under the following parameters: pH of 5-9, at a short hydraulic residence time (HRT) at range 5–10 min, current density. The laboratory results showed that the removal of COD was greater than 70%, the surfactant, a methylene blue active substance (MBAS), P-phosphate ($P\text{-}PO_4^{3-}$) could be reached above 90% and turbidity was increased with increasing current and HRT.

Ulucan and Kurt, 2015, they found treatability of bilge water by electrocoagulation/electroflotation process is investigated by using aluminum and iron electrodes. In order to determine optimum conditions, the experiments were conducted in different ranges pH (4.5–10), time (5–120 min), temperature (10–60) ^oC and current density (2.5–25 mA/cm^2). For Al and Fe electrode, the best results can be investigated after 10 min, temperature of 20 ^oC, current density equal to 7.5 mA/cm^2, pH=6.5,6.86, COD efficiency equal to 64.8,36.2% and oil–grease removal efficiency was equal to 64% and 53%, respectively. While these values were increases after 60 min. Table (2.2), shows that the optimum removal is occurres in the first

Table (2.2) Comparison of EC/EF processes for Al, Fe Electrodes.**Ulucan&Kurt,2015**

Parameters	Electrocoagulation/electroflotation	
	Aluminum	Iron
Reaction time (min)	10	10
Applied current (A)	1.0	1.0
Applied current density (mA/cm^2)	7.5	7.5
Initial voltage (V)	6.5	6.5
Dinal voltage (V)	6	6.2
Influent pH	6.86	6.86
Effluent pH	6.95	6.90
Conductivity (mS/cm)	29.8	29.5
Sludge produced (ml/500 ml)	40	55
Turbidity, ntu	24.4	276
Influent COD concentration(mg/L)	2247	2247
Effluent COD concentration (mg/L)	792	1433
Removal rate of COD (%)	64.8	36.2
Influent Oil&Grease concentration (mg/L)	93	93
Effluent Oil&Grease concentration (mg/L)	40	81.4
Removal rate of Oil&Grease (%)	57	12.5
Influent BOD concentration (mg/L)	490	490
Effluent BOD concentration (mg/L)	167	200
Removal rate of BOD, %	66	59
Influent TSS concentration (mg/L)	111	111
Effluent TSS concentration (mg/L)	13	213
Removal rate of TSS, %	88	0
Electricity consumption (kWh/m^3)	2.17	2.13

10 min. In addition, from the first moments of EC/EF process onwards, oil became visible on the surface.

da Mota et al, 2015, explained the performance of batch EC/EF technique for the treatment of synthetic solutions simulating wastewater from washing soil contaminated by drilling fluids from oil wells. The effects of different parameters, including the pH, the electrolysis time, the current density, ionic strength and the supporting electrolyte dosage were evaluated. pH and EC/EF time were very important for design optimal conditions of the treatment. The experimental results revealed that it was feasible to remove up to 97% of the Pb, Ba and Zn by EC/EF attaining 97% of removal using stainless steel mesh electrodes with a total energy consumption of 14 Kwh/m^3. The optimum conditions found were, current density 350 Am^{-2}, ionic strength 3.2×10^{-3} M, pH = 10.0 and 20min of EC/EF, molar ratio 3:1 SDS: heavy metal, and 0.1% ethanol (as a foamy).

Jiménez et al, 2016, they concluded the electroflotation processes is a good alternative to the removal of oil micro drops and dyes during a combined treatment of wastewater through a combined electrocoagulation and electroflotation techniques and used response surface methodology (RSM).The experiments were practiced, taking into account the effect of current density, residence time, oil micro drops concentration and the ratio floated /settled solids, an achieved good results in the removal of (oil micro drops and dye solutions) that form low density solids during the EC stage (dye solutions and oil-in water emulsions). These types of solids can be easily dragged to the reactor surface by the hydrogen bubbles produced during the EF process. RSM has been used which allows modelling the results obtained in a combined EC/EF reactor for the removal of (kaolin, as a model of suspended mater pollution, (EBT), as a model of soluble organic matter pollution; eriochrome black T) that form hight density solids and oil concentration of an oil-in-water emulsion and for the floated-settled solid ratio achieved inside the reactor. As compared to iron, the use of aluminium

electrodes during the EC leads to better results in the separation of the oil droplets formed during the treatment of oil-in water emulsions because of the lower density of the aluminium flocs formed.

Aoudj et al, 2017, studied removal of organic and inorganic pollutants such as (SDS), fluorine and ammonia from the special liquid wastes of the semiconductor industry with their proposal to be treated by the combined process of electrocoagulation and electroflotation as a post-treatment after precipitation for simultaneous clarification and removal of pollutants. In EC step, a hybrid Fe–Al was used as the soluble anode in order to avoid supplementary EC step and with hybrid Al-Fe makes a good compromise. EC-Fe is more suitable for SDS removal, while EC-Al is more suitable for fluoride removal. The final concentrations may reach 0.27, 6.23, and 0.22 mg/L for SDS, fluoride, and ammonia, respectively.

Safwat et al., 2019, studied investigate the performance of EC/EF to treat printing wastewater under various experimental conditions using copper electrodes. The effects of several variables, including different electrode materials (copper and aluminum), different current densities, electrolysis time, and spacing between electrodes on the removal efficiency of various parameters were investigated. The results showed that the maximum removal efficiencies for COD, TDS, and oil and grease were obtained when using a copper electrode. The maximum removal efficiencies were obtained at a gap distance of 4 cm.

Mazumder et al, 2020, discussed the proposed benefits of electrocoagulation and electroflotation with the membrane separation, for a novel hybrid electrocoagulation and electroflotation enhanced membrane module (ECEFMM) was used. Polyethersulfone (PES) and polysulfone (PSf) membranes were employed with each of the modes. The synergistic effect of applied voltage and membrane operation facilitates demulsification for emulsified oily wastewater. Voltage was applied both continuously and periodically. The minimum flux decline for PSf membrane can be achieved

with periodical voltage application at 10 V with substantial oil rejection of 94–96 %. Substantial increase in the steady state permeate flux, which was around 43–72 %, was observed on the application of the voltage. It was seen that the oil rejection through membrane separation was high and permeate conductivity was low as the intensity of the applied voltage was increased to 15 V. Moreover, the operational energy consumption is minuscule with the ECEFMM that made it a promising and cost-effective hybrid technology for oily wastewater treatment.

2.6 The Literature Review Summary

By reviewing the researchers' literature, it became clear to us that the use of the electrocoagulation/electroflotation method for oily wastewater demulsification yields the desired results within a shorter time, higher removal efficiency and lower cost by sacrificing the cheap and effective in-process anode compared to other possible removal processes, Therefore, the hybrid EC/EF is considered one of the most promising and scalable operations.

1- Previous studies of ECEF removal operations have helped in improving operations, optimum condition and reducing costs.

2- Aluminum is often used for its availability, cheapness and effectiveness in removal.

3- The efficiency of the removal of oil and organic pollutants increases with the increase in current density and the passage of time.

No.	Author	Year	Method	Electrodes	Type of wastewater	pollutants	Notes, Optimum operating conditions
1	**Mazumder et al**	2020	ECEFMM	Al –SS	oily wastewat-er	oil	The oil removal efficiency through separation membrane (PES, PSf) is high, SEEC is low and the

							separate conductivity is low as the applied voltage is increased to 15V.
2	**Ulucan & Kurt**	2015	EC/EF	Al, Fe	Bilge water	oil	For Al, Fe electrode, time=10 min, T=20 ^{o}C, CD=7.5 mA/cm^{2}, pH=6.5,6.86, COD efficiency equal to 64.8,36.2% and oil–grease removal efficiency was equal to 64% and 53%, respectively.
3	**Jiménez et al**	2016	EC/EF, RSM	Al	oily wastewat-er	Kaolin, EBT	Current density, residence time, oil micro drops concentration and the ratio floated /settled solids, achieved good results in the removal of (oil micro drops and dye solutions).
4	**Mota et al**	2015	Batch EC/EF	SS mesh	Synthetic solutions simulating wastewater (drilling fluids oil wells)	SDS, Pb, Ba and Zn	Current density 350 Am^{-2}, ionic strength 3.2 × 10^{-3} M, pH = 10.0 and 20min of EC/EF, molar ratio 3:1 SDS: heavy metal and 0.1% ethanol.
5	**Dimoglo**	2004	EC/EF	EF(C-SS) EC(Fe-Al)	PCWW	oils, greases, oil-fuel products	EC removes the contaminants of (PCWW) more effectively than EF, Turbidity removal 83% for EF and 88% for EC
6	**Ge et al**	2004	Bipolar EC/EF	Monopolar Ti,Bipolar Al	laundry wastewat-er	COD, MBAS, P-PO_4^{3-}	Under the following parameters: pH of 5-9, at a short hydraulic residence time (HRT) at range5–10 min, current density16-40mAcm^{-2}. The laboratory

							results showed that the removal of COD was greater than 70%., MBAS, P-phosphate (P-PO_4^{3-}) could be reached above 90% and turbidity was increased with increasing current and HRT.
7	**Akarsu & Deniz**	2021	EC/EF, RSM	Al-Al, Al-Fe, Fe-Fe, and Fe-Al	laundry wastewat-er	COD, Color, Anionic surfacta nt, Micropl astic and Phospha te	Effective removal was obtained with 2.16 A current, pH 9, and 60min reaction time using Fe-Al electrodes. Here, 91, 94, 100 and 98% removal efficiencies were achieved for COD, surfactant, color and microplastic, respectively.
8	**Aoudj et al**	2017	EC/EF	Hybrid Fe–Al	liquid wastes of the semicondu ctor industry	(organic, SDS), (inorgan ic, fluorine and ammoni a)	EC-Fe is more suitable for SDS removal while EC-Al is more suitable for fluoride removal. The final concentrations may reach 0.27, 6.23 and 0.22 mg/L for SDS, fluoride and ammonia respectively.
9	**Safwat**	2019	EC/EF	AL-Al, Cu-Cu	printing wastewate r	oil and grease	maximum removal efficiencies for COD, TDS, and oil and grease were obtained when using a copper electrode. The maximum removal efficiencies were obtained at a gap distance of 4 cm.

1

3 CHAPTER three

EXPERIMENTAL WORK

Aqeel Talib

Chapter Three
Experimental Work

3.1 Introduction

This chapter describes an oil/water emulsion that has been prepared by mixing crude oil brought from a Najaf refinery and deionized water purchased from the local market, for the purpose of treatment and study by hybrid EC/EF method. In addition, study the effect of operating parameters on COD removal, electric power consumption(SEEC), instantaneous current efficiency(ICE) , Zeta potential and further study, the study of turbidity, pH, total solids(TS),total dissolved solids(TDS) and total suspended solids(TSS) from oil refining wastewater under the conditions of different: 10, 20, 30 mA/cm^2 current density, 100,200, and 300 ppm initial Crude oil concentration , Al and Carbon felt electrode materials,2,4 and 6 L/hr, O/W flowrate in case of fixed 1 cm distance between electrodes . The materials and devices used in this study are listed below. The tests that will be approved during the research are also mentioned.

3.2 Experimental Objectives

The Experimental objectives of the study work are:

3.2.1 Experimental Reactor Design

As shown in Figure 3.1, 3.2, the experiments were carried out in a laboratory making electrochemical cell (reactor) of pure transparent Perspex(cuboid) plate thickness 6 mm.With internal dimensions (5 * 11.3 * 17.7 cm), the continuous flow EC/EF reactor is made of Perspex (Poly (methyl methacrylate)) with a fixed volume that provides an emulsion flow of 1000 ml (counter current flow). The reactor contains three holes, two at the top (one with a diameter of one cm to enter the

emulsion through a perforated tube with holes 5 mm in diameter, and the other as a groove for the exit of sludge in front of it), and the last hole at the 1.5 cm from the bottom of the cell, for the removal of treated water through a tube like the upper tube, its holes are for the bottom to not blocked by sedimentary solid sludge contaminants). The electrodes used in the continuous conduction process were aluminum - aluminum and aluminum - carbon felt. The electrodes dimensions are1.5mm thick and 5, 5 cm wide and 10,10 cm thick for aluminum and carbon felt, respectively, Figure 3.5,3.6, connected to other parts of the treatment system water emulsion, treated by the hybrid EC/EF process. The system consists of the following parts.

Figure.3.1 Shape of the electrocoagulation/electroflotation experiment reactor

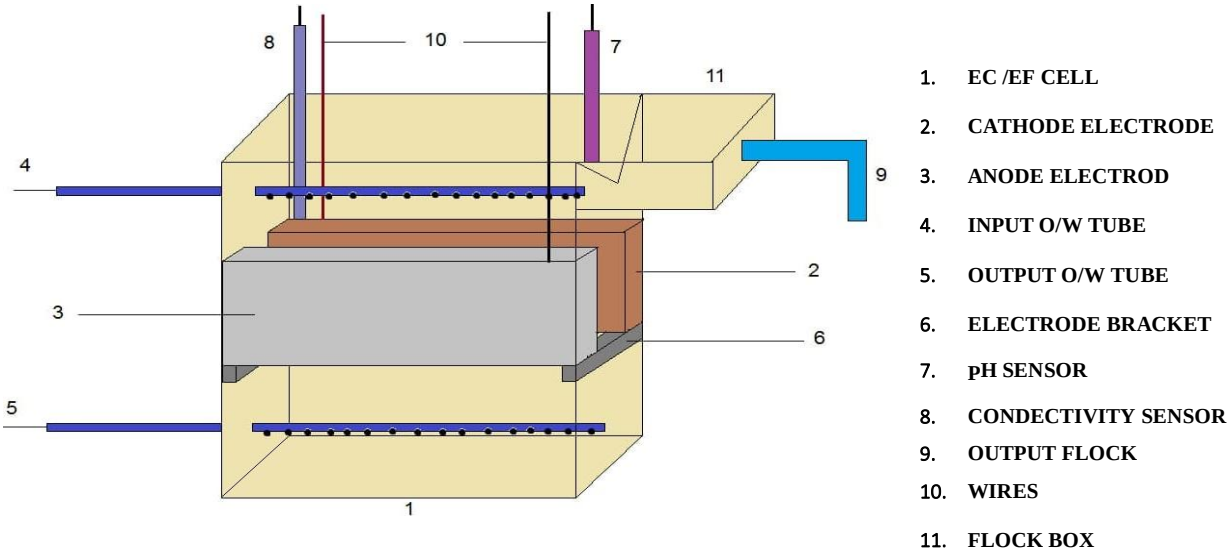

Figure.3.2 Schematic Diagram of EC/EF Reactor Experimental Desig

3.2.2 Anode Electrode

This electrode is the sacrificial anode electrode used as the anode electrode in the two cases where the cathode is aluminum or carbon felt. The aluminum dimensions were, thickness of 1 mm, width 5 cm and length 10 cm, with a high purity that reached 99. 178 %.as it was tested by VAC 34mm analysis by Brucker AXS-D- 76187 Karisruhe, Germany, Figure 3.3, A.

3.2.3 Cathode Electrode

Two cathodes were used made of aluminum (above mentioned) and carbon filtrate, with the following characteristics thickness of 5 mm, width of5 cm, length of10 cm, porosity; 0.94, weight per unit volume; 0.5 kg/m^2.Density; 0.12 kg/ m^3 , carbon content;> or = 99% and ash content; < 0.01, supplied by Shanghai Carbon Material Company (Taiwan), Figure 3.3, B,C.

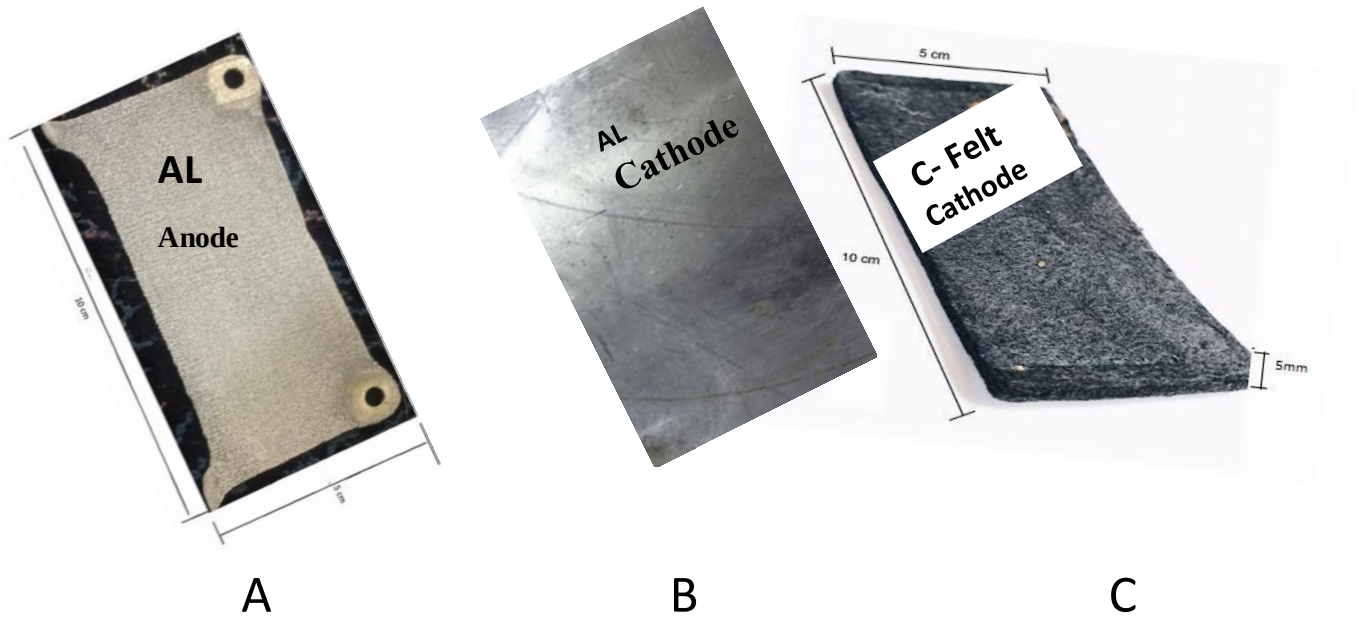

Figure.3.3 Treatment electrodes for EC/EF processors, A- sacrificial anode, B and C, cathodes

3.3 Preparation of Wastewater Samples

1. A laboratory-stable emulsion for use in the EC/EF reactor, prepared by mixing the specified amount of crude oil (100,200, and 300 ppm) with deionized water at room temperature with a high-speed blender (IKA® RW 16 basic overhead stirrers) mixing system at 1600 rpm, for 90 -100 minutes, which is checked by a digital laser (rpm) tachometer (VICTOR DM6234P+). 50 ppm of Sodium dodecyl sulphate (SDS) was used as an emulsifier and is absorbed at the oil-water interface, a sufficient amount of Sodium Chloride solution(1500ppm), produced separately, was added to the emulsion. The resultant emulsion will be referred to as the O/W emulsion here on.

2. The analysis of deionized water was carried out in the laboratories of the Al-Hilla water department and the Al-Muimira sewerage, as for the analysis of crude oil,

which its details are listed in Table (3-1). it was carried out in the Quality control laboratory within the Al-Najaf Al-Ashraf Refinery.

3.The emulsion O/W was tested for its properties as shown in Table (3-2) using a method or instrument for each test and then acidified and kept at a temperature of less than 4°C in the refrigerator to be prepared for analysis operations after adding the digestion solutions and catalyst.

Table (3-1): Al-Najaf Al-Ashraf Refinery Crude Oil and Deionized Water Characteristics**.**

NO	Characteristics	Crude Oil Value	NO	Characteristics	Deionized Water Value
1.	API Gravity @ 15.6 °C	29.3	**1.**	Turbidity. NTU	0.54
2.	SP.Gravity @15.6°C	0.8878	**2.**	Alkalinity of water. mg/L	16
3.	Density @15.6°C mg/ml	0.8795	**3.**	Total water hardness. mg/L	10.3
4.	Sulfur Content Wt.%	3.44	**4.**	Calcium. mg/L	2
5.	Kin.Viscosity@37.8mm^2/s	13.1	**5.**	Chloride. mg/L	0.91
6.	Water&Sediment Vol%	0.05	**6.**	Magnesium. mg/L	1.3
7.	Salt mg/L	98.5	**7.**	Sodium. mg/L	0.8
8.	pH	7.1	**8.**	Potassium. mg/L	0.2
9.	Cl^- Wt.%	3.55	**9.**	Iron. mg/L	0.15
10.	Hardness as $CaCO_3$ mg/L	200	**10.**	Aluminum. mg/L	0.0
11.	Alkalimity as $CaCO_3$ mg/L	177	**11.**	pH	6.7

12.	H_2S Dissolived in Crudeoil ppm	6.4	**12.**	E.c. μ seminice	47
13.	$Fe^{2+,3+}$ ppm	4.2	**13.**	TDS. ppm	6
14.	Carbon Residue wt%	10.5	**14.**	TSS. ppm	3

Table (3-2): Synthetic petroleum oily wastewater emulsion properties.

No	Parameter, Unit	value
1	pH	7.8
2	Temperature (˚C)	36
3	Total Hardness (TH)	200
4	Alkalinity (as $CaCO_3$mg/L)	238
5	Conductivity Ec (μs/cm)	3400
6	Turbidity (NTU)	130
7	Sulfates as SO^{4-} (mg/L)	14.4
8	Chlorides as CL^- (mg/L)	101.2
9	Nitrates as NO_3^- (mg/L)	0.007
10	Total Solids (TS mg/L)	2050
11	Total Dissolved Solid (TDS mg/L)	1730
12	Total Suspended Solid (TSS mg/L)	320
14	Chemical Oxygen Demand (COD mg/L) for 100 ppm crude oil	1108
15	Chemical Oxygen Demand (COD mg/L) for 200 ppm crude oil	1124
16	Chemical Oxygen Demand (COD mg/L) for 300 ppm crude oil	1141

3.4 Laboratory equipment and tools

Specification of the laboratory tools used as given in Table (3.3).

Table (3.3): Laboratory tools specification

Name	model	Company	Specification
Power supply	PS-305DM	LONG WEI	0.01%, Max Range 30 V and 5A.

pH and Conductivity meter	pH, Ec Model 3540	Jenway UK bu Bibby scientific Ltd	Voltage 9VAC Frequency 50/60HZ and Power 6VA
Digital Thermometer	-100.0 to 199.9	VWR	Temperature 211˚C, Temperature range (100-199.9) ˚C
Electrical Rheostat	(1-100k) ohm	Dambrige	Resistance box with maximum range 10k Ohms.
Multi-range Ammeter	DT-830D	Hewlett-Packard	USA (type 3466A), Max Range 20
Multi-range Voltmeter	DT-9205A	Hewlett-Packard	USA (type 3466A) Max Range 20V
Drying Oven	DHG-9055A	Memmert Germany	Volts220V/50Hz Watts 1100w Temp.RangRT+10˚C≈300˚C Temp. Stability ±1˚C Dimensions of the working room 420*395*350 mm Date 2012.04
Sensitive Balance	BL 210S	Sartorius AG GÖttingen Germany	Max 250g
Perspex	RKQ-6mm	PMMA Acrylic plate -China	220x150mm Perspex Sheet Acrylic Stamping Blocks

3.5 Chemicals

Types and qualities of the chemical Properties required for the experiments are showed in Table (3.4)

Table (3.4): Chemicals material Properties

Material and Formula	Purity and Properties
Mercury Sulfate (**$HgSO_4$**)	White powder, insoluble (<0.01g/l of H_2O) 0.051g/100ml(25°C), and soluble in hot H_2SO_4
Potassium Dichromate (**$K_2Cr_2O_7$**)	The solubility in water is 125g/l at 20°C clear orange
Potassium Hydrogen Phthalate **($C_8H_5KO_4$)**	Solubility 10%in water is clear and colorless Minimum assay (after drying) 99.9-100.1% Maximum limits of impurities: insoluble matter 0.003% phthalic acid 0.005%, sodium 0.025%, chloride 0.002%and loss on drying at 110°C 0.05%
Silver Sulfate (**Ag_2SO_4**)	Minimum assay (ex Ag) 98.5% Maximum limits of impurities: Nitrate (NO_3) 0.004%,iron (Fe) 0.003%, and alkalis (sulphated) 0.4%.
Sodium Dodecyl Sulphate(**SDS**)	Alpha Chemika Company, India. $C_{12}H_{25}O_4SNa$. Purity.92%
Sulfuric Acid (**H_2SO_4**)	Minimum assay 98%, Sp.gr. (1.84) and non-volatile matter (0.002%).
Sodium Chloride (**NaCl**)	HIMedla Laboratories Pvt.Ltd. purity.99%.

3.6 Experimental Setup

1. The reactor (cell) made from perspex material dimensional (5 *11.3 * 17.7 cm), with capacity 1L.
2. The anode and cathode were positioned vertically and parallel to each other

with an inner constant gap of 1 cm.

3. The anode electrode was connected to Multi-range ammeter to measure the applied current with galvanostatic operational options for controlling the current density.
4. The cathode electrode was connected to a DC power supply to complete connecting the circuit.
5. The conductivity and pH sencer in the reactor to measure the conductivity and pH of the solution to follow the experiments.
6. The current passing through the circuit remains constant, so it is controlled through the voltage source and the variable resistance. Figure (3.4) shows the experimental setup, and Figure (3.5) shows the schematic diagram.

Figure.3.4 Continuous Electrocoagulation/Electroflotation Experimental Setup System.

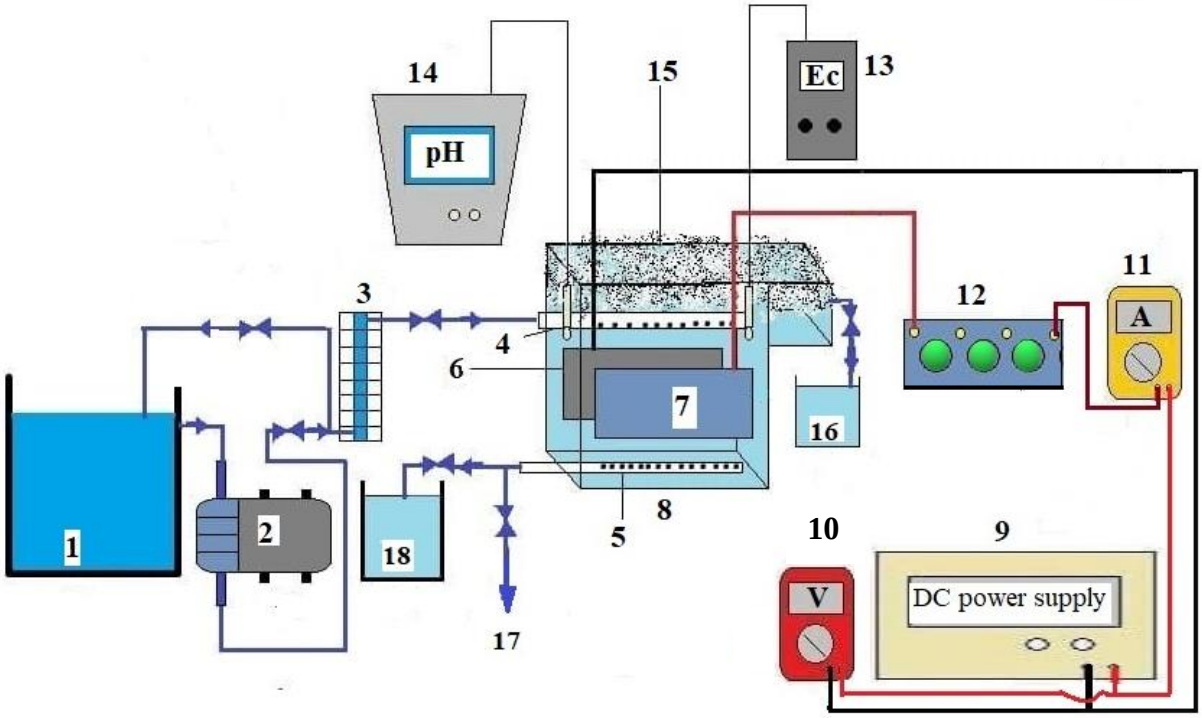

Figure (3.5) Schematic view of experiment setup EC/EF continues reactor processes., **1.** Feed tank,**2.** Diaphragm Booster Pump, **3.** Flowmeter, **4.** Inlet Perforated Feed Tube, **5.** Outlet Perforated Exit Tube, **6.** Cathode, **7.** Anode, **8.** Reactor (cell), **9.** Power Supply, **10.** Multi-range Voltmeter, **11.** Multi-range Ammeter, **12.** Electrical Rheostat,**13.** Conductivity Meter **,14.** pH Digital Meter,**15.** Flock Skimming, **16.** Flock Collecting Vessel, **17.** Sampling **18.** Collection Tank.

3.7 Emulsion Preparation and Experimental Procedure

1. After complete preparation of the stable emulsion for the first experiment of 100 ppm crude oil, 50 ppm SDS and 1500 ppm NaCl per liter of deionized water (for 20 liters O/W emulsion mixing 2g crude oil ,1g SDS and 30g NaCl). The liquid circuit and electrical connection were connected as shown in Figures (3.4), (3.5).

2. Before starting the first experiment, a sample of the emulsion was taken for the purpose of checking the absorbance and then the concentration of the first initial

emulsion, in addition to enhancing the work with other tests such as electrical conductivity, turbidity, pH, TDS, TSS and TS, temperature.

3. The interaction started according to the design of the experiments with the stability of the variables except for one for each experiment.

4. The first experiment was carried out using aluminium-aluminum electrodes, the crude oil concentration was 100 parts per million, the constant current density was 10mA/cm^2 and the emulsion flow rate was 2 liters per hour.

5. More than 1 ml of sample was taken from the exit tube from the reactor every 20 minutes for the length of time specified 120 minutes for one experiment.

6. The above data is recorded in Figure 2 after taking each sample.

7. The samples were kept in a refrigerator at a temperature of less than 4°C and acidified with H_2SO_4 pH lower or equal to 2 prior to analysis.

8.The sample was analyzed in a UV spectrophotometer.

3.8 UV-Spectrophotometer

3.8.1 Principle of the Method

Absorption measurements are made using a (6800 Double Beam Spectrophotometer), in which all oxidants in water can be determined from 3 to 900 mg/L COD. Oxidants are essentially organic components that are oxidized during a two-hour heating step at 150°C. The strong oxidizing agent in the reaction mixture is the dichromate present. During the reaction green chromate ions are formed from

yellow dichromate. This increase in absorption at 600 nm (wavelength) is related to the amount of oxidants in the sample. As for chlorides, they are quantitatively oxidized by dichromate and represent a positive interaction. Mercury sulfate is added to the digestion tubes to complicate the chlorides. Table (3.5) shows the device and reagents that were used **(Pisal, 2010 and EPA based on standard methods for water and wastewater examination, 2007). O'Dell,1993**

- **Digestion solution:** Addition of 10.2 g of potassium dichromate $K_2Cr_2O_7$ after drying at 105˚C for 2-hour drying oven, 167 mL of concentrated sulfuric acid H_2SO_4 and 33.3 g of mercury sulfate $HgSO_4$ to 500 mL of distilled water then cooling and dilution to 1000 mL with deionized water in 1000 mL volumetric flask **EPA based on standard methods**. O'Dell,1993
- **Catalyst solution:** Addition 22 g of silver sulfate Ag_2SO_4 to a 4.09 kg bottle (2.22L) of concentrated sulfuric acid H_2SO_4 and let stand for 2 days until dissolved **EPA based on standard methods**. O'Dell,1993
- **Potassium hydrogen phthalate stock solution ($C_8H_5KO_4$):** Dissolving 0.850 g of ($C_8H_5KO_4$) dried at 105˚C for 2 hours in 800 mL of deionized water in a 1000mL volumetric flask and diluting up to the mark **EPA basedon standard methods**. O'Dell,1993

Table (3.5): Apparatus and reagents for KPH & samples

Apparatus	**Description**
Wavelength	600 nm
Measurement Mode	Absorbance
Cell	10-mm glass cell

Volumetric flasks, volume 50 mL	Digestion solution
Volumetric flasks, volume 100 mL	Catalyst solution
Volumetric flasks, volume 250 mL	Wash solution, H_2SO_4 20%
Volumetric flasks, volume 100 mL	Potassium Hydrogen Phthalate stock solution (1g/L COD)
Culture tubes 25* 100 mm	Block digestor or oven 150 °C

3.8.2 References (Standards) Solutions Preparation for Calibration Curve

All culture tubes (15 ml) and screw caps should be washed with clean solution before being used to prevent contamination and prepar a series of reference solutions, as follows in Table (3.6) by pipetting suitable volumes of the ($C_8H_5KO_4$) solution in 50mL volumetric flasks and making up the mark with deionized water **EPA based on standard methods** O'Dell,1993and following the steps.

1. Transfer 2.5 mL of the reference solutions to the culture tubes.
2. Addition of 1.5 mL of digestion solution to each of the references and mix thoroughly.
3. Addition 3.5 mL of catalyst solution to each of the references, down the side of the culture tube.
4. Capping tightly and shaking to mix the layers (the mixture becomes hot).
5. Placing the culture tubes in an oven at 150 °C for 2 hours.
6. Cooling and allowing any precipitate to settle.
7. Perform background correction with the blank solution and measure the absorbance of the solutions at 600 nm using the 10mm glass cuvette. Figure (3.6) shows the preparation standard solution after heating, the appendix A shows the calibration curve of the reference's solution.

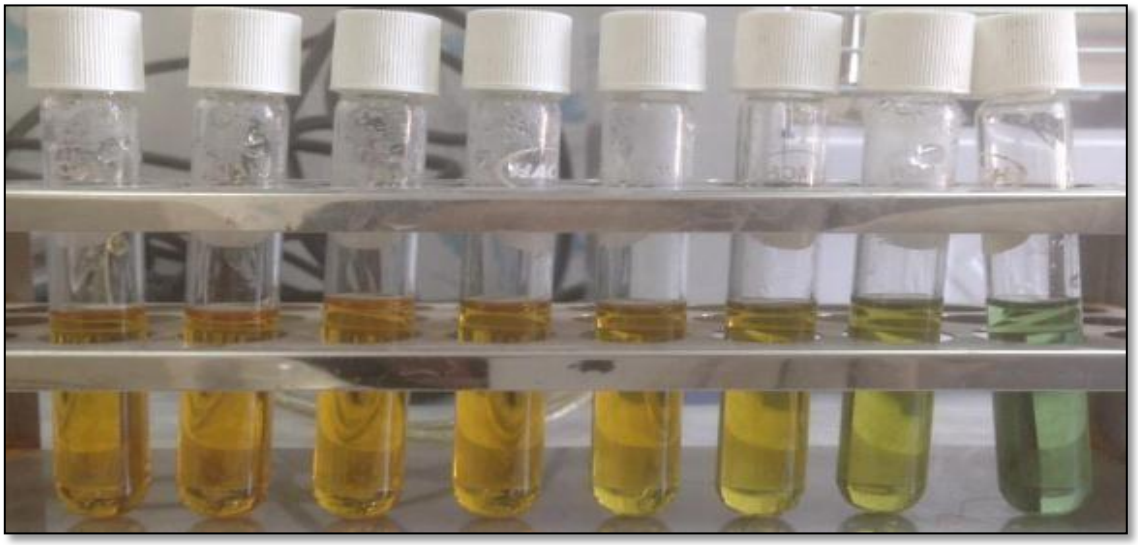

Figure (3.6) Calibration reference solutions during cooling

Table (3.6): Calibration Reference Solutions

	Amount of $C_8H_5KO_4$solution in 50mL Volumetric flasks	Concentration (mg/L) COD
Blank (deionized H_2O)	…	0
Reference 1	1 mL in 49 mL deionized water	20
Reference 2	2.5mL in 47.9 mL deionized water	50
Reference 3	5 mL in 45 mL deionized water	100
Reference 4	10 mL in 40 mL deionized water	200
Reference 5	20 mL in 30 mL deionized water	400
Reference 6	30 mL in 20 mL deionized water	600
Reference 7	45mL in 5 mL deionized water	900

3.9 UV-Spectrophotometer Measuring Method

The concentration of the COD determined by using the (Double Beam Spectrophotometer 6800 Jenway) Figure (3.7)

- Start the device and leave it for 20 minutes to complete the preparation and run the application program from the computer.
- The cuvettes should be cleaned clearly with distilled water then acetone.
- Select the calibration curve estimation mode, set the wavelength to 600 nm (one wavelength) and enter the standard concentration from 0 to 900 ppm.
- Auto zero the instrument with the blank sample then measuring the concentration for the standards samples by using the cuvettes.
- For sample measurements, we followed the same previous step.

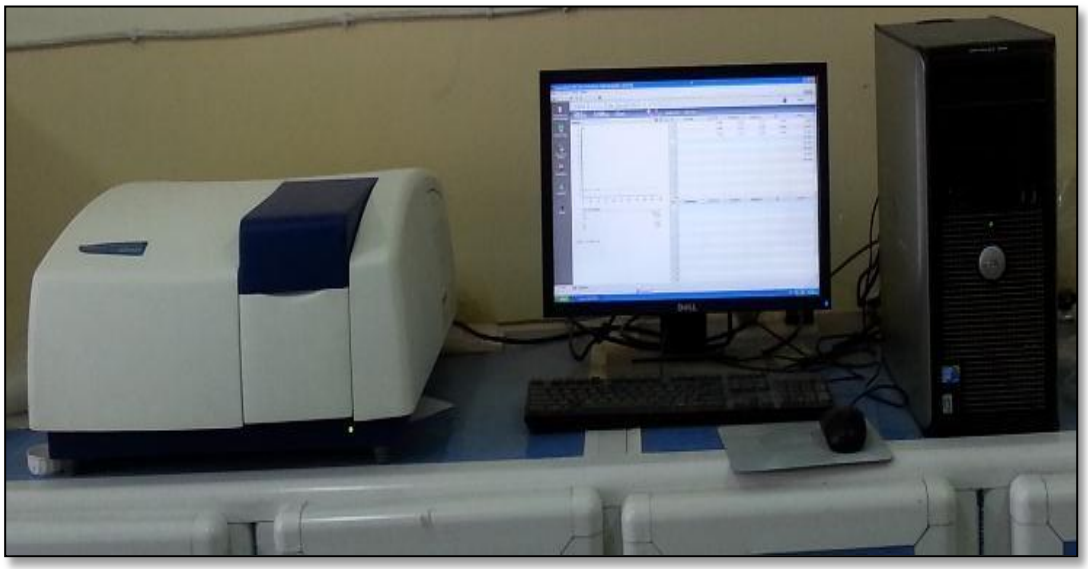

Figure (3.7) System of measurement absorbance by Double Beam Spectrophotometer 6800

4 Chapter four

RESULTS AND DISCUSSION

Aqeel Talib

Chapter Four
Results And Discussion

4.1 Background

Most studies of oily wastewater treatment are based on separate electrocoagulation, and electroflotation processes, with electrocoagulation carried out in one electrochemical reactor, and electroflotation in another, [Jiménez et al., 2016].

An integrated electrochemical treatment for oily wastewater reclamation is provided in this study, which includes the hybrid EC/EF process, using a dissolution aluminum electrode in a well-designed continuous electrochemical reactor was executed [Mazumder et al, 2020].

The experiments were conducted using synthetic wastewater to find the efficiency of demulsification of oily wastewater in accordance with COD removal efficiency. To find the optimum conditions of demulsification process, several parameters such as current density i (mA/cm^2), initial O/W emulsion concentration C_o (ppm), and O/W emulsion flow rate Q (L/hr), with constant 12 V applied potential, and a constant electrode gap of 1cm. All experiments were done at atmospheric pressure, and 30 temperature.

For the majority of experiments, other parameters such as turbidity, TSS, TDS, and pH were measured in order to explain the mechanism of demulsification. A comparison of the Al-Al, and Al-C felt electrode pairs revealed that theAl-C felt electrodes achieved the highest COD removal, and demulsification efficiencies, but required a higher current density to maintain the same efficiency, and thus additional power consumption. Decreases in O/W emulsion flow rate had a positive effect on COD removal, whereas increasesin initial O/W concentration had a negative effect [Mazumder et al, 2020].

4.2 Al-Al Electrode Material

Two pairs of electrodes have been used for most of the experiments, Al- Al electrode pair, and the Al-Carbon felt electrode pair. The efficiency of the EC/EF process was primarily assessed by monitoring DOC. The efficiency of DOC removal was expressed as:

$$COD \text{ Removal } (\%) = \frac{COD_{(t=0)} - COD_t}{COD_{(t=0)}} \times 100$$

4.2.1 Influence of Current Density

The effect of current density (*i*) on COD removal efficiency with an initial O/W concentration of 100 ppm (C_o equal 1108 mg/L) is shown in Figures (4.1- 4.9). Results gave a reasonable demulsification efficiencies (COD removal efficiency) for current densities of 10, 20, and 30 mA/cm^2. The results data are given in appendix B, Table (B.1).

After 20 minutes of treatment (effective removal period). Results revealed that the COD removal efficiencies of 50.36,63.89,79.96%, for 2 L/hr emulsion flowrate, and 39.16, 52.88,75.63%, for 4 L/hr, and were 36.55, 47.78, 71.11%, for 6L/hr, respectively.

At the total treatment time (120 min), the EC/EF results of the O/W treatment showed that the current density had a significant effect on COD removal efficiency, The improved COD removal efficiency increases with increasing current density of 10-20-30mA/cm^2 significantly In fact, these observations are largely in agreement with previous investigations by [Panizza & Cerisola, 2010], [Rocha et al., 2012]. Using O/W emulsion with an initial concentration of 100ppm, and a volumetric flow rate of 2 L/hr, Figure (4-1) shows the COD removal efficiency with time at various current densities. It was obvious that increasing current density led to a higher final COD removal efficiency of contaminants.

This may be explained by the fact that when current density rises, the rate of anodic dissolution of aluminum rises due to the formation, and release of Al^{3+}on the anode's surface. Resulting in a greater amount of coagulant, and flocs formation. As a result, the removal of organics has become more efficient[Mazumder et al, 2020].

Furthermore, increasing current density reduces bubble size while increasing bubble formation rate, resulting in better efficiency of organics removal by H_2 flotation along with the coagulation effect, and the formation of flocs, as previous studies have made similar observations [Song et al., 2008].

Figures (4.4-4.6) shows the COD removal efficiency with the effect of different current densities after 20 minutes of treatment with an initial concentration of 200 ppm of O/W emulsion and flow rates of emulsion of 2, 4 and 6 L/hr. The results indicated that the COD removal efficiency of 37.36,50.08and 67.17% were obtained for 2 L/hr, the COD removal efficiency of 17.79,43.59,and 56.93% were obtained for 4 L/hr, and the COD removal efficiency of 5.33,11.12 and 47.46 %were obtained for 6 L/hr O/W flow rates.

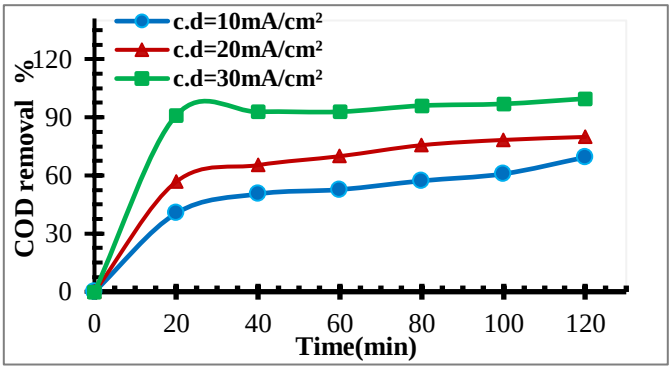

Figure (4.1) Influence of current density on COD removal efficiency during EC/EF of oily wastewater treatment, Al-Al electrode; initial O/W conc. **100** ppm, volumetric flow rate **2** L/hr.

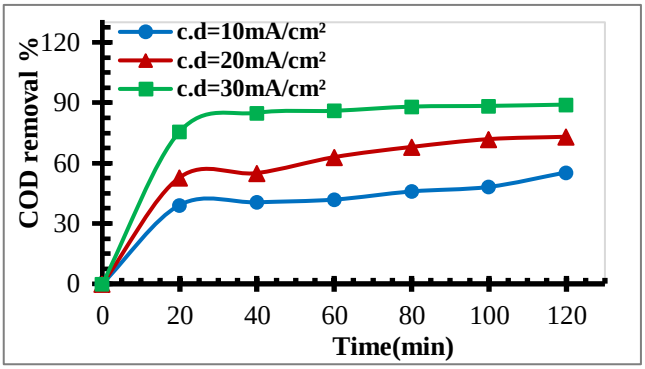

Figure (4.2) Influence of current density on COD removal efficiency during EC/EF of oily wastewater treatment, Al-Al electrode; initial O/W conc. **100** ppm, volumetric flow rate **4** L/hr.

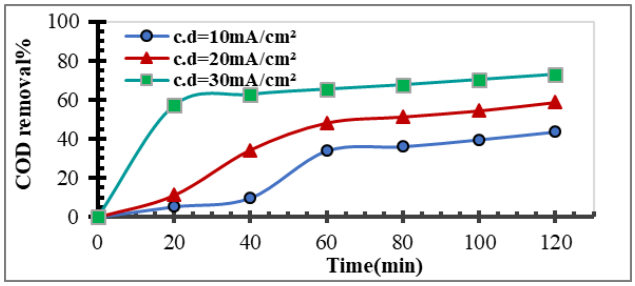

Figure (4.3) Influence of current density on COD removal efficiency during EC/EF of oily wastewater treatment, Al-Al electrode; initial O/W conc. **100** ppm, volumetric flow rate **6** L/hr.

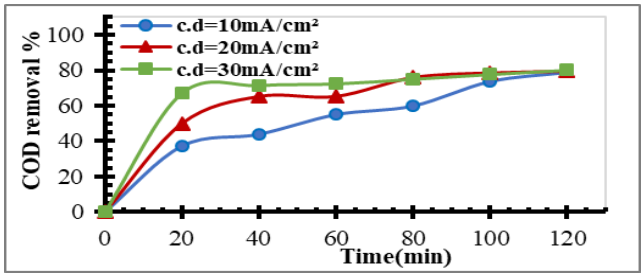

Figure (4.4) Influence of current density on COD removal efficiency during EC/EF of oily wastewater treatment, Al-Al electrode; initial O/W conc. **200** ppm, volumetric flow rate **2** L/hr.

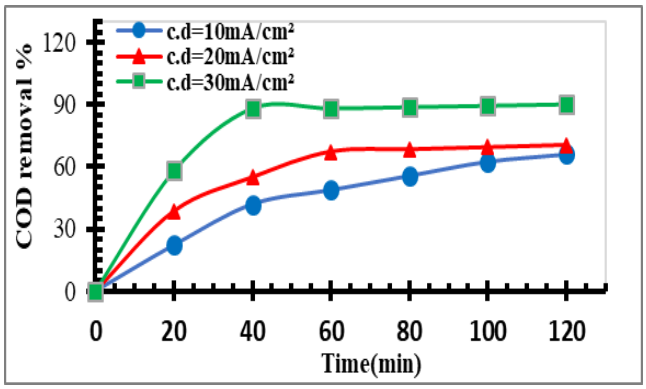

Figure (4.5) Influence of current density on COD removal efficiency during EC/EF of oily wastewater treatment, Al- Al electrode; initial O/W conc.**200** ppm; volumetric flow rate **4** L/hr.

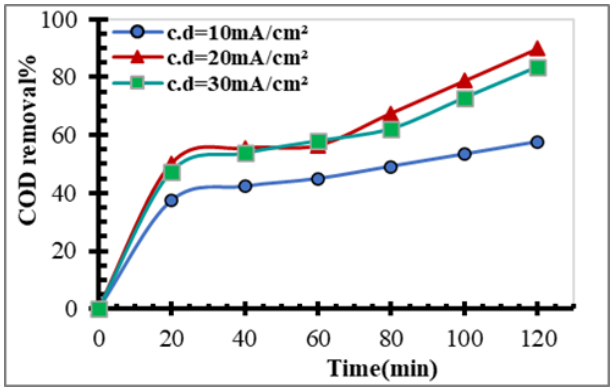

Figure (4.6) Influence of current density on COD removal efficiency during EC/EF of oily wastewater treatment, Al-Al electrode; initial O/W conc. 2**00** ppm; volumetric flow rate **6** Lt/hr

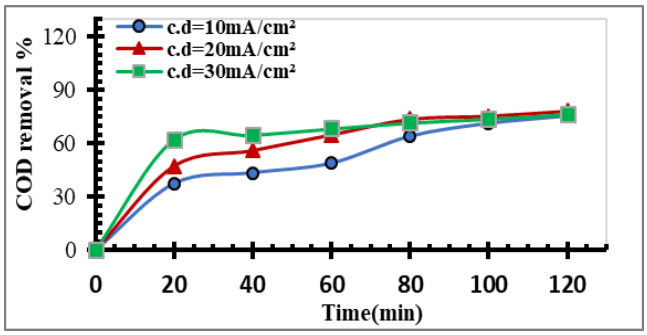

Figure (4.7) Influence of current density on COD removal efficiency during EC/EF of oily wastewater treatment, Al-Al electrode; initial O/W conc. 3**00** ppm; volumetric flow rate **2** Lt/hr

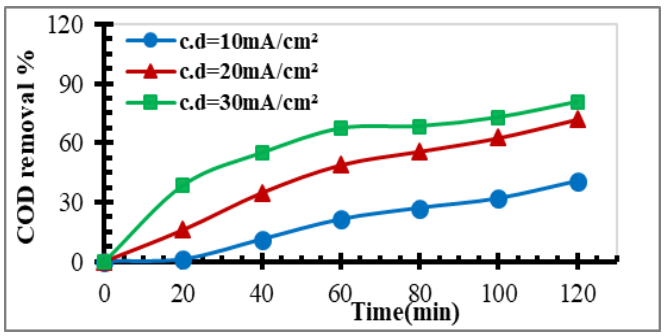

Figure (4.8) Influence of current density on COD removal efficiency during EC/EF of oily wastewater treatment, Al-Al electrode; initial O/W conc. 3**00** ppm; volumetric flow rate **4** Lt/hr

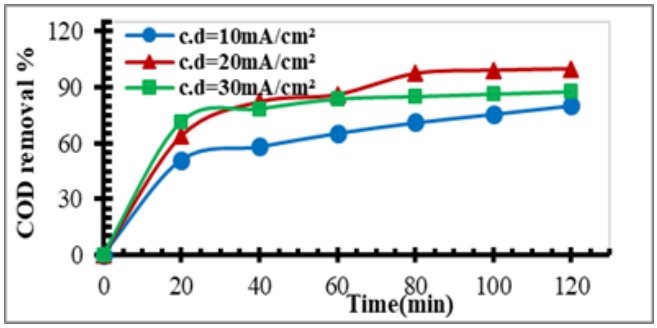

Figure (4-9) Influence of current density on COD removal efficiency during EC/EF of oily wastewater treatment, Al-Al electrode; initial O/W conc. 3**00** ppm; volumetric flow rate **6** L/hr.

Also, Figures (4.7 - 4.9) shows the effective removal occurs in the first period of the treatment(20minutes), the effect of current density on the COD removal efficiency at different current densities after 20 minutes of treatment with an initial O/W concentration 300 ppm (C_o equal to 1141 mg/L) and for O/W emulsion flow rates of 2, 4 and 6 L/hr. The COD removal efficiency were 37.5,47.41 and 62.31%, for 2 L/hr flowrate, and 33.21,51and 61.6% for 4 L/hr and for 6 L/hr, were 1.05,11.12 and 38.51%, respectively.

Frequently, the COD removal efficiency is sharp at the start of the electrocoagulation/electroflotation process, and is increased on a regular basis for more than 20 minutes, then it gradually declines to approach equilibrium. Furthermore, the increase in current density induces an increase in the coagulant formation rate.

At galvanostatic condition where a constant current density is applied, the hydrogen gas evolution increased proportionally with current. On the other hand, a higher H_2 gas bubbles evolutionimproves hydrodynamics of EC/EF by increasing the mass transfer, and the collision rates between coagulant, and oil droplets. The removal of pollutants has become more efficient by H_2 flotation, which it becomes more efficient along with the coagulation effect. So, increasing current density decreases thesize of bubble while boosting the pace

of bubble creation, and this is what theresearchers has explained [Esfandyari et al.,2015] & [Song et al., 2008].

4.2.2 Influence of Emulsion Flow rate

Increasing the O/W emulsion flow rate reduces the hydraulic residence time, and facilitates the possibility for oil droplets to interact with gas bubbles. As a result, optimal O/W emulsion flow rates at constant current densities must be considered in order to keep O/W emulsion concentrations in effluent streams within allowable limits.

Because of the large amount of O/W in the refinery wastewater industry, the treatment procedure must be accelerated, and intensified. A system that performs under continuous flow, and does not require frequent electrode substitution is needed. Despite this expanding industrial need, there are few investigations in the literature employing EC/EF for O/W water treatment in continuous flow, and with a mechanism to enhance electrode durability. This research is evaluated the usage of a cuboid electrocoagulation/electroflotation reactor working in the continuous regime in the synthetic oily wastewater treatment of crude oil emulsified in water. This is consistent with the authors' assessment [Shonza et al., 2020].

The results show that COD removal efficiency from O/W emulsion by EC/EF treatment increased with decreasing flow rate at constant current density. So, the effect of emulsion flow rate at any constant current density was more pronounced at the lowest emulsion flow rate. The results data are given in appendix B, Table (B.1)

The effect of increasing flow rate on decay COD removal efficiency ratio is shown in the Figures (4.10- 4.12), using Al-Al electrodes, 100 ppm initial O/W concentration of O/W emulsion, and current density of 10,20,30 mA/cm^2,

respectively. It can be seen that increasing the emulsion flow rate from 2 to 4, then 6 L/h leads to a decrease in COD removal efficiency.

At a current density of 10 mA/cm^2, and a minimum flow rate of 2L/hr, the total COD removal efficiency increased from 50.36% after 20 min to 69.40% at the end of the treatment time (120 minutes). While, by increasing the flow rate to 4 L/hour, the COD removal efficiency increased from 39.16% to 55.4%. Moreover, if the emulsion flow rate increased to 6 L/hr, the COD removal efficiency increased from 36.55% after 20 minutes to 45.39% for the same current density.

The above results clearly show that most decrease in COD removal efficiency was occurred during the period of 20-30 minutes in all demulsification experiments with flow rates (2, 4, 6 L/hr) where the COD removal efficiency of estimated to be 50.36%,39.16 and 36.55%, respectively.

The results showed that the COD removal efficiency at a current density of 20 mA / cm^2 and flow rate of 2, 4 and 6 L/hr were increased from 63.89% during the period of 20 minutes to 78.97% at the end of the treatment time (120 minutes). However, the COD removal efficiency increased from 52.88-73.10% and 47.78-62.22% for a change of flowrate from 4-6 L/hr, respectively.

Moreover, the results showed that the COD removal efficiency at a current density of 30 mA / cm^2 and flow rate of 2, 4 and 6 L/hr were increased from 79.96% to 96.93% at the end of the treatment time for2 L/hr flow rate. However, the COD removal efficiency increased from 75.63% to 89.07% and 71.11% to 84.11%for a change of flowrate from4-6 L/hr, respectively.

The above results of 30 mA / cm^2 clearly show that most decrease in COD removal efficiency was occurred with flow rates (2, 4, 6 L/hr) where the COD removal efficiency of estimated to be 96.93, 89.07 and 84.11%, respectively.

Similarly, for initial O/W concentration of 200 ppm the results showed in Figure (4.13- 4.15). At a current density of 10 mA/cm^2, and a minimum flow rate of 2 L/hr, the COD removal efficiency increased from 37.36% after 20 min to 79% at the end of the treatment time 120 min. While, by increasing the flow rate to 4 L/hr, the COD removal efficiency increased from 17.79% to 57.6%. Moreover, if the emulsion flow rate increased to 6 L/hr, the COD removal efficiency increased from 5.33 % after 20 min to 43.5% for the same current density.

The results showed that the COD removal efficiency at a current density of 20 mA / cm^2 and flow rate of 2, 4 and 6 L/hr were increased from 50.08% to 79.35% at the end treatment time of the 2L/hr flow rate. However, the COD removal efficiency increased from 43.6-73.3% and 16.03-63.43% for a change of flowrate from 4-6 L/hr, respectively. The above results of 20 mA / cm^2 clearly show that most decrease in COD removal efficiency was occurred with flow rates (2, 4, 6 L/hr) where the COD removal efficiency of estimated to be 79.35,73.3 and 63.43%, respectively

Moreover, the results showed that the COD removal efficiency at a current density of 30 mA / cm^2 and flow rate of 2, 4 and 6 L/hr were increased from 67.17% to 80.24%at the end of the treatment time. However, the COD removal efficiency increased from 56.9% to 74.19.9% and 47.46% to 66.37% for a change of flowrate from 4-6 L/hr, respectively.

Figures (4.16-4.18) showed the results of the COD removal efficiency for 300 ppm initial O/W concentration. At current density of 10 mA/cm^2 and O/W emulsion flow rates of 2, 4 and 6 L/hr ,the results of the COD removal efficiency increase from 37.51 -75.28% after 20 min,33.2 – 73.7 % and 1.05-40.49%, at the total treatment time.

Also the results in Figure (4.17) showed that the COD removal efficiency at a current density of 20 mA / cm^2 and flow rate of 2, 4 and 6 L/hr were increased

from 47.41% after 20 minutes to 78.267% at the end of the treatment time (120 minutes). However, the COD removal efficiency increased from 51-80.36% and 11.12-60.49% for a change of flowrate from 4-6 L/hr, respectively.

Moreover, the results in Figure (4.18) showed that the COD removal efficiency at a current density of 30 mA / cm^2 and flow rate of 2, 4 and 6 L/hr were decreased from 87.81% for 2 L/hr O/W emulsion flow rate to 80.54% for 4 L/hr O/W emulsion flow rate and 76.5 % for 6 L/hr O/W emulsion flow rate, respectively. This is consistent with the researcher's investigation [Tir & Moulai-Mostefa, 2008].

However, higher operating current density resulted in better removal efficiency, but higher emulsion flow rates required in lower COD removal efficiency since the emulsion residence time in the active reactor volume was shorter, as noted by other researchers [Mohora et al.,2012].

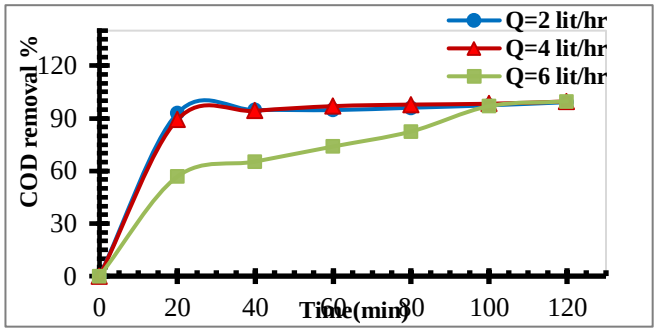

Figure (4-10) COD removal efficiency vs time with different O/W emulsion flow rates, **100** ppm O/W. Al-Al electrodes, current density **10** mA/cm^2.

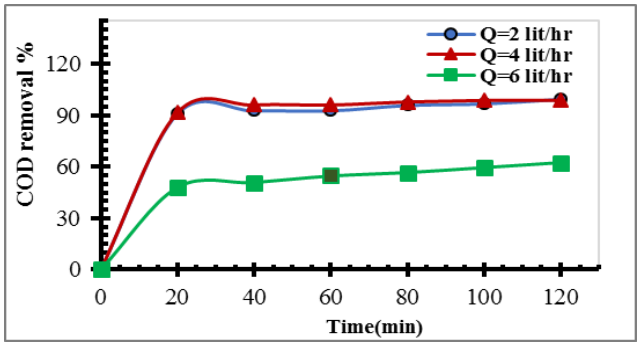

Figure (4-11) COD removal efficiency vs time with different O/W emulsion flow rates, **100** ppm O/W. Al-Al electrodes, current density **20** mA/cm^2.

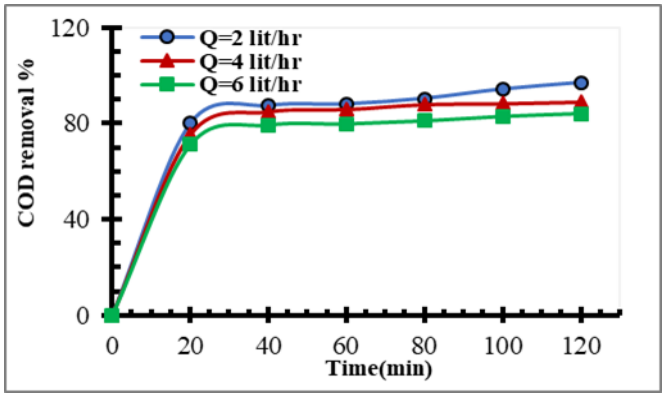

Figure (4-12) COD removal efficiency vs time with different O/W emulsion flow rates **100** ppm O/W. Al- Al electrodes, current density **30** mA/cm^2

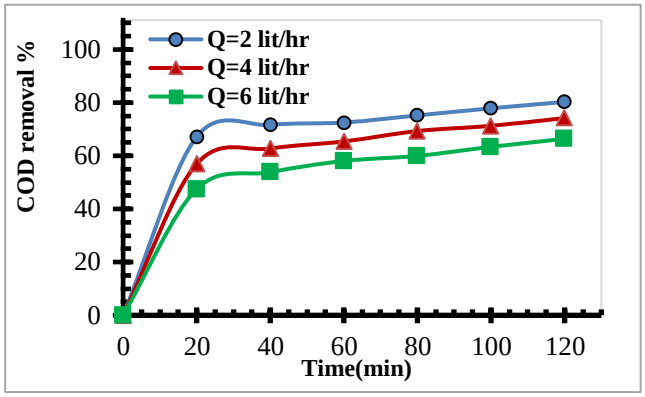

Figure (4-13) COD removal efficiency vs time with different O/W emulsion flow rates **200** ppm O/W. Al- Al electrodes, current density **10** mA/cm^2.

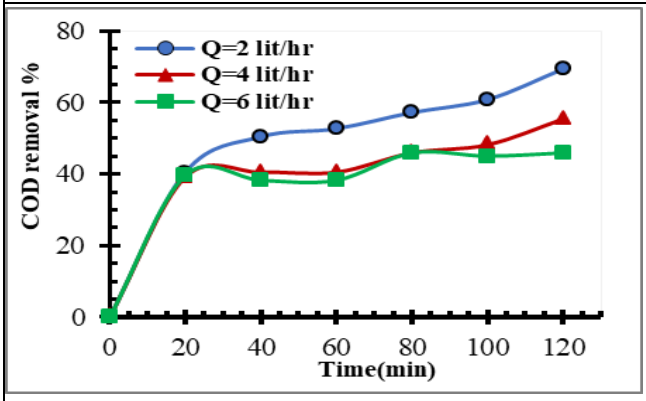

Figure (4-14) COD removal efficiency vs time with different O/W emulsion flow rates **200** ppm O/W. Al-Al electrodes, current density **20** mA/cm^2

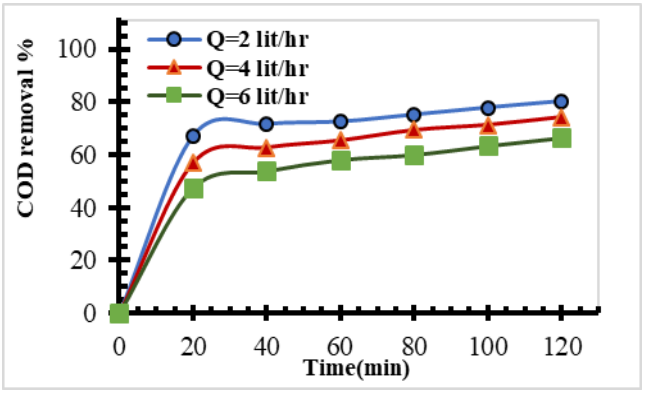

Figure (4-15) COD removal efficiency vs time with different O/W emulsion flow rates **200** ppm O/W. Al- Al electrodes, current density **30** mA/cm^2 .

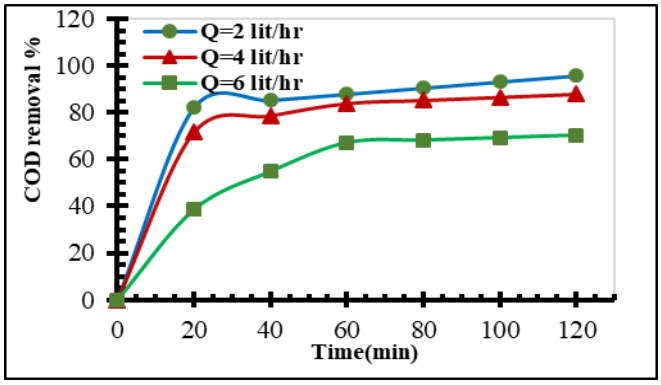

Figure (4-16) COD removal efficiency vs time with different O/W emulsion flow rates **300** ppm O/W. Al-Al electrodes, current density **10** mA/cm^2.

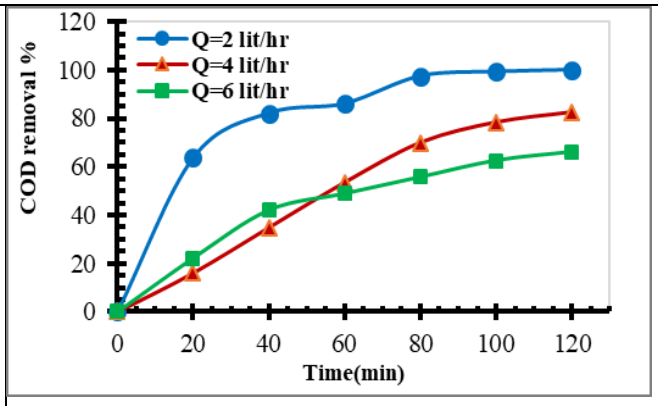

Figure (4-17) COD removal efficiency vs time with different O/W emulsion flow rates **300** ppm O/W. Al-Al electrodes, current density **20** mA/cm^2 .

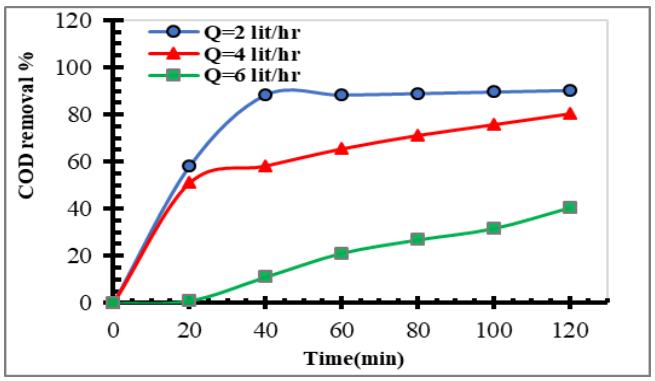

Figure (4-18) COD removal efficiency vs time with different O/W emulsion flow rates **300** ppm O/W. Al-Al electrodes, current density **30** mA/cm^2 .

4.2.3 Influence of Initial O/W Emulsion Concentration

The effect of increasing initial O/W emulsion concentrations on decay COD removal efficiency is shown in Figures (4.19-4.27). Results gave reasonable demulsification efficiencies (COD removal efficiency) with different initial O/W emulsion concentration (100,200, and 300 ppm) for each Figure, the results data are given in appendix B, Table (B.1).

Figures (4.19 - 4.21) shows the COD Removal efficiency with the effect of increase an initial O/W emulsion concentration (100,200, and 300 ppm) for 10

mA/cm^2 current density with O/W flow rate 2, 4 and 6 L/hr. The COD removal efficiency decreased with increase the initial O/W emulsion concentration were 79, 75.28 and 69.4%, for 2 L/hr O/W emulsion flow rate , the COD removal efficiency were73.7,57.6 and 55.4% for 4 L/hr O/W emulsion flow rate , the COD removal efficiency were 45.93, 43.5 and 40.49 for 6 L/hr O/W flow rate, respectively.

Also Figures (4.22 - 4.24) shows the COD Removal efficiency with the effect of increase an initial O/W emulsion concentration (100,200, and 300 ppm) for 20 mA/cm^2 current density with O/W flow rate 2, 4 and 6 L/hr. The COD removal efficiency decreased with increase the initial O/W emulsion concentration were 79.53, 78.98 and 78.26 %, for 2 L/hr O/W emulsion flow rate , the COD removal efficiency were 80.36, 73.33 and 73.1% for 4 L/hr O/W emulsion flow rate , the COD removal efficiency were 63.43, 62.22 and 60.49 for 6 L/hr O/W flow rate, respectively.

Similarly, Figures (4.25 - 4.27) shows the COD Removal efficiency with the effect of increase an initial O/W emulsion concentration (100,200, and 300 ppm) for 30 mA/cm^2 current density with O/W flow rate to the treatment reactor 2, 4 and 6 L/hr. The COD removal efficiency decreased with increase the initial O/W emulsion concentration were 96.93,80.24 and 76.51%, for 2 L/hr O/W emulsion flow rate, the COD removal efficiency were 89.07, 87.81 and 74.19% for 4 L/hr O/W emulsion flow rate, the COD removal efficiency were 84.11,80.54 and 66.37 for 6 L/hr O/W emulsion flow rate, respectively. From the above results it appears very clearly that the efficiency of demulsification is directly proportional to the residence time of the emulsion in reactor (low O/Wemulsion flow rate), also, the COD removal efficiency is directly proportional to the increase in current density applied, while it is inversely proportional to the increase in the concentration of the initial O/W emulsion concentration.

One can remark, that the COD removal efficiency at various O/W emulsion concentrations is influenced not only by oil droplet coalescence mechanism, but also by the capacity of electrocoagulation (EC).). The results data of drop size are given in appendix E, Table (E.1).

The decomposition of oil droplets resulting from anode dissolution is particularly effective at low oil concentrations. Less efficient breakdown of oil droplets can occur with higher emulsion O/W concentration. Hence, EC process isless effective at emulsion O/W concentrations o4ver 100 ppm, this finding was largely agreed with another researcher [Dermentzis et al.,2014], [Xu & Zhu, 2004]

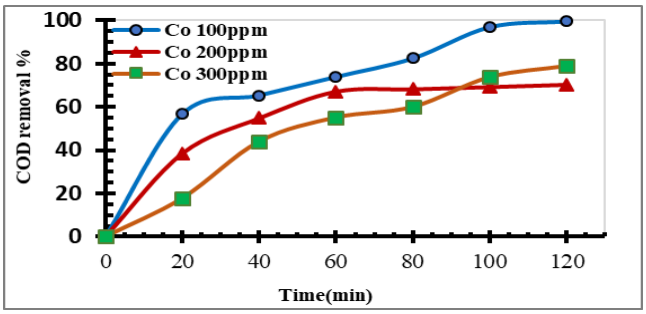

Figure (4-19) COD removal efficiency vs Time with different concentrations of O/W (a) Al-Al electrode, current density **10** mA/cm^2, volumetric flow rate **2**L/hr.

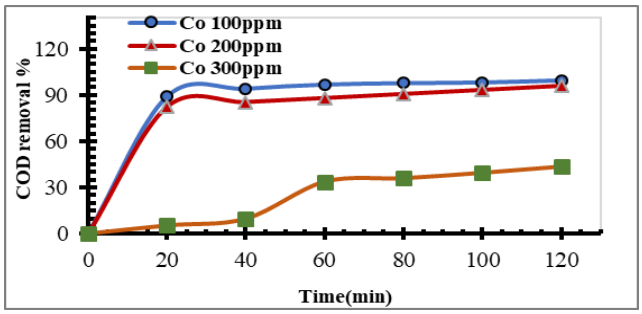

Figure (4-20) COD removal efficiency vs Time with different concentrations of O/W (a) Al-Al electrode, current density **10** mA/cm^2, volumetric flow rate **4**L/hr

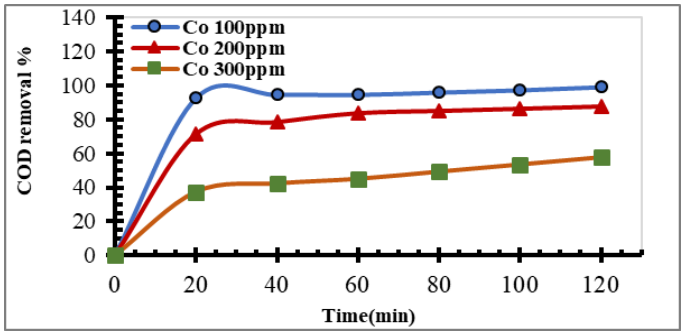

Figure (4-21) COD removal efficiency vs Time with different concentrations of O/W (a) Al-Al electrode, current density **10** mA/cm^2, volumetric flow rate **6**L/hr

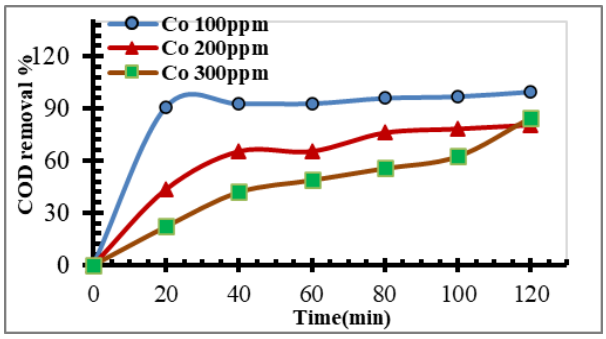

Figure (4-22) COD removal efficiency vs Time with different concentrations of O/W (a) Al-Al electrode, current density **20** mA/cm^2, volumetric flow rate **2**L/hr

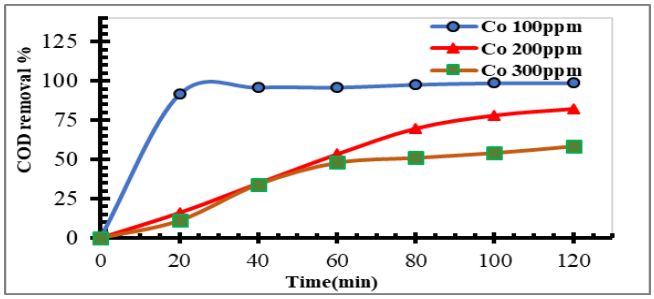

Figure (4-23) COD removal efficiency vs Time with different concentrations of O/W (a) Al-Al electrode, current density **20** mA/cm^2, volumetric flow rate **4**L/hr.

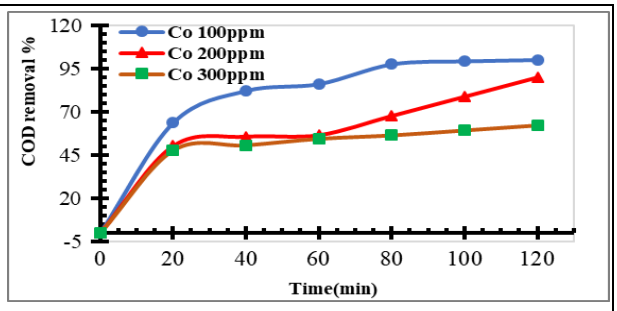

Figure (4-24) COD removal efficiency vs Time with different concentrations of O/W (a) Al-Al electrode, current density **20** mA/cm^2, volumetric flow rate **6**L/hr.

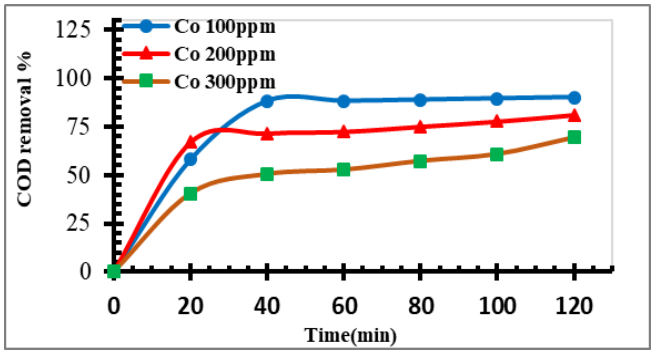

Figure (4-25) COD removal efficiency vs Time with different concentrations of O/W (a) Al-Al electrode, current density **30** mA/cm^2, volumetric flowrate **2**L/hr.

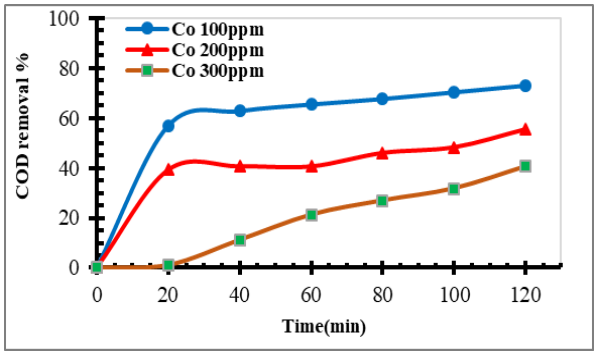

Figure (4-26) COD removal efficiency vs Time with different concentrations of O/W (a) Al-Al electrode, current density **30** mA/cm^2, volumetric flowrate **4**L/hr.

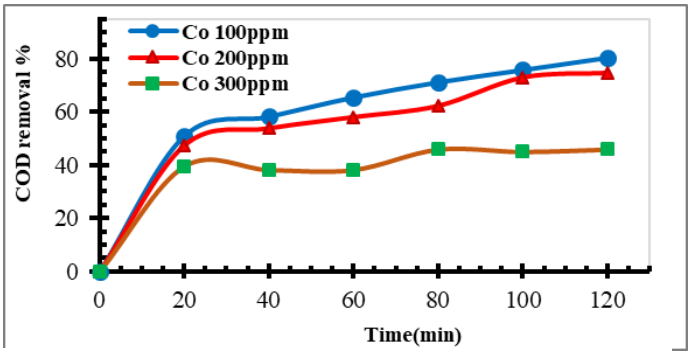

Figure (4-27) COD removal efficiency vs Time with different concentrations of O/W (a) Al-Al electrode, current density **30** mA/cm^2, volumetric flowrate **6**L/hr.

4.2.4 Current efficiency Variation

The current efficiency (CE) values are often more than 100%, especially at low current density, for example, 10 mA/cm^2 for hybrid EC/EF processes due to the ease of sacrifice aluminum electrode, and its transformation into ions because the working or applied voltage is much higher than that of standard aluminum charge,noting that CE here is calculated based on the concentration of metal ions. The Current efficiency Variation was expressed as:-

$$\text{The Currant Efficiency } \emptyset\ (\%) = \frac{(\Delta m_{exp}/\Delta t)}{(\Delta m_{th}/\Delta t)} \times 100 = \frac{C_{exp}}{C_{th}} \times 100$$

$$\text{were} \quad \boldsymbol{C_{exp} = \frac{1}{Q}\frac{\Delta m}{\Delta t}} \quad \text{„} \ \boldsymbol{C_{theor} = \frac{(\Delta m_{th}/\Delta t)}{Q} = \frac{M}{Q}\frac{I}{zF}}$$

In this expression, **M** is the molar mass of the metal, I is current, z is the number of electrons transferred, **F** is Faraday's constant and **Q** is the inlet volumetric flow rate of the liquid phase. The experimental mass loss of the electrodes per unit of time (**Δm/Δt**) was derived from a mass balance on Al species and measured in the form of experimental concentration ($\mathbf{C_{exp}}$) at the outlet of the EC cell.

$\mathbf{M_{Al}}$=26.9815386 (g/mol), **Δm**=(g), **Δt=**2 hr time of experiment, **Q=** (L/hr), **Z=3,F**=96485.332(As/mol)=26.80148(Ahr/mol),**zF=**80.40444(Ahr/mol**).**

$\mathbf{C}_{exp}$= (**Δm**/2**Q**) , $\mathbf{C}_{thor}$= (26.80148***I**) / (80.40444***Q**)

In addition, the increase in the current density led to a decrease in the current efficiency, and the process was said to be controlled by mass transfer. However, at a low current density of 10 mAcm^{-2} the CE was higher or equal to 100%, and the hybridization process is said to be kinetic control. It can be assumed that higher current density leads to lower current efficiency because side reactions such as (electrolyte breakdown involving O_2, and H_2 evolution) will be improved, while

these interactions have a detrimental effect on the overall currentefficiency, and this behavior seems to agree with the researchers [Chen, (2004) , and Rodrigo et al., (2001)].

The results in Figure (4.28–4.33), show the current efficiency (CE) variation against the O/W emulsion flow rate of EC/EF of petroleum refinery wastewater demulsification under different conditions of current densities (10,20, and 30 mA/cm^2) , and initial O/W concentrations (100, 200 , and 300 ppm).

It was noted that the efficiency of the current reaches more than 100% in some circumstances, it is possible that there will be major side reactions such as the generation of oxygen on the anode electrode and hydrogen, since the applied voltage is much higher than the electrode voltage, oxygen and nitrogen, So we found $\mathbf{C}_{exp}$ higher than $\mathbf{C}_{thor}$, this behavior seems to agree with the researchers [Guinea et al 2010].

The difference in a current efficiency (CE) against the increase in an O/W emulsion flow rate of 2.4, and 6 L/hr shown in Figure (4.28). The results data are given in appendix B, Table (B.3).

For 100ppm initial O/W concentrations, the applied current density was 10 mA/cm2, it is illustrated in Figure (4.28), where it was 126%, 126.48%, and 135. 72%, respectively. Also, values of the current efficiency at current density of 20 mA/cm2 are illustrated in the same Figure: 120.75%, 120.15% , and 205.5%, respectively.

As for the current density of 30 mA/cm2, shown in the same Figure, in which the current efficiency values were 126.96%,147.24% , and 143%, respectively.

For 200ppm initial O/W concentration, and for 10 mA/cm2 current density, Figure (4.29) shows the variation in a current efficiency (CE)values against the increases of an O/W emulsion flow rate of 2.4 , and 6 L/hr were: 114%,285% , and 27%, respectively. For 20 mA/cm2 current density, a current efficiency (CE)value was: 120.06%, 116.4%, and183.6%, respectively. For 30 mA/cm2 current density,

a current efficiency (CE) were: 119.88%, 125.22%, and 117.06%, respectively.

For 300ppm initial O/W concentration, and for 10 mA/cm2 current density, Figure (4.30) show the difference in a current efficiency (CE)values against the increase in an O/W emulsion flow rate of 2,4, and 6 L/hr were: 48.69%, 131.88%, and170.52, respectively. For 20 mA/cm2 current density, a current efficiency (CE)values were: 85.26%, 164.97%, and64.2% respectively. For 30 mA/cm2 current density, a current efficiency (CE)value was: 124.22%,117.5%, and117.5, respectively.

Similarly, Figures (4.31-4.33) show the influence of current efficiency variation verses volumetric O/Wemulsion flow rate under different initial O/W concentration (100,200 and300 ppm), under different current density (10,20, and 30 mA/cm2).

Figure (4-31) show variation of current efficiency verses volumetric O/W emulsion flow rate as a function of initial O/W concentration, and 10 mA/cm2 current density during 120 minutes of EC/EF method of petroleum oily wastewater demulsification.

For 100ppm initial O/W concentration and 10 mA/cm2, current efficiency were; 126% at 2L/hr,126.48% at 4L/hr and 135.72% at 6L/hr, respectively. For 200ppm initial O/W concentration and 10 mA/cm2, current efficiency were; 114% at 2 L/hr,285% at 4L/hr and 27% at 6L/hr, respectively. For 300ppm initial O/W concentration and 10 mA/cm2, current efficiency were; 48.69% at 2L/hr,131.88% at 4L/hr and 170.52% at 6L/hr, respectively.

Figure (4-32) shows the variation of current efficiency verses volumetric flow rate as a function of initial O/W concentration and 20 mA/cm2 current density during 120 minutes of EC/EF method of petroleum oily wastewater demulsification.

For 100ppm initial O/W concentration, and 20 mA/cm2, current efficiency were; 120.75% at 2 L/hr,120.15% at 4L/hr, and 205.5% at 6L/hr, respectively. For 200ppm initial O/W concentration, and 20 mA/cm2, current efficiency were:

120.06% at 2 L/hr, 116.4% at 4L/hr, and 183.6% at 6L/hr, respectively. For 300ppm initial O/W concentration, and 20 mA/cm2, current efficiency were; 85.26% at 2 L/hr, 164.97% at 4L/hr, and 64.2% at 6L/hr, respectively.

Figure (4-33) show variation of current efficiency verses volumetric flow rate as a function of initial O/W concentration, and 30 mA/cm2 current density during 120 minutes of EC/EF method of petroleum oily wastewater demulsification.

For 100ppm initial O/W concentration, and 30 mA/cm2, current efficiency were; 126.96% at 2L/hr,14.24% at 4L/hr, and 143% at 6L/hr, respectively. For 200ppm initial O/W concentration, and 30 mA/cm2, current efficiency were;119.88% at 2 L/hr, 125.22 % at 4L/hr, and 117.06% at 6L/hr, respectively. For 300ppm initial O/W concentration, and 30 mA/cm2, current efficiency were; 124.22% at 2 L/hr, 117.5% at 4L/hr, and 117.5 % at 6L/hr, respectively.

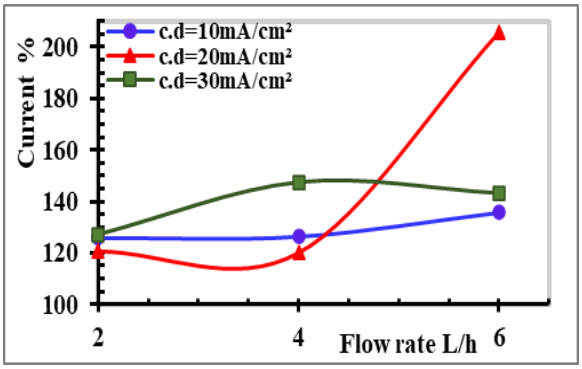

Figure (4-28) Variation of Current efficiency with O/W emulsion flow rate at different current densities, Al-Al electrode; initial O/W concentration 1**00** ppm

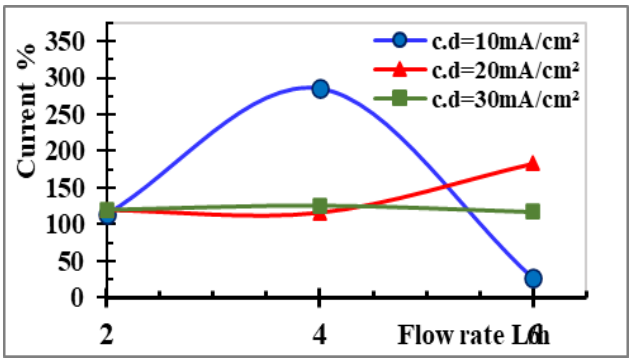

Figure (4-29) Variation of Current efficiency with O/W emulsion flow rate at different current densities, Al-Al electrode; initial O/W concentration **200** ppm

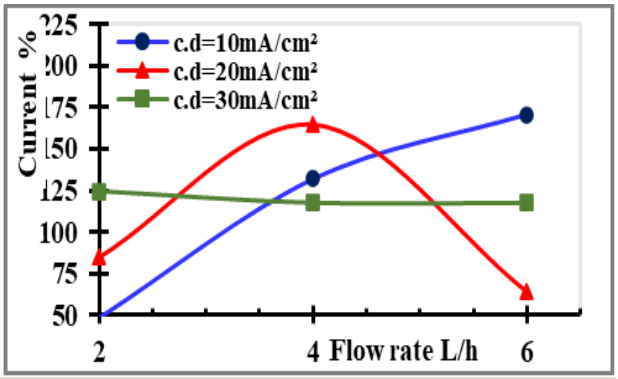

Figure (4-30) Variation of Current efficiency with O/W emulsion flow rate at different current densities, Al-Al electrode; initial O/W concentration **300** ppm.

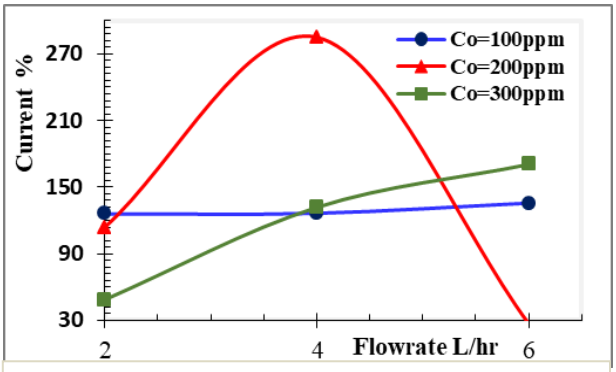

Figure (4-31) Variation of Current efficiency with O/W em ulsion flow rate at different current densities, Al-Al electrode; **10** mA/cm^2 current density

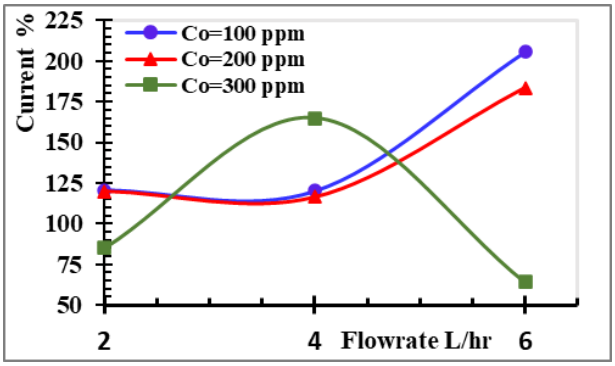

Figure (4-32) Variation of Current efficiency with O/W emulsion flow rate at different current densities, Al-Al electrode; **20** mA/cm^2 current density.

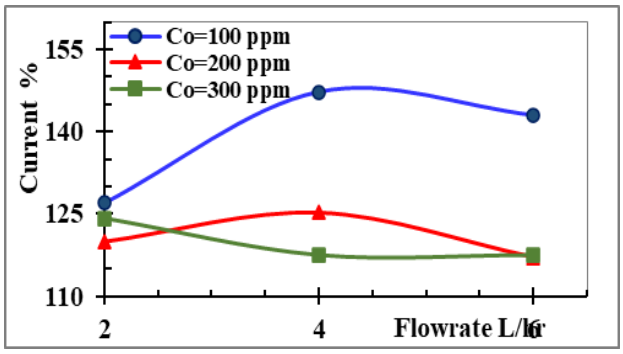

Figure (4-33) Variation of Current efficiency with O/W emulsion flow rate at different current densities, Al-Al electrode; **30** mA/cm^2 current density.

4.2.5 Specific Electrical Energy Consumption

Figures (4.34-4.60) show an important parameter in an oily wastewater treatment reactor using the hybrid electrocoagulation/ electroflotation (EC/EF) method, which is the specific electrical energy consumption (SEEC) versus time. SEEC(kWh/m^3) can be characterized as quantity of used electric energy for each unit volume of electrolyte removed.

Energy consumption, and its cost is one of the most efficient parameters in applying any approach of wastewater treatment, so the consumption of electric energy, and aluminum electrodes consumption are of the highest importance.

The specific electrical energy consumption SEEC($\frac{kWh}{m^3}$)of wastewater pretreated by EC/EF process was calculated as a function of cell potential (V), current intensity (I) and inlet emulsion flow rate (Q) as follows:

$$SEEC\left(\frac{kWh}{m^3}\right) = \frac{V\ I}{Q}$$

To study the effect of SEEC when using aluminum electrodes for different initial O/W concentrations of 100,200, and 300ppm, different current densities 10,20, and 30mA/cm^2, and different O/W emulsion flow rate of 2, 4, and 6 L/hr. The

effect of SEEC is shown in Figure (4.34- 4.36), at 100 ppm initial O/W emulsion concentration and current density of 10, 20, 30 mA/cm^2, respectively. It can be seen that increasing the O/Wemulsion flow rate from 2 to 4, and 6 L/hr leads to a decrease in SEEC.In Figure (4.34), as seen the specific electrical energy consumption was 6.4 kWh/m^3 for 2L/hr O/W emulsion flow rate, the specific electrical energy consumption was 3.55kWh/m^3 at 4L/hr, and 2.32kWh/m^3 when O/W emulsion flow rate rises to 6L/hr, respectively. The results data are given in appendix B, Table (B.2).

For 20 mA/cm^2 current density, with different O/W emulsion flow rate 2,4, and 6L/hr is shown in Figure (4.35). As seen the specific electrical energy consumption was 12.7 kWh/m^3 for 2L/hr O/W emulsion flow rate up to 120 minutes treatment, the specific electrical energy consumption was 6 kWh/m^3 at 4L/hr, and 1.68kWh/m^3 when the flow rate rises to 6L/hr, respectively.

For 100 ppm initial O/W concentration ,30 mA/cm^2 current density, and different O/W flow rate 2,4, and 6L/hr is shown in Figure (4.36). As seen the SEEC value for 2L/hr O/W emulsion flow rate, were 9 kWh/m^3,4.76 kWh/m^3 for 4L/hr O//W emulsion flow rate, and 3kWh/m^3 when the flow rate rises to 6L/hr, respectively.

Similarly, for 200 ppm initial O/W concentration ,10 mA/cm^2 current density, and different O/W flow rate 2,4 , and 6L/hr is shown in Figure (4.37). As seen the SEEC value for 2L/hr O/W emulsion flow rate, was 2.8 kWh/m^3,1.46 kWh/m^3 at 4L/hr, and 0.87kWh/m^3 when the flow rate rises to 6L/hr, respectively.

For 200 ppm initial O/W concentration ,20 mA/cm^2 current density, and different O/W flow rate 2,4, and 6L/hr is shown in Figure (4.38). As seen the SEEC value for 2L/hr O/W emulsion flow rate, were 5.94 kWh/m^3, 3.12kWh/m^3 for 4L/hr O//W emulsion flow rate, and 1.9kWh/m^3 when the flow rate rises to 6L/hr, respectively.

For 200 ppm initial O/W concentration ,30 mA/cm^2 current density, and different O/W flow rate 2,4, and 6L/hr is shown in Figure (4.39). As seen the SEEC value for 2L/hr O/W emulsion flow rate, were 9.05 kWh/m^3, 4.23kWh/m^3 for 4L/hr O//W emulsion flow rate, and 2.97 kWh/m^3 when the flow rate rises to 6L/hr, respectively.

Figure (4.40) show the specific electrical energy consumption with the effect of different flow rate of emulsion of 2, 4 and 6 L/hr of initial concentration of 300 ppm of O/W emulsion and 10 mA/cm^2 current density. The results indicated that the specific electrical energy consumption of 3, 1.62 and 1 kWh/m^3 were obtained for 2 ,4 and 6 L/hr O/W emulsion flowrate, respectively.

Figure (4.41) show the specific electrical energy consumption with the effect of different flow rate of emulsion of 2, 4 and 6 L/hr of initial concentration of 300 ppm of O/W emulsion and 20 mA/cm^2 current density. The results indicated that the specific electrical energy consumption of 5.88, 2.914 and 2.14 kWh/m^{3}were obtained for 2 ,4 and 6 L/hr O/W emulsion flowrate, respectively.

Figure (4.42) show the specific electrical energy consumption with the effect of different flow rate of emulsion of 2, 4 and 6 L/hr of initial concentration of 300 ppm of O/W emulsion and 30 mA/cm^2 current density. The results indicated that the specific electrical energy consumption of 9.22,4.53 and 3.02 kWh/m^{3}were obtained for 2 ,4 and 6 L/hr O/W emulsion flowrate, respectively.

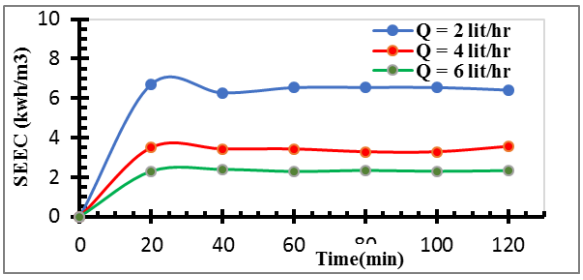

Figure (4.34) Variation of the specific electrical energy consumption SEEC (kwh/m3) with Time atdifferent emulsion flow rates, **100 ppm** initial O/Wemulsion conc., Al-Al electrode, and current density**10mA/cm^2**

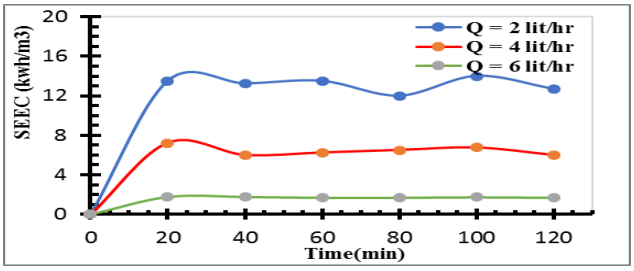

Figure (4.35) Variation of the specific electrical energy consumption SEEC (kwh/m3) vs Time during EC/EF treatment for **100 ppm** initial crude oil concentration of O/W emulsion, Al-Al electrode and current density **20mA/cm^2**

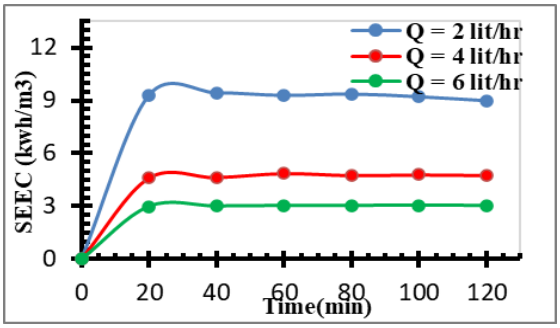

Figure (4.36) Variation of the specific electrical energy consumption SEEC (kwh/m3) vs Time during EC/EFtreatment for **100 ppm** initial crude oil concentrationof O/W emulsion, Al-Al electrode, and current density**30mA/cm^2**

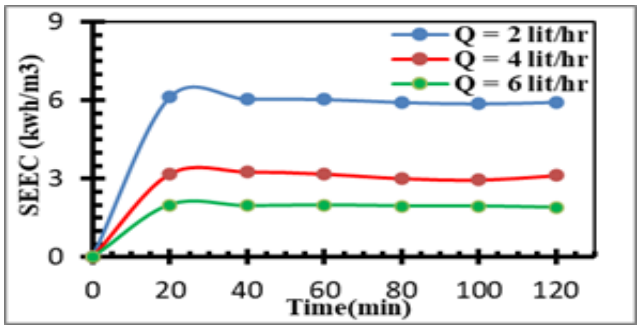

Figure (4.37) Variation of the specific electrical energy consumption SEEC (kwh/m3) vs Time during EC/EF treatment for **200 ppm** initial crude oil concentration of O/W emulsion, Al-Al electrode, and current density **10mA/cm^2**

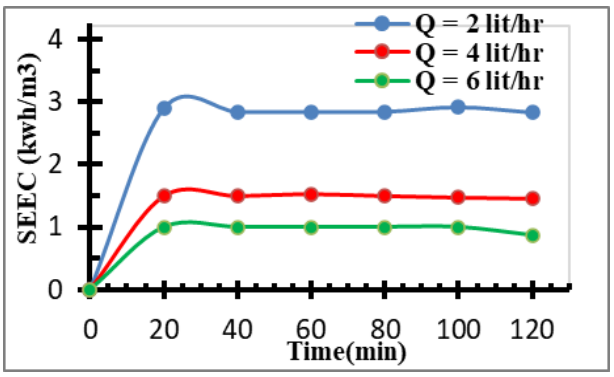

Figure (4.38) Variation of the specific electrical energy consumption SEEC (kwh/m3) vs Time during EC/EF treatment for **200 ppm** initial crude oil concentration of O/W emulsion, Al-Al electrode, and current density **20mA/cm^2**

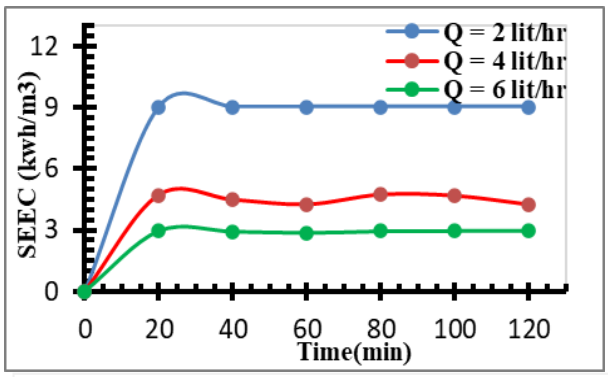

Figure (4.39) Variation of the specific electrical energy consumption SEEC (kwh/m3) vs Time during EC/EF treatment for **200 ppm** initial crude oil concentration of O/W emulsion, Al-Al electrode, and current density **30mA/cm^2**

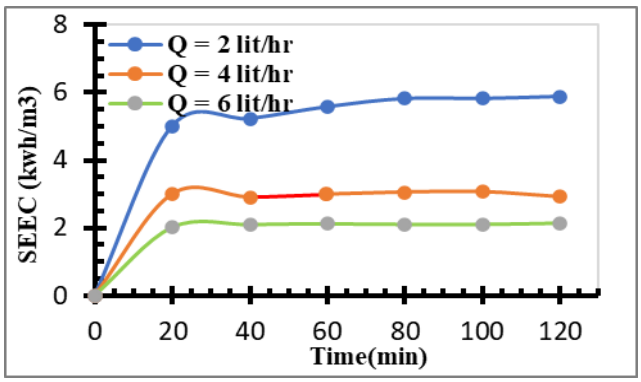

Figure (4.40) Variation of the specific electrical energy consumption SEEC (kwh/m3) vs Time during EC/EF treatment for **300 ppm** initial crude oil concentration of O/W emulsion, Al-Al electrode, and current density **10mA/cm^2**

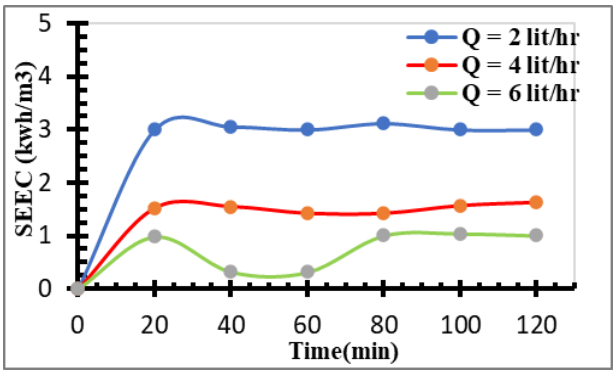

Figure (4.41) Variation of the specific electrical energy consumption SEEC (kwh/m3) vs Time during EC/EF treatment for **300** ppm initial crude oil concentration of O/W emulsion, Al-Al electrode, and current density **20mA/cm^2**

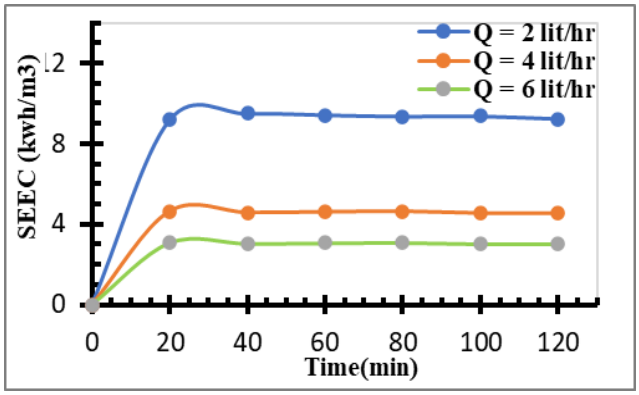

Figure (4.42) Variation of the specific electrical energy consumption SEEC (kwh/m3) vs Time during EC/EF treatment for **300 ppm** initial crude oil concentration of O/W emulsion, Al-Al electrode, and current density **30mA/cm^2**

Figure (4.43-4.51) illustrates the effect of the specific electrical energy consumption with time at different current densities using O/W emulsion by hybrid EC/EF method with deferent initial O/W concentration, and flow rate, the results show with increasing current density, the specific electrical energy consumption increases.

As seen in Figure (4.43), For 100 ppm initial O/W emulsion concentration, and 2 L/hr O/W emulsion flow rate with different current density (10,20, and30 mA/cm^2), the specific electrical energy consumption were: 6.49kWh/m^3 at 10 mA/cm^2,9kWh/m^3 at 20mA/cm^2, and 12.7kWh/m^3 when current density was 30mA/cm^2, respectively.

Also for 100 ppm initial O/W emulsion concentration, as seen in Figure (4.44), 4 L/hr O/W emulsion flow rate with different current density (10,20, and30 mA/cm^2), the specific electrical energy consumption were: 3.5kWh/m^3 for 10 mA/cm^2,4.76 kWh/m^3 for 20mA/cm^2, and 6kWh/m^3 when current density was 30mA/cm^2, respectively.

For 100 ppm initial O/W emulsion concentration, and O/W emulsion flow rate 6L/hr with different current density (10,20, and30 mA/cm^2), Figure (4.45)

shown the specific electrical energy consumption were:3.5kWh/m^3 for 10 mA/cm^2,4.76kWh/m^3 for 20mA/cm^2, and 6kWh/m^3 for current density 30mA/cm^2, respectively.

Also, for 200 ppm initial O/W emulsion concentration, and O/W emulsion flow rate 2L/hr with different current density 10,20, and30 mA/cm^2, Figure (4.46) shown the specific electrical energy consumption 2.8kWh/m^3 at 10 mA/cm^2, 5.94kWh/m^3 at 20mA/cm^2, and 9kWh/m^3 for current density 30mA/cm^2, respectively.

For 200 ppm initial O/W emulsion concentration, and 4L/hr O/W emulsion flow rate with different current density 10,20, and30 mA/cm^2, Figure (4.47), shown the specific electrical energy consumption were 1.46 kWh/m^3 at 10 mA/cm^2, 3.12 kWh/m^3 at 20mA/cm^2, and 4.23 kWh/m^3 forcurrent density was 30mA/cm^2, respectively.

Also for 200 ppm initial O/W emulsion concentration, and 6L/hr O/W emulsion flow rate with different current density 10,20, and30 mA/cm^2, Figure (4.48), shown the specific electrical energy consumption were 0.87 kWh/m^3 at 10 mA/cm^2, 1.9 kWh/m^3 at 20mA/cm^2, and 2.9 kWh/m^3 when current density was 30mA/cm^2, respectively.

Similarly, for 300 ppm initial O/W emulsion concentration, and O/W emulsion flow rate 2L/hr with different current density 10,20, and30 mA/cm^2, Figure (4.49), shown seen the specific electrical energy consumption were: 3 kWh/m^3 at 10 mA/cm^2, 5.83 kWh/m^3 at 20mA/cm^2, and 9.225 kWh/m^3 when current density was 30mA/cm^2, respectively.

for 300 ppm initial O/W emulsion concentration, and 4L/hr O/W emulsion flow rate with different current density 10,20, and30 mA/cm^2, Figure (4.50), shown the specific electrical energy consumption were: 62 kWh/m^3 at 10

mA/cm^2, 2.9 kWh/m^3 at 20mA/cm^2, and4.53 kWh/m^3 for current density 30mA/cm^2, respectively.

For 300 ppm initial O/W emulsion concentration , and 6L/hr O/W emulsion flow rate with different current density 10,20 , and 30 mA/cm^2, Figure (4.51), shown the specific electrical energy consumption were: 1 kWh/m^3 at 10 mA/cm^2, 2.14 kWh/m^3 at 20mA/cm^2, and 3.02 kWh/m^3 when current density was 30mA/cm^2, respectively.

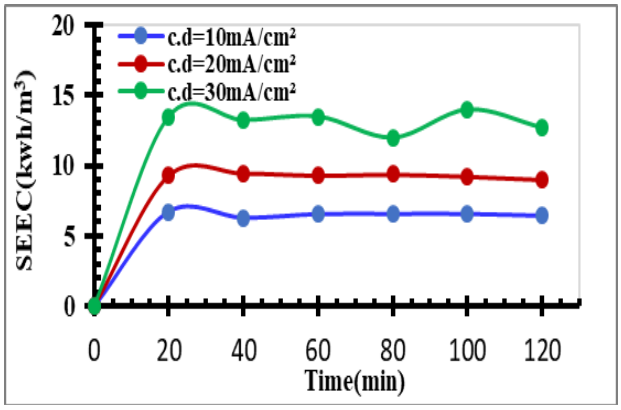

Figure. **(4.43)** Variation of specific electrical energy consumption SEEC (kWh/m^3) with Time at different current densities; Al-Al electrode,**100 ppm** initial O/W concentration, volumetric flow rate **2 L/hr.**

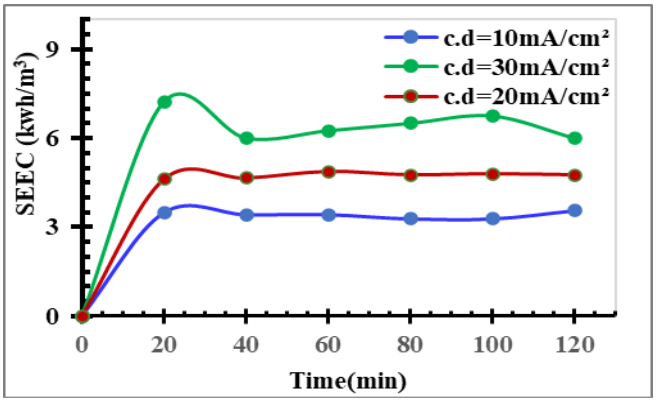

Figure. **(4.44)** Variation of specific electrical energy consumption SEEC (kWh/m^3) with Time at different current densities; Al-Al electrode,**100 ppm** initial O/W concentration, volumetric flow rate **4 L/hr.**

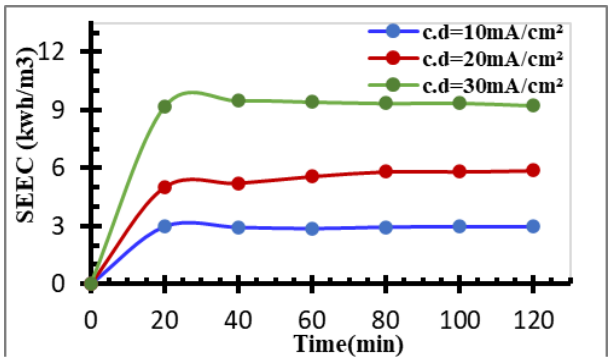

Figure. **(4.45)** Variation of specific electrical energy consumption SEEC (kWh/m^3) with Time forAl-Al electrode,**100 ppm** initial O/W concentration, volumetric flow rate **6 L/hr**.

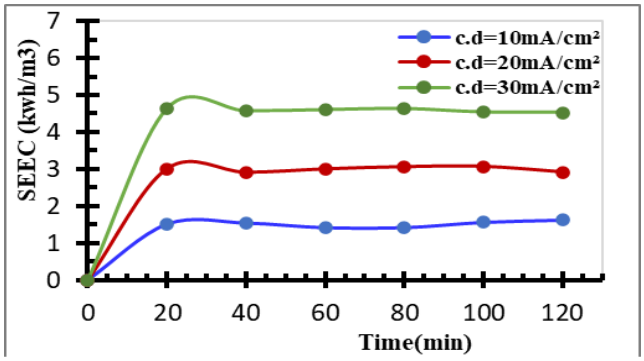

Figure. **(4.46)** Variation of specific electrical energy consumption SEEC (kWh/m^3) with Time forAl-Al electrode,**200 ppm** initial O/W concentration, volumetric flow rate **2 L/hr.**

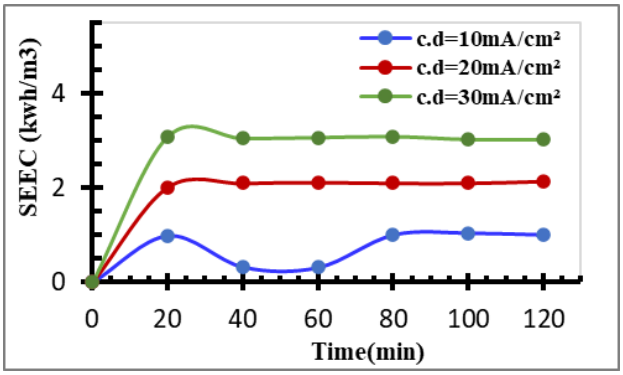

Figure (4.47) Variation of specific electrical energy consumption SEEC (kWh/m^3) with Time forAl-Al electrode,**200 ppm** initial O/W concentration, volumetric flow rate **4 L/hr**.

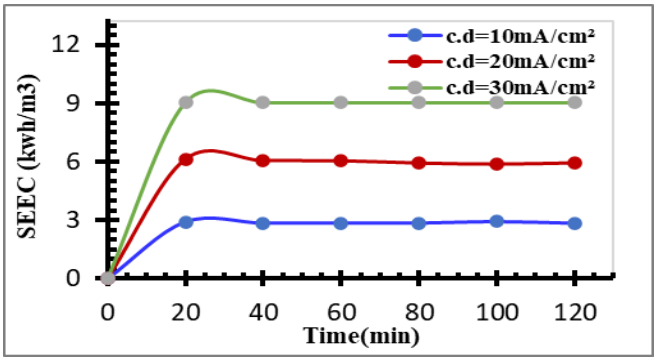

Figure (4.48) Variation of specific electrical energy consumption SEEC (kWh/m^3) with Time forAl-Al electrode,**200 ppm** initial O/W concentration, volumetric flow rate **6 L/hr**.

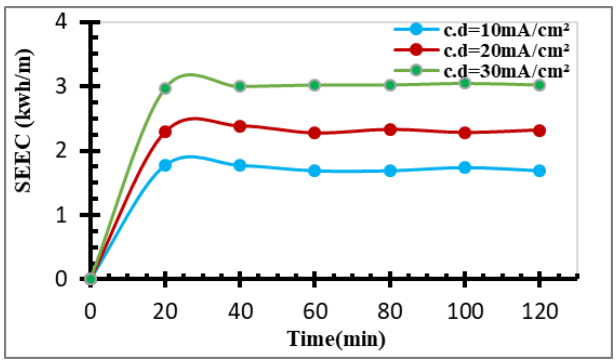

Figure. **(4.49)** Variation of specific electrical energy consumption SEEC (kWh/m^3) with Time forAl-Al electrode,**300 ppm** initial O/W concentration, volumetric flow rate **2 L/hr.**

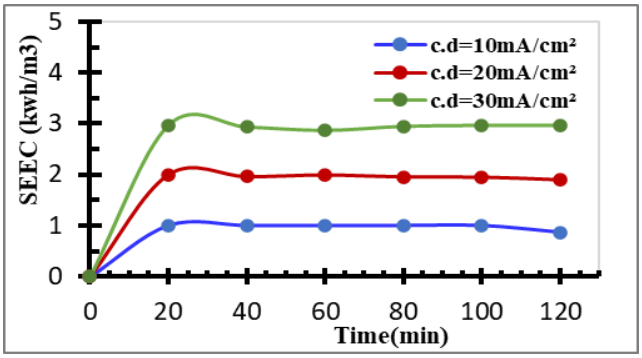

Figure. **(4.50)** Variation of specific electrical energy consumption SEEC (kWh/m^3) with Time forAl-Al electrode,**300 ppm** initial O/W concentration, volumetric flow rate **4 L/hr.**

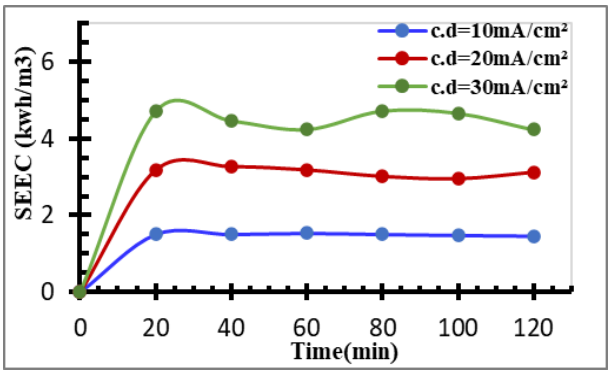

Figure. **(4.51)** Variation of specific electrical energy consumption SEEC (kWh/m^3) with Time for Al-Al electrode,**300 ppm** initial O/W concentration, volumetric flow rate **6 L/hr**.

The effect of increasing initial O/W emulsion concentration on behaviour specific electrical energy consumption SEEC is shown in Figure (4.52-4.60), using Al-Al electrodes, different initial O/W concentration emulsion for each Figure (100,200, and 300 ppm), at current densities of 10,20, and 30 mA/cm^2, and different O/W emulsion flow rate 2,4,6L/hr, respectively.

For current density 10 mA/cm^2, O/W emulsion flow rate 2L/hr with different initial O/W concentration, Figure (4.52), shown the specific electrical energy consumption SEEC behaviour when increasing initial O/W emulsion concentration during hybrid EC/EF treatment were : 6.4 kWh/m^3 at 2L/hr O/W emulsion flow rate, 3 kWh/m^3 at 4L/hr O/W emulsion flow rate, and 2.83 kWh/m^3 when O/W emulsion flow rate was 6L/hr, respectively.

For current density 10 mA/cm^2, O/W emulsion flow rate 4L/hr with differentinitial O/W concentration, Figure (4.53), shown the specific electrical energy consumption SEEC decreasing when increasing initial O/W emulsion concentration during hybrid EC/EF treatment were : 3.5 kWh/m^3 at 2L/hr O/W emulsion flow rate, 1.6 kWh/m^3 at4L/hr, and1.46 kWh/m^3 when O/W emulsion flow rate was 6L/hr, respectively.

For current density 10 mA/cm^2, O/W emulsion flow rate 6L/hr with differentinitial O/W concentration, Figure (4.54), shown the specific electrical energy consumption SEEC decreasing when increasing initial O/W emulsion concentration during hybrid EC/EF treatment were: 2.32 kWh/m^3 at 2L/hr O/W emulsion flow rate, 1 kWh/m^3 at 4L/hr, and 0.87 kWh/m^3 when O/W emulsion flow rate was 6L/hr, respectively.

Also, for current density 20 mA/cm^2, O/W emulsion flow rate 2L/hr with differentinitial O/W concentration, Figure (4.55), shown the specific electrical energy consumption SEEC decreasing when increasing initial O/W emulsion

concentration during hybrid EC/EF treatment were: 12.7 kWh/m^3 at 2L/hr O/W emulsion flow rate, 5.94 kWh/m^3 at 4L/hr, and5.88 kWh/m^3 when O/W emulsion flow rate was 6L/hr, respectively.

For current density 20 mA/cm^2, O/W emulsion flow rate 4L/hr with different initial O/W concentration, Figure (4.56), shown the specific electrical energy consumption SEEC decreasing when increasing initial O/W emulsion concentration during hybrid EC/EF treatment were: 6 kWh/m^3 at 2L/hr O/W emulsion flow rate, 3.12 kWh/m^3 at 4L/hr, and 2.9 kWh/m^3 when O/W emulsion flow rate was 6L/hr, respectively.

For current density 20 mA/cm^2, O/W emulsion flow rate 6L/hr with differentinitial O/W concentration, Figure (4.57), shown the specific electrical energy consumption SEEC decreasing when increasing initial O/W emulsion concentration during hybrid EC/EF treatment were: 1.68 kWh/m^3 at 2L/hr O/W emulsion flow rate, 1.9 kWh/m^3 at 4L/hr, and2.14 kWh/m^3 when O/W emulsion flow rate was 6 L/hr, respectively.

Similarly, for current density 30 mA/cm^2, O/W emulsion flow rate 2L/hr with different initial O/W concentration, Figure (4.58), shown the specific electrical energy consumption SEEC decreasing when increasing initial O/W emulsion concentration during hybrid EC/EF treatment were: 9.225 kWh/m^3 at 2L/hr O/W emulsion flow rate, 9.03kWh/m^3 at 4L/hr, and9 kWh/m^3 when O/W emulsion flow rate was 6L/hr, respectively.

F or current density 30 mA/cm^2, O/W emulsion flow rate 4L/hr with differentinitial O/W concentration, Figure (4.59), shown the specific electrical energy consumption SEEC decreasing when increasing initial O/W emulsion concentration during hybrid EC/EF treatment were: 4.76 kWh/m^3 at 2L/hr O/W emulsion flow rate, 4.53kWh/m^3 at 4L/hr, and4.23 kWh/m^3 when O/W emulsion

flow rate was 6L/hr, respectively.

F or current density 30 mA/cm^2, O/W emulsion flow rate 6L/hr with differentinitial O/W concentration, Figure (4.60), shown the specific electrical energy consumption SEEC decreasing when increasing initial O/W emulsion concentration during hybrid EC/EF treatment were: 3.025 kWh/m^3 at 2L/hr O/W emulsion flow rate, 3.02 kWh/m^{3}at 4L/hr, and 2.97 kWh/m^3 when O/W emulsion flow rate was 6L/hr, respectively.

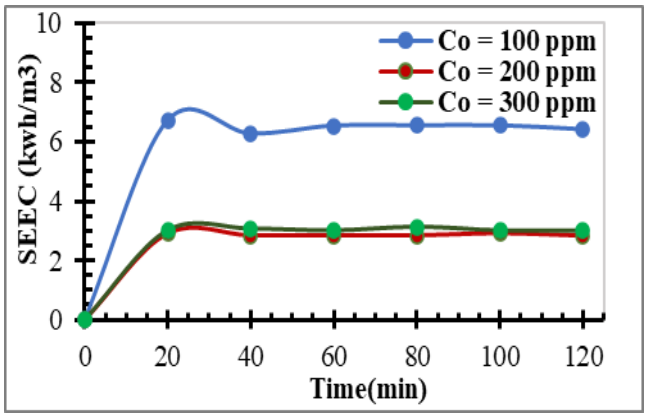

Figure (**4.52**) Variation of specific electrical energy consumption SEEC (kWh/m^3) with Time during EC/EF method, with different O/W emulsion concentration, current density **10 mA/cm^2**, volumetric flow rate **2 L/hr** .

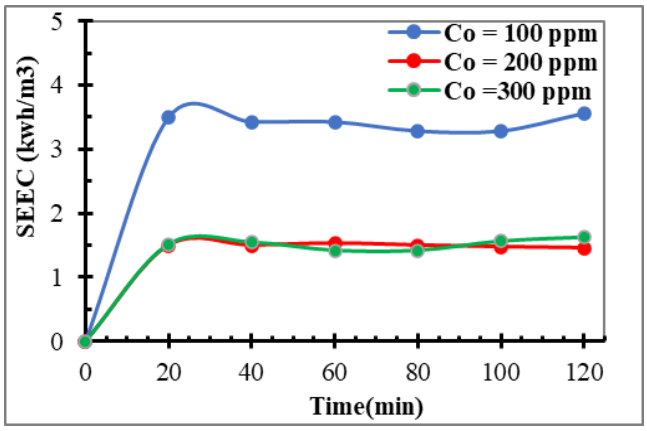

Figure (**4.53**) Variation of specific electrical energy consumption SEEC (kWh/m^3) with Time during EC/EF method, with different O/W emulsion concentration, current density **10 mA/cm^2,** volumetric flow rate **4** L/hr .

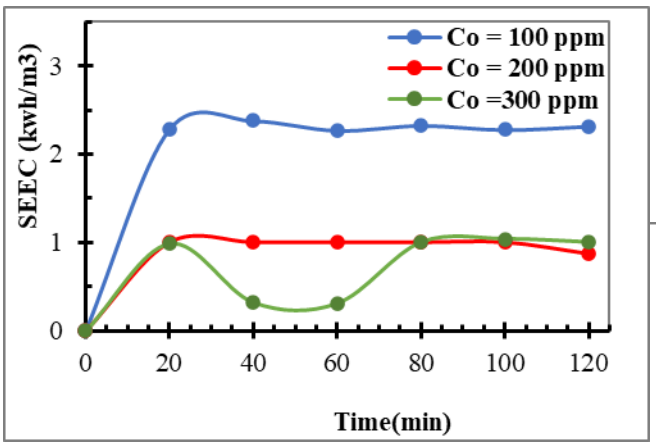

Figure. (**4.54**) Variation of specific electrical energy consumption SEEC (kWh/m^3) with Time during EC/EF method, with different O/W emulsion concentration, current density **10 mA/cm^2**, volumetric flow rate **6 L/hr.**

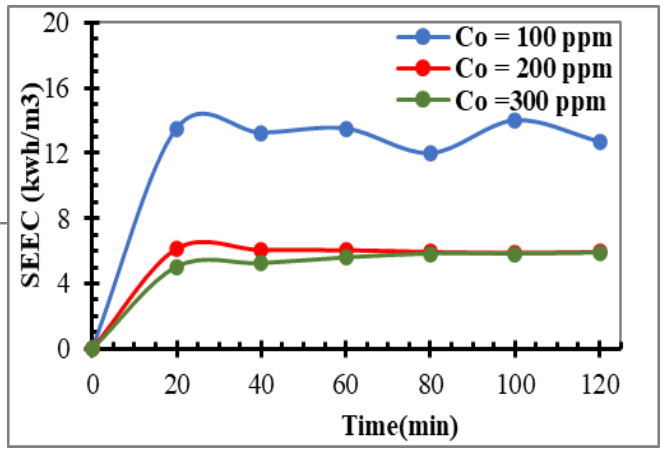

Figure. (**4.55**) Variation of specific electrical energy consumption SEEC (kWh/m^3) with Time during EC/EF method, with different O/W emulsion concentration, current density **20 mA/cm^2**, volumetric flow rate **2 L/hr.**

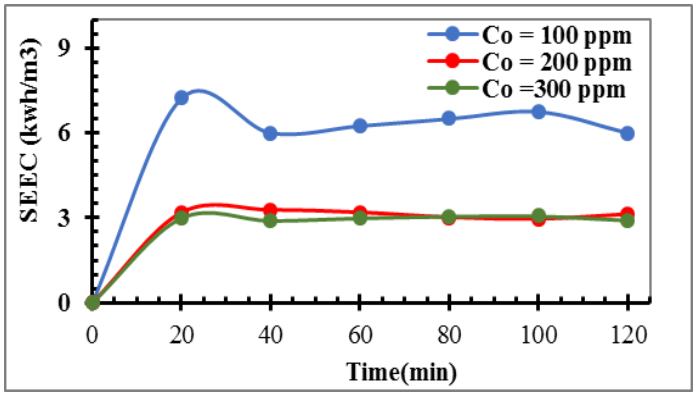

Figure. (**4.56**) Variation of specific electrical energy consumption SEEC (kWh/m^3) with Time during EC/EF method, with different O/W emulsion concentration, current density **20** mA/cm2, volumetric flow rate **4** L/hr.

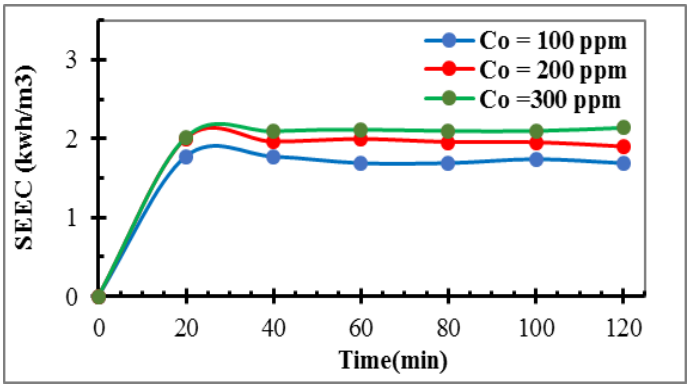

Figure (**4.57**) Variation of specific electrical energy consumption SEEC (kWh/m^3) with Time during EC/EF method, with different O/W emulsion concentration, current density **20** mA/cm2, volumetric flow rate **6** L/hr.

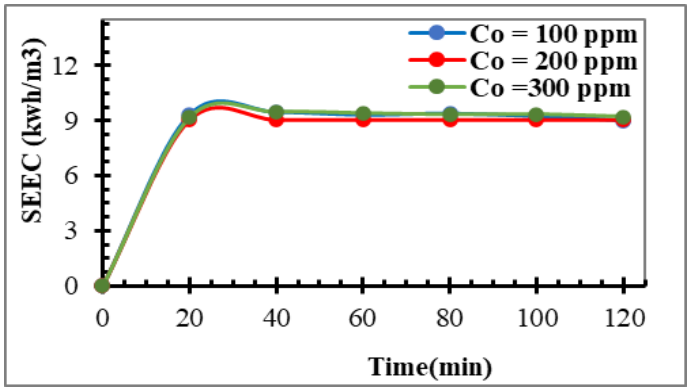

Figure (**4.58**) Variation of specific electrical energy consumption SEEC (kWh/m^3) with Time during EC/EF method, with different O/W emulsion concentration, current density **30** mA/cm^2, volumetric flow rate **2** L/hr..

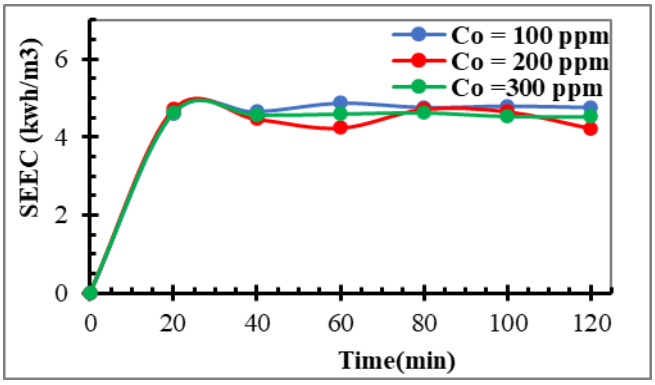

Figure. (**4.59**) Variation of specific electrical energy consumption SEEC (kWh/m^3) with Time during EC/EF method, with different O/W emulsion concentration, current density **30** mA/cm^2, volumetric flow rate **4** L/hr

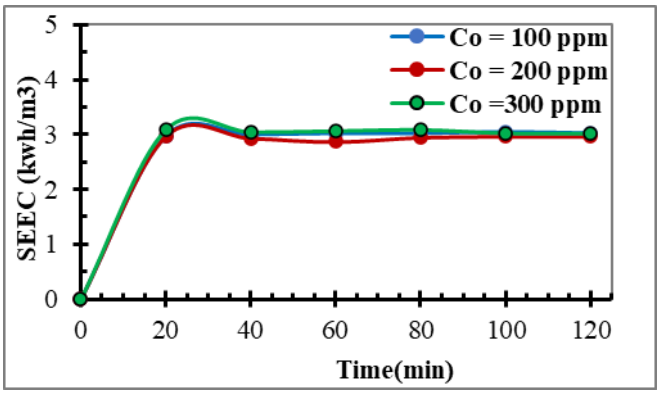

Figure. (4.60) Variation of specific electrical energy consumption SEEC (kWh/m^3) with Time during EC/EF method, with different O/W emulsion concentration, current density **30** mA/cm2, volumetric flow rate **6** L/hr

Figures showed the behavior of the specific electrical energy consumption SEEC during the two-hour experiment period for each treatment a slight increase or nearly steady up to 120 minutes' time, the results showed a decrease of SEEC with the increase of O/W emulsion flow rate, and the initial O/W emulsion concentration, on the other hand, increasing with the increase of current density.

The specific electrical energy consumption SEEC behavior can be explained by the fact that due to fluctuations, occurs electrode coverage causing blockages, lower COD removal efficiency, and higher current density. It has been observed that power consumption is affected by electrode voltage, current, and emulsion flow rate. Similar observations were found in previous researches [Un et al., 2009]; [Esfandyari et al., 2015].

4.2.6 pH Measurement

pH values obtained from oil wastewater treatment were studied by EC/EF hybrid method to enhance the research in this important parameter, studies were conducted on three different main parameters of the initial O/W concentration, current density, and O/W emulsion flow rate, as well as to investigate their effects on COD removal efficiency as shown in Figure (4.61- 4.63) based on optimum conditions. It was found that the results of all initial pHstudies were not similar. So, acidic initial pH values caused some significant changing on the COD removal efficiency. The results revealed that the acidic condition enhance the free radical ($OH^{\bullet}$) formation, and therefore the adsorbedorganic matter was easily reacting at the electrode surface. definitely, the present results agreed with [Tasic et al.,2014].

The pH value increased when the running period of the EC process, which was responsible for flocs generation, was extended, which appears to correspond with the findings of [kobya et al., 2010].

Because the procedure took place at ambient temperature, which was around 20-40 ^{o}C, the pH rise was minor. The pH of the emulsion was observed to fall linearly when the temperature was raised. When the emulsion temperature rise, the esters in the oil appear to breakdown into alcohols, and acids, lowering the pH of the water-oil emulsion, this explanation agrees with what was mentioned by [Sangal et al.,2013].

The pH of O/W emulsion's, for all expements, the pH very little gradually increased from 5.80 to 8.81 over a 120-minute treatment time. In the following 60 minutes, the pH rose very slightly to 7.3, and remained nearly steady for the next 120 minutes.

During all the electrolysis periods, the O/W emulsion pH changed optimally with different current density, and initial O/W concentration,as shown in Figure (4.61-4.63) for experimental run performed at an optimum O/W emulsion flow rate of 2L/hr, and an optimum initial pH of 6.5.

Because the optimal starting pH was determined to be 6.5, it can be inferred that charge neutralization of anionic colloids by monomeric cationic aluminum species Al^{+3}, $Al(OH)_2^{+2}$, $Al(OH)_2^{+}$ $_2$as well as sweep EC/EF with amorphous $Al(OH)_3$ aid in maximum pollutant removal at pH_o= 6.5. As, variousresearchers have shown that the optimum electrocoagulation effectiveness occurs when the starting pH is between 6.5, and 7.0, [Cañizares et al., 2007].

During electrocoagulation therapy, this equilibrium pH is due to a dynamic balance between the complicated chemical processes involving an H^+ donor or OH^- acceptor. Because cathodic water reduction predominates over anodic water oxidation, the pH is slight alkaline.

Figure (4.61-4.63) shows the pH-time trend, as an optimum condition for 2L/hr O/W emulsion flow rate, studying the effect of increasing the applied

current density on the pH when the initial O/W concentration (100, 200, and300 ppm), respectively. For initial O/W concentration 100 ppm, and current densities (10, 20, and30mA/cm^2), the pH increased from its initial value of 7.1 to 8.3, from 6.93 to 8.8, and from 7.1 to 8.1, respectively, as shown in the Figure (4.61).

For 200 ppm initial O/W concentration, and current densities (10, 20, and30 mA/cm^2), the pH increased from its initial value of 7.3 to 8.4, from 7.2 to 8.4, and from 7.4 to 8.4, respectively, as shown in the Figure (4.62), For 300 ppm initial O/W emulsion concentration, and current densities (10, 20, and30 mA/cm^2), the pH increased from its initial value of 6.8 to 7.9, from 6.93 to 8.8, andfrom 7.1 to 8.1, respectively, as shown in the Figure (4.63). The results data are given in appendix B, Table (B.4a).

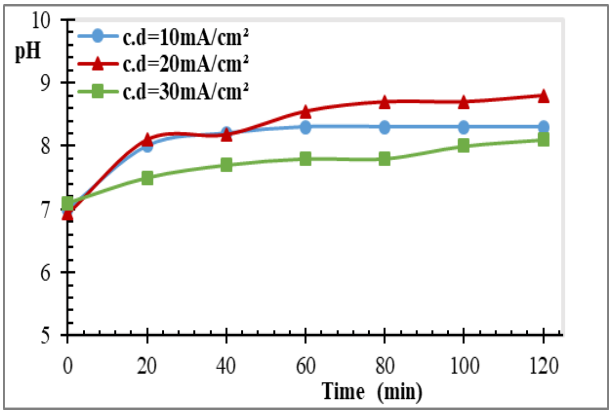

Figure (4.61) pH variation with time at different current densities; initial O/W emulsion conc.**100** ppm, Al-Al electrode, volumetric flow rate **2** L/hr.

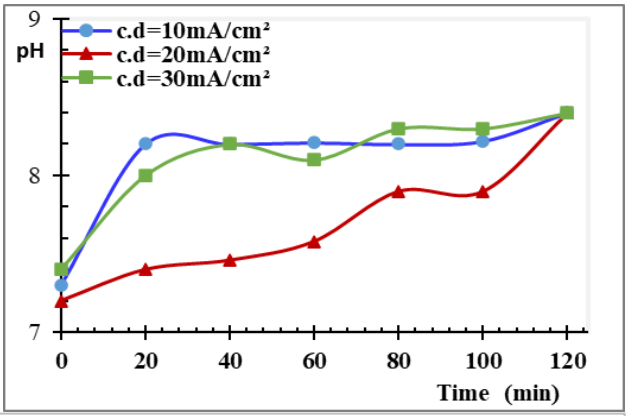

Figure (4.62) pH variation with time during EC/EF process for initial crude oil concentration **200** ppm of O/W emulsion, Al-Al electrode, volumetric flow ate **2**L/hr.

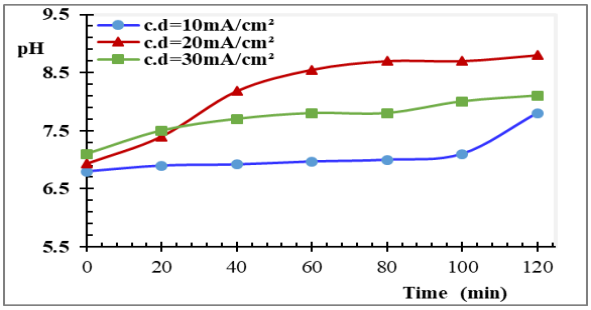

Figure (4.63) pH variation with time during EC/EF process for initial crude oil concentration **300** ppm of O/W emulsion, Al-Al electrode, volumetric flow ate **2**L/hr

4.2.7 Zeta Potential Evaluations

Zeta potential decreases with increasing electrolyte concentration. So, increasing of zeta potential causes increasing of emulsion, and addition of the anionic surfactant (Sulfate Dodecyl Sodium) adds more negative charge to O/Wemulsion so causes increasing of zeta potential.

Figure (4.64) , and appendix D,Table (D.1) showed analysis of the most optimal samples at optimal conditions (current density 30 mA/cm^2, emulsion flow rate 2L/hr) , and for the initial O/W concentrations (100, 200 , and 300 ppm), for zeta potential. The results data are given in appendix D (Table D.1).

The results give zeta potential of -35.32 mV for initial O/Wemulsion analysis (time zero minutes) , and gives the potential -21 mV at the end of the treatment (120 minutes), for the first concentration of 100 ppm.

In the case of increasing the initial concentration of O/W emulsion to 200 ppm, this gives a zeta potential of -39.37 at the beginning of the treatment, and 27.98 at the end of the treatment.

In the case of the initial O/W concentration of 300ppm, gives zeta potential -66.41, and 32.32 at start, and end of the treatment, respectively.

The results showed that, zeta potential was more positive during the time of treatment for 100ppm O/W concentration, while it was negative when the concentration increased to 300 ppm O/W, this is in agreement with [Kuo, & Lee ,2010].

Figure (4.65) shows the best behavior of zeta potentials verses time for different initial O/W concentrations, during EC/EF of demulsification OWemlsion at condition of current density 30 mA/cm², and volumetric flow rate 2L/hr, it shows a positive behavior of the removal process of solutions

with concentrations of 100, and 200 ppm, in the form of oil effort at the points of intersection with the time axis, assuming that each solution behaves in a straight line during the treatment period. Moreover, the concentration curve approaches 300 ppm, but at the end of the treatment (120 minutes).

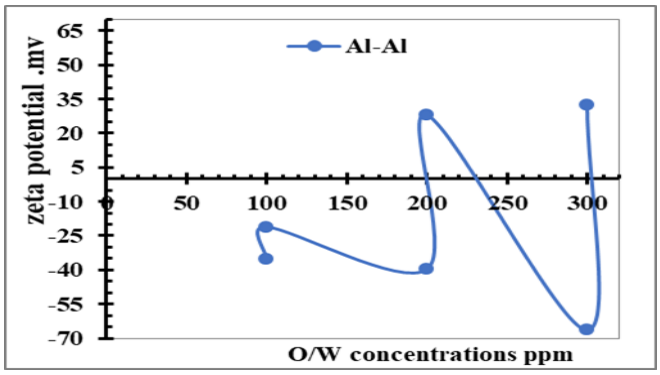

Fig (**4.64**) Behavior of zeta potentials (mv) before and after treatment during EC/EF of demulsification OWemlsion, Al-AL electrodes, current density **30**mA/cm^2, volumetric flow rate **2** L/hr

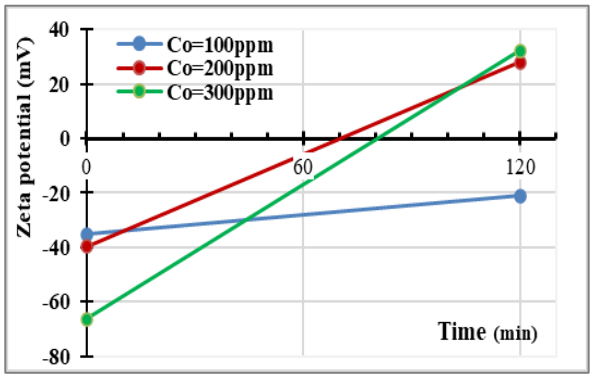

Fig (**4.65**) Best Behavior of zeta potentials (mv) Vs. Time(min) for different initial crude oil concentrations, during EC/EF of demulsification OWemlsion, Al-Al electrodes, current density **30** mA/cm^2, volumetric flow rate **2** L/hr

This negative charge came from the adsorption of hydroxyl ion on the surface of oil droplet. Subsequently, that increase indicates that more ions are adsorbed on to oil droplets, resulting in a drop in zeta potential. This is in agreement with [Kuo & Lee, (2010); Al-Shamrani et al., (2002)].

The higher the ionic strength, the more compressed the double layer becomes. The valency of the ions will also influence double layer thickness A trivalent ion such as Al^{3+} will compress the double layer to a greater extent in comparison with a monovalent ion such as Na^{+}, That means that it has a higher ability to reduce zeta potential. Previous research has shown a similar pattern. [Abbas,2011].

Oil recovery increases when zeta potential decreases. The EC/EF treatment produced H, and OH radicals, reducing the zeta potential of particulates, the liquid layer around the particle is divided into two sections: aninner area (Stern

layer) where the ions are strongly bound, and an outer (diffuse)region where they are less securely bound. A hypothetical border exists insidethe diffuse layer, within which the ions, and particles form a stable entity. Ionsinside the boundary move a particle when it moves.

Ions that cross the border remain with the bulk dispersant. The zeta potential exists at this point. The zeta potential's magnitude indicates the colloidal system's potential stability. Suppose all of the particles in beyond the barrier, the ions stay with the bulk dispersant. The zeta potential is the potential at this point. The colloidal system's potential stability is determined by the amplitude of the zeta potential. If all of the particles in suspension have a large negative or positive zeta potential, they will resist each other, and have no inclination to join together. However, if the particles' zeta potential levels are low, there will be no force to keep them from colliding, and flocculating [Abbas, 2011].

4.2.8 Turbidity Evaluations

This study was enhanced by analyzing samples taken at the beginning,after 20 minutes, and at the end of each EC/EF test. Turbidity, TS, and TSS of each sample are measured (total 162 data for each parameter). The results data are given in appendix B (Table B.5).

The turbidity of an O/W emulsion stabilized by surfactant has a positive relationship with the oil concentration. The effectiveness of the main operating factors (flow rate, current density, and initial O/W concentration) on demulsification can be determined by comparing the turbidity of emulsions before, and after treatment, and determining the effectiveness of the main operating factors (flow rate, current density, initial crude oil concentration), and their agreement with the work of researchers [Yang, 2007].

Appendix B, Table (B.5) shows one of the optimum results of turbidity reduction during electrocoagulation/electroflotation test at the indicated times when the current density increased 10, 20, and 30 mA/cm^2 for the initial O/W concentration of 100 ppm, 2 L/hr the volumetric O/Wemulsion flow rate .The results showed that the turbidity decreases with the increase in the current density, in other words, the removal efficiency of turbidity increases with an increasein the current density.

The turbidity of the O/W emulsion decreased sharply for 20 minutes of analysis at a current densityof 10 mA/cm^2 from 28.4 to 14.3 **NTU**, 28.3 to 17 **NTU** at 20 mA/cm^2 , and from 28 to 5.3 **NTU** at 30 mA/cm^2, followed by a small decrease at end test as shown in Appendix B,Table (B.5) .Moreover, the turbidity increases with the increase in the concentration of pollutants in O/W emulsion, that is, increase in initial O/W concentration the efficiency of removing turbidity decreases. The results data are given in Appendix B, Table (B.5).

4.2.9 Total Dissolve Solid, Total Suspended Solid, and Total Solid Evaluation

This study was enhanced by analyzing samples taken at the beginning,after 20 minutes, and end of each EC/EF test, TS, and TSS of each sample are measured. The results data are given in Appendix B, Table (B.5).

For measuring Absorption, pH, Ec, temperature(T), and TDS, the results data are given in Appendix B, Table (B.5b)., analyzing samples taken at the beginning of each experiment, and in periods of 20 minutes, and end of each EC/EF test at 120 minutes (total 162 data for each parameter).The exceptional effectiveness of the EC/EF treatment in the removal of TSS can be related to the turbidity removal efficiency. The results data are given in Appendix B, Table (B.5).

TSS for each sample was calculated by weighing a suitable filter paper after drying it in an oven dryer at 90-100 ^{0}C for 15 minutes, and then placing it in Desiccator containing silica gel for the purpose of drying the filter paper, and cooling it down. Record its weight as W1. Buckner Funnel installed to a mechanicalvacuum pump to filter the sample completely, then repeat the process of drying, cooling, withdrawing moisture, and weighing the paper with the suspended solids, record its weight as W2, and the difference between the two weights is theamount of total suspended solids (TSS).

The total solids (TS) are the sum of total (TSS) suspended solids, and total dissolved solids (TDS)

In Appendix B, Table (B.4), (B.5), models showing the results of TDS, TSS, and TS, respectively,during hybrid EC/EF at optimum conditions, current, and fluorite density of initial O/W concentration of 100 ppm. The tables clearly show a decrease of total dissolved solid, total suspended solid, and total solid, evaluation against a timeof 20 minutes, sharply, and then a slight decrease until the end of the analysis time.

4.2.10 Flocs Composition

The identification of phases presents in the flocs collected during the process of oily sewage de-emulsification by skimmed it, was analyzed by the X-ray diffraction machine device (LabX, XRD-6000model, SHIMADZU company. Japan). The phenomenon of diffraction occurs when the flocs samples is exposed to X-rays. The phases in it were diagnosed by conforming the results of crystal clearing values(d-spacing), we get from the diffraction pattern, and comparing them with standard X-ray diffraction cards containing information on standard patterns from the International Center for Diffraction Data (ICDD).

Aluminum hydroxide Al $(OH)_3$, main compound, which appeared when diagnosing the phase at the values of intensity162,121, and 201 counts/second at 38.8409,49.4135, and 37.9354 $2\theta^0$ (deg) respectively, as shown in Figure (4.66).

The flocs created by the hybrid EC/EF process may be absorbed by hydrogen bubblesformed on the cathode, ensuring their float it.

High charges of the electrogenerated cations efficiently neutralize the surface charges on the surfactant molecules. At the same time, and the colloidal oil particles begin to agglomerate. The destabilized oil droplets eventually absorb into the highly distributed aluminum hydroxide colloid created by the electrogeneratedAl^{3+}, and hydroxyl ions. Finally, the oil-rich flocs rise to the surface, where it is skimmed away, similar observations were noticed by [Zongo et al., 2009][Yang,2007].

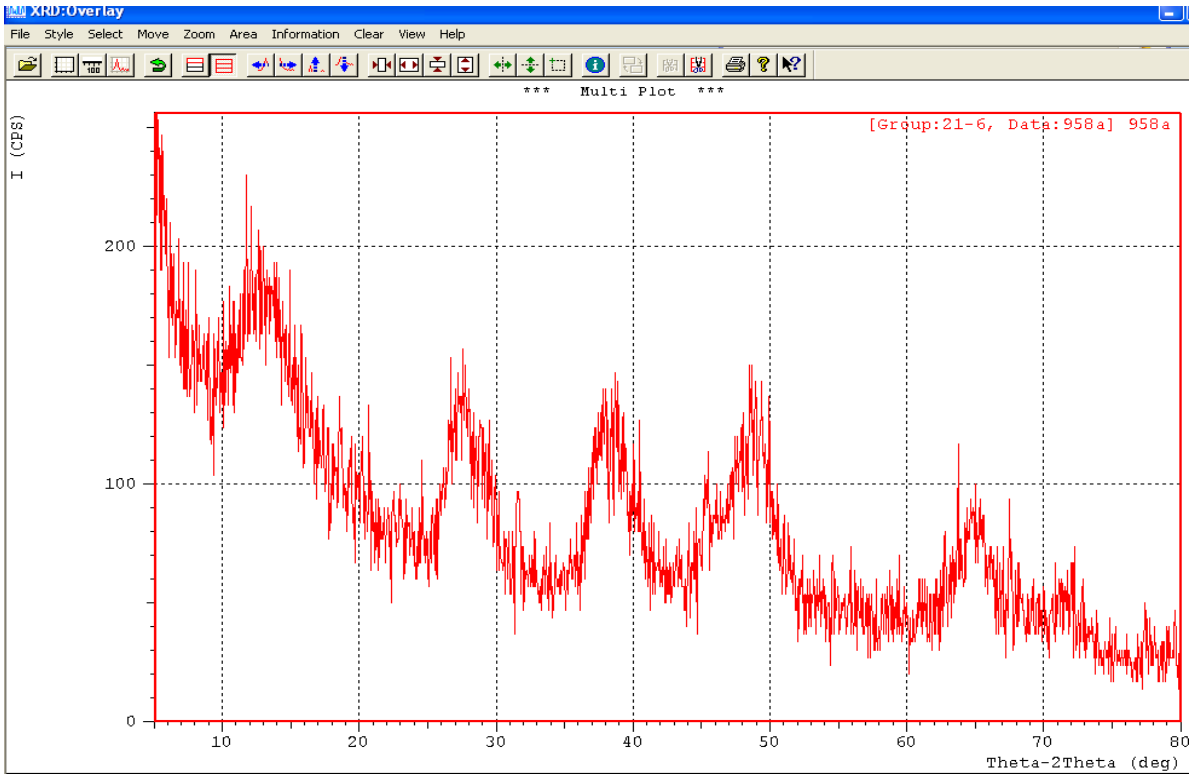

Figure (4.66) Intensity graph (count) versus $2\theta^0$ (deg) showing the peaks ofaluminum compounds corresponding to the X-ray diffraction results.

4.2.11 Bubbles Electrogeneration (Electroflotation)

Metal hydroxides are formed when these ions mix with hydroxyl ions, which are by-products of hydrogen production. The dissolution Aluminum anode is oxidized into Al^{3+} ions during electrolysis.

The design of the reactor, which favored the creation of big hydrogen bubbles, causing disrupted flow, and decreasing the contact between bubbles, and particles, is one factor that impacts the size, and generation of hydrogen bubbles; another factor is the electrode surface. Because of the passivation, the electrode has a rough surface, which reduces the production of hydrogen bubbles by giving a higher sticking force to bubbles than smooth surfaces Previous research has shown a similar pattern. [chen et al.,2000]. Positively charged hydrolyzed aluminum compounds such as Al^{+3}, $Al(OH)_2^{+2}$, $Al(OH)_2^{+}$, and others destabilize negatively charged oil globules in water. As aresult, oil globules clump together, and hydrogen bubbles generated at the cathode can bind to coagulated suspended particles, and droplets, causing them to float. this explanation agrees with what was mentioned by [Tasic et al.,2014].

4.3 Al - Carbon.felt Electrode

4.3.1 The Influence of Current Density

The performance of an electrocoagulation process is said to be totally influenced by current density, among other operational elements, because current density determines the pace at which the coagulant is dissolved from the electrode into the solution, agree with the researchers [Un et al.,2009].

Figure (4.67-4.75) shows effect of current density on COD removal efficiency for O/W emulsion treatment for various conditions of O/W emulsion flow rate, and initial O/W concentration. The results data are given in Appendix B,

Table(B.6).

For an initial O/W concentration of 100 ppm (C_o equal to 1108 mg/L initial O/W initial emulsion concentration) with increase current density(10,20 and 30 mA/cm^2) and O/W emulsion flow rate. Figure (4.67-4.69) shows the COD removal efficiency were 66.6,82 and 99.8% for 2L/hr O/W emulsion flow rate, for 4L/hr O/W emulsion flow rate, the COD removal efficiency were 36.9,43.6 and 98% and for 6 L/hr O/W emulsion flow rate the COD removal efficiency were: 45.9 ,52.7and 83.73%, respectively.

Figure (4.70-4.72) show effect of current density at initial O/W concentration 200 ppm (C_o equal to 1124 mg/L initial O/W emulsion concentration), at 2 L /hr O/Wemulsion flow rate, the COD removal efficiency for different current density (10,20,30 mA/cm^2) were: 75.8, 76.87, and 84.5% . For 4 L/hr O/W emulsion flow rate, the COD removal efficiency were: 60.58%,72.6%, and 79.2 %, and for 6 L/hr O/W emulsion flow rate, the COD removal efficiency were: 53.66,69.73 and 68.87%, respectively.

Similarly, Figure (4.73-4.75) illustrated COD removal efficiency for the concentration of 300 ppm of O/W in the emulsion (C_o equal to 1141 mg/L initial O/W emulsion concentration). For O/W emulsion flow rate of 2 L/hr, the COD removal efficiency were: 70,73.22and 81.56 %. Also, for 4L/hr were, 68,71.88 and 79.35% , lastly, , the COD removal efficiency were 68.91, 71.25 and 80.48 % for 6 L/ hr O/W emulsion flow rate, sequentially**.**

The efficiency of COD removal at different levels of current density is shown in Figure (4.70-4.72). For state of Carbon field analyzes show higher removal efficiency than aluminum cathode at the end of analysis time, due to higher formation of H_2 gas on electrode surface, and because of larger surface area of carbon felt, but aluminum electrode shows us higher removal efficiency after 20 minutes of analysis compared to carbon field for the same time, it

matches what has been done previously [Un et al., 2009]. Applying a current density of 20 mA/cm^2 using a carbon felt cathode can result in a higher COD removal efficiency than the Al cathode as it has been shown to require a higher current density of 30 mA/cm^2 for higher removal.

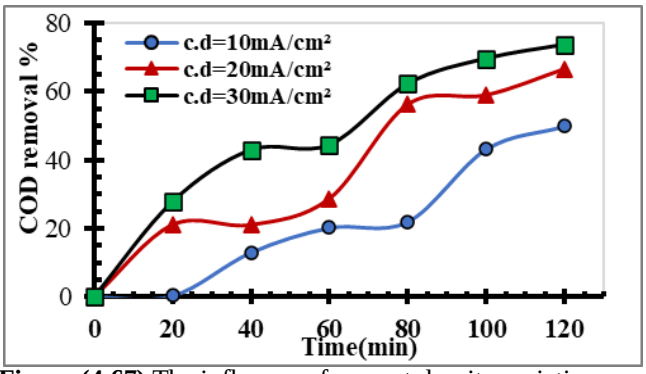

Figure (4.67) The influence of current density variation on COD removal efficiency during EC/EF of O/W treatment, Al- C. felt electrode; initial O/W conc.**100**ppm; volumetric flow rate **2** L/hr.

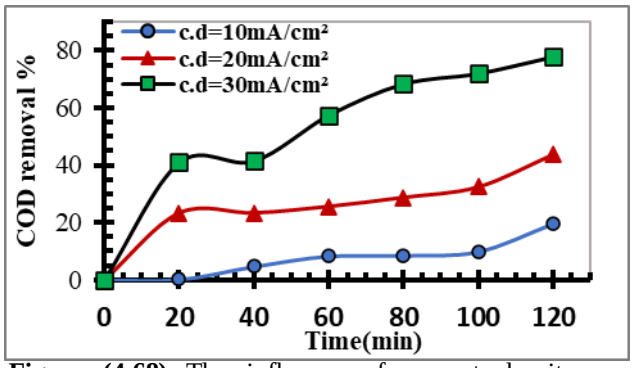

Figure (4.68) The influence of current density variation on COD removal efficiency during EC/EF of O/W treatment, Al-C.felt electrode; initial O/W conc.**100**ppm; volumetric flow rate **4** L/hr.

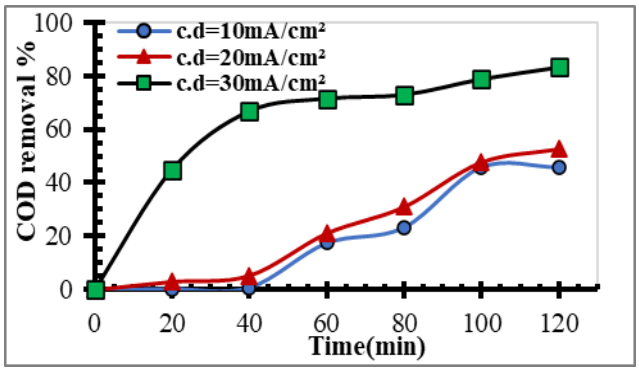

Figure (4.69) The influence of current density variation on COD removal efficiency during EC/EF of O/W treatment, Al- C. felt electrode; initial O/W conc.**100**ppm;volumetric flow rate **6** L/hr.

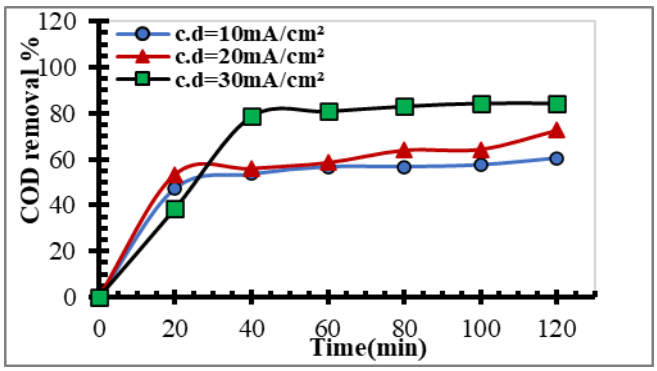

Figure (4.70) The influence of current density variation on COD removal efficiency during EC/EF of O/W treatment, Al-C. felt electrode; initial O/W conc.**200**ppm; volumetric flow rate **2**L/hr.

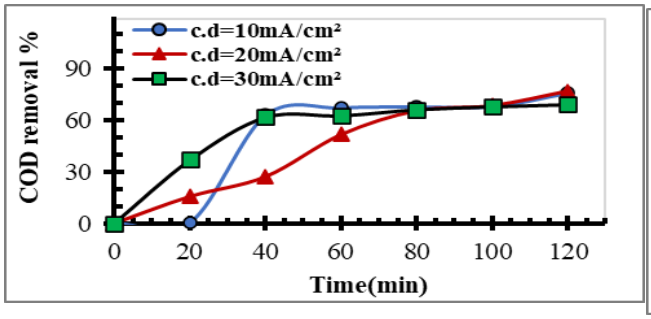

Figure (4.71) The influence of current density variation on COD removal efficiency during EC/EF of O/W treatment, Al- C.felt electrode; initial O/W conc.**200**ppm; volumetric flow rate **4** L/hr.

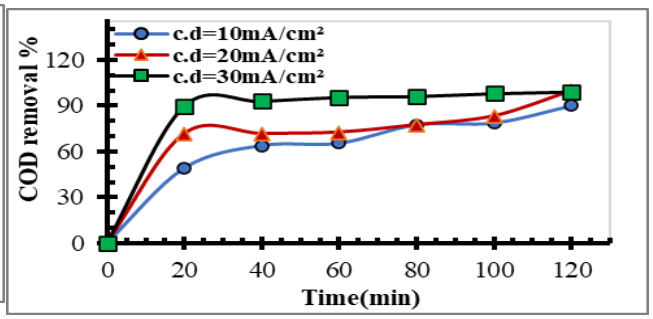

Figure (4.72) The influence of current density variation on COD removal efficiency during EC/EF of O/W treatment, Al- C.felt electrode; initial O/W conc.**200**ppm; volumetric flow rate **6**L/hr.

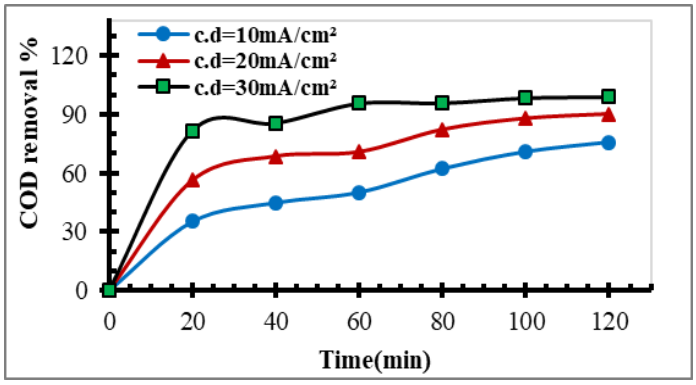

Figure (4.73) The influence of current density variation on COD removal efficiency during EC/EF of O/W treatment, Al-C.felt electrode; initial O/W conc.**300**ppm; volumetric flow rate **2** L/hr.

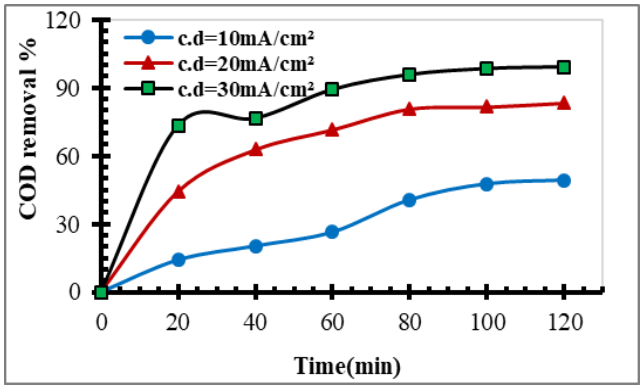

Figure (4.74) The influence of current density variation on COD removal efficiency during EC/EF of O/W treatment, Al- C.felt electrode; initial O/W conc.**300**ppm; volumetric flow rate **4** L/hr.

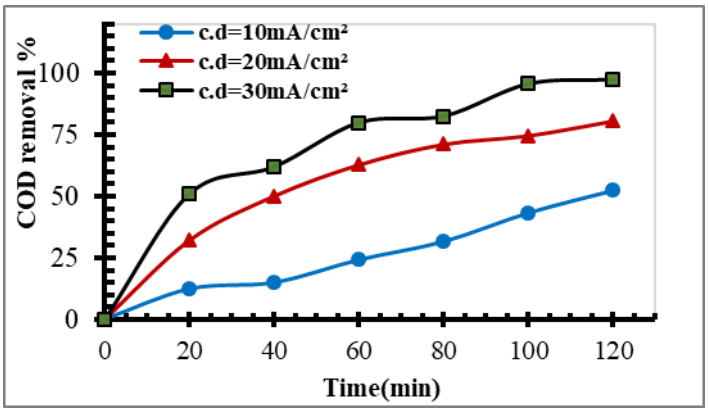

Figure (4.75) The influence of current density variation on COD removal efficiency during EC/EF of O/W treatment, Al-C.felt electrode; initial O/W conc.**300**ppm; volumetric flow rate **6** L/hr.

4.3.2 The Influence of Emulsion Flowrate

The effect of increasing flow rate on decay COD removal efficiency ratio is shown starting in the Figure (4.76- 4.78), initial O/W emulsion concentration 100 ppm, and current density of 10,20,30 mA/cm^2, respectively. at a current density of 10mA/cm^2, emulsion flow rate of 2 L/hr, the accumulated COD% increased from 0.32 % (after 20 min) to 50% at the end of the analysis time (120 minutes),at the O/W emulsion flow rate of 4 L/hr, the COD removal efficiency was 45% while at the highest O/Wemulsion flow rate 6 L/hr the COD removal efficiency decreased to 19.5%, respectively.

The COD removal efficiency at 100 ppm initial O/W concentration and 20 mA/cm^2 current density with different O/W emulsion flow rate 2,4, and 6 L/hr 66.7% at the end of the analysis (120 minutes), for 4 L/hr the COD removal efficiency 53.7% , and 38.14% for 6L/hr.

Also, for a current density of 30 mA/cm^2, the COD removal efficiency was decreased from optimum results 99.8% at 2L/hr O/W emulsion flow rate to 98% at 4L/hr O/W emulsion flow rate and 83.73% for 6L/hr O/W emulsion flow rate, respectively.

Similarly, for initial O/W emulsion concentration of 200 ppm , and a current density of 10 mA/cm^2 , the effect of different flow rate on the COD removal efficiency is shown in Figure (4.79 - 4.81) as follows, at a minimum flow rate of 2 L/hr, the COD removal efficiency was 89.9% , for O/W emulsion flow rate 4 L/hr, the COD removal efficiency 75.8%, while at the highest flow rate of 6 L/hr, the COD removal efficiency decreased to 60% , respectively .

For 200ppm initial O/W concentration, and a current density of 20 mA/cm^2 with different O/W emulsion flowrate,2,4,and 6L/hr the COD removal efficiency were decreased from: 89.96% for 2L/hr O/W emulsion flow rate, 76.88% for 4L/hr O/W emulsion flow rate, and 72% for 6L/hr O/W emulsion flow rate, respectively.

For 200ppm initial O/W concentration, and a current density of 30 mA/cm^2 with different O/W emulsion flowrate,2,4,and 6L/hr the COD removal efficiency were decreased from: 92% for 2L/hr O/W emulsion flow rate, to 85.16% for 4L/hr O/W emulsion flow rate, and 78% for 6L/hr O/W emulsion flow rate, respectively.

Figure (4.82-4.84) showed the results of the COD removal efficiency for the highest concentration of O/W at 300 ppm , and current densities of

10mA/cm² at O/W emulsion flow rates of 2,4, and 6 L/hr, the COD removal efficiency were from: 90.5% for 2L/hr O/W emulsion flow rate, 82.82 % for 4L/hr O/W emulsion flow rate, and from 74% for 6L/hr O/W emulsion flow rate.

Similarly, for 300 ppm initial O/W concentration and a current density of 20mA/cm²,the COD removal efficiency were: 91.5% for 2L/hr O/W emulsion flow rate, 83.98 % for 4L/hr O/W emulsion flow rate, and from 76.17% for 6L/hr O/W emulsion flow rate.

Lastly, for 300 ppm initial O/W concentration and a current density of 30 mA/cm², the COD removal efficiency were: 90% of 2L/hr O/W emulsion flow rate,83.4% for 4L/hr O/W emulsion flow rate, and 79.89% for 6L/hr O/W emulsion flow rate, respectively.

The O/W emulsion flow rate does appear to have an effect on COD removal efficiency by EC/EF reactor (Figure.4.76-4.84), and after 20–120min of treatment, the average COD removal efficiency reductions were 99.8–49%, depending on the flow rate values (2,4 and 6L/h). The best COD removal efficiency (99.8%) results were obtained with a flow rate of 2 L/hr and current density of 30mA/cm^2.

By comparison, for the best conditions ,in the case of using Al-Al electrodes ,the COD removal efficiency as a function of different flow rate under optimal conditions were depicted in Figure (4.12) .It shown, when O/W emulsion flow rate increased from 2 to 4 then to 6L/hr, the COD removal efficiency rates decreased (96.93, 89.07 and 84.11 %) under condition of 100ppm O/W concentration , and for a currant density is 30 mA/cm^2.Also for state of using the Al-Carbon.felt electrode, Figure (4-78) show the optimum condition which give the most efficient removal of COD under 100ppm O/W concentration,30mA/cm^2 current density were (99.8%, 98% to 83.73%)

respectively.

Exactly as expected, the COD removal efficiency of emulsions O/w was found to decrease when the flow rate was increased from 2,4-6L/hr in the continuous operating mode. As slower flow rate increases uptime. A higher run time means that the untreated wastewater solution stays in the EC/EF reactor for a longer time, which in turn provides a longer reaction time. This is consistent with what was achieved by researchers [Kobya et al., 2010].

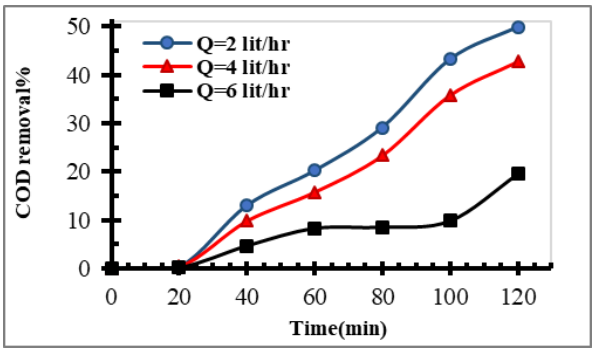

Figure (4-76) COD removal efficiency vs time with different O/W emulsion flowrates **100** ppm O/W. Al- Carbon.felt electrodes, current density **10** mA/cm^2.

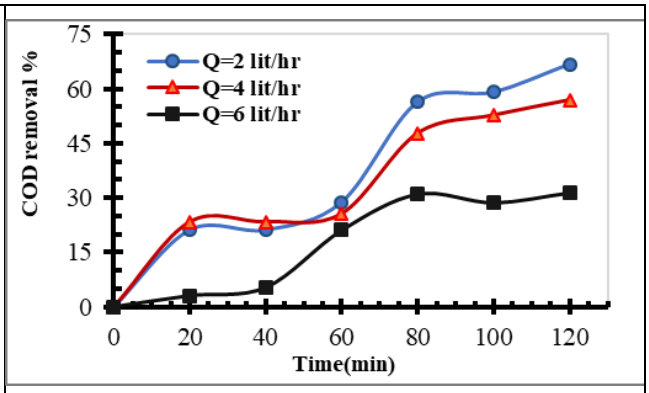

Figure (4-77) COD removal efficiency vs time with different O/W emulsion flowrates **100** ppm O/W. Al-Carbon.felt electrodes, current density **20** mA/cm^2.

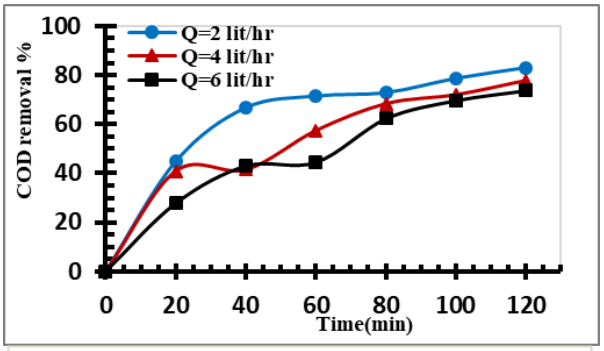

Figure (4-78) COD removal efficiency vs time with different O/W emulsion flowrates **100** ppm O/W. Al- Carbon.felt electrodes, current density **30** mA/cm^2.

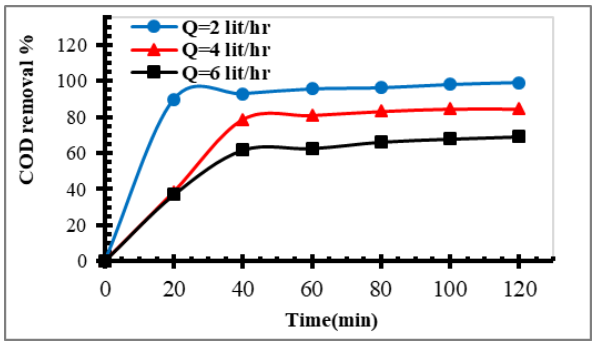

Figure (4-79) COD removal efficiency vs time with different O/W emulsion flowrates **200** ppm O/W. Al- Carbon.felt electrodes, current density **10** mA/cm^2.

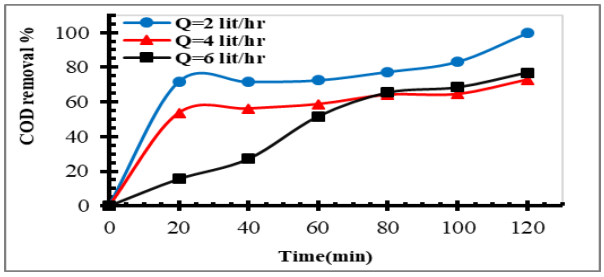

Figure (**4-80)** COD removal efficiency vs time with different O/W emulsion flowrates **200** ppm O/W. Al-Carbon.felt electrodes, current density **20** mA/cm^2.

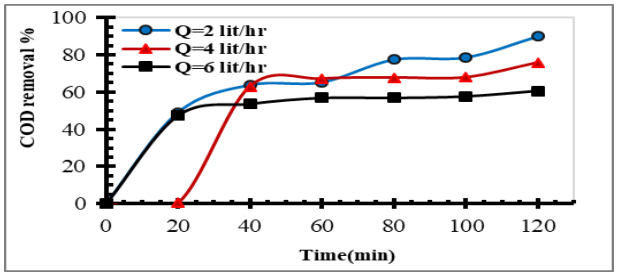

Figure (**4-81)** COD removal efficiency vs time with different O/W emulsion flowrates **200** ppm O/W. Al-Carbon.felt electrodes, current density**30** mA/cm^2.

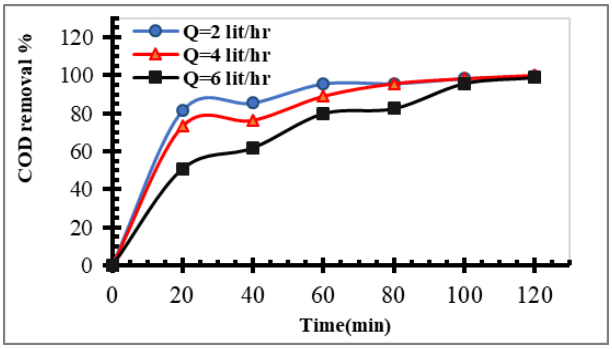

Figure (**4-82)** COD removal efficiency vs time with different O/W emulsion flowrates **300** ppm O/W. Al-Carbon.felt electrodes, current density **10** mA/cm^2.

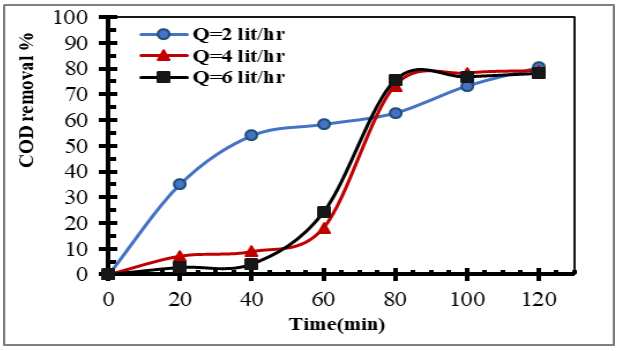

Figure (**4-83)** COD removal efficiency vs time with different O/W emulsion flowrates **300** ppm O/W. Al-Carbon.felt electrodes, current density **20** mA/cm^2.

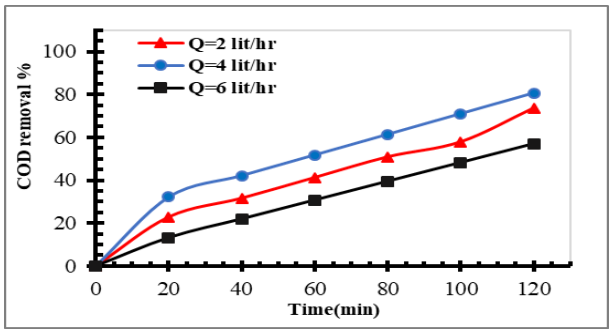

Figure (**4-84)** COD removal efficiency vs time with different O/W emulsion flowrates **300** ppm O/W. Al-Carbon.felt electrodes, current density 3**0** mA/cm^2

4.3.3 The Influence of Initial Crude Oil Concentration

The effect of increasing the initial crude oil concentration (100, 200 , and 300 ppm) on decay COD removal efficiency was studied under different condition of emulsion flowrate and current density parameter, as seen in Figure (4.85- 4.93).current density(10,20,30mA/cm^2),the effect of increase initial O/W concentration at different O/W emulsion flow rate, 2,4 , and 6L/hr.

For 10mA/cm^2 a current density, and 2L/hr, O/W emulsion flow rate, Figure (4.85-4.87) shown the COD removal efficiency decreased from 99 % for 100ppm initial O/W concentration to82% for 200ppm initial O/W concentration then 72.6% for 300ppm initial O/W concentration respectively. The results data are given in appendix B (Table B.6).

Also for 10mA/cm^2 a current density, and 4L/hr, O/W emulsion flow rate, Figure (4.86) shown the COD removal efficiency decreased from 98.7 % for 100ppm initial O/W concentration to 75.8% for 200ppm initial O/W concentration then 43.6% for 300ppm initial O/W concentration respectively.

Figure (4.87) show a decrease in the COD removal efficiency at 6 L / hr O/W emulsion flowrate, 10 mA/cm^{2}current density, the COD removal efficiency decreased from 97.6 % for 100ppm initial O/W concentration to 73.7% for 200ppm initial O/W concentration then 42% for 300ppm initial O/W concentration respectively.

Also, for current density 20 mA/cm^2 with different O/W emulsion flow rate 2,4, and 6 L/hr, Figure (4.88-4.90) explain the decrease of COD removal efficiency with increasing O/W emulsion flowrate.

At current density 20 mA/cm^2 and 2L/hr O/W emulsion flow rate, the COD removal efficiency were 99.37 for 100ppm initial O/W concentration , 76.7%

for 200ppm initial O/W concentration then 66.6% for 300ppm initial O/W concentration respectively.

. At 20 mA/cm^2 current density and 4L/hr O/W emulsion flow rate, the COD removal efficiency were 90.3% for 100ppm initial O/W concentration ,83.4 % for 200ppm initial O/W concentration and 43.6% for 300ppm initial O/W concentration respectively.

For 20 mA/cm^2 current density and 6 L/hr O/W emulsion flow rate, , the COD removal efficiency were 90% for 100ppm initial O/W concentration ,83.73 % for 200ppm initial O/W concentration and 41.26% for 300ppm initial O/W concentration respectively.

Similarly, For 30 mA/cm^2 current density, Figures (4.91-4.93) explain the decrease of the COD removal efficiency with increasing the O/W emulsion flow rate. At 2L/hr O/W emulsion flowrate, the COD removal efficiency were 99.8% for 100ppm initial O/W concentration ,84.5 % for 200ppm initial O/W concentration and 83.4% for 300ppm initial O/W concentration respectively.

At For 30 mA/cm^2 and 4L/hr O/W emulsion flowrate, the COD removal efficiency were : 98% for 100ppm initial O/W concentration ,75.8 % for 200ppm initial O/W concentration and 79% for 300ppm initial O/W concentration respectively.

At For 30 mA/cm^2 and 6L/hr O/W emulsion flowrate, the COD removal efficiency were: 83.73% for 100ppm initial O/W concentration ,73.7 % for 200ppm initial O/W concentration and 78.1% for 300ppm initial O/W concentration respectively.

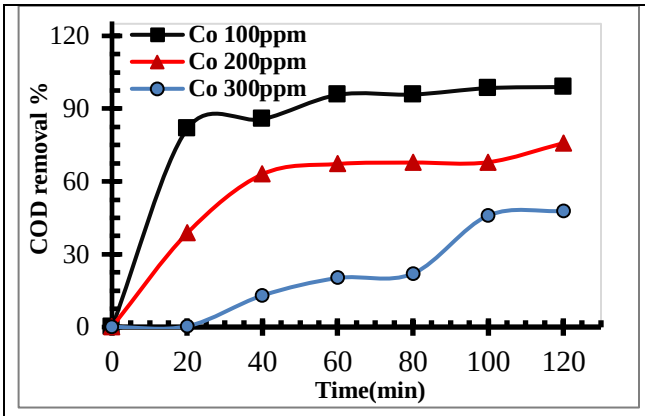

Figure (**4-85**) COD removal efficiency vs time with different O/W emulsion flow rates, **100** ppm O/W. Al-Al electrodes, current density **10** mA/cm^2.

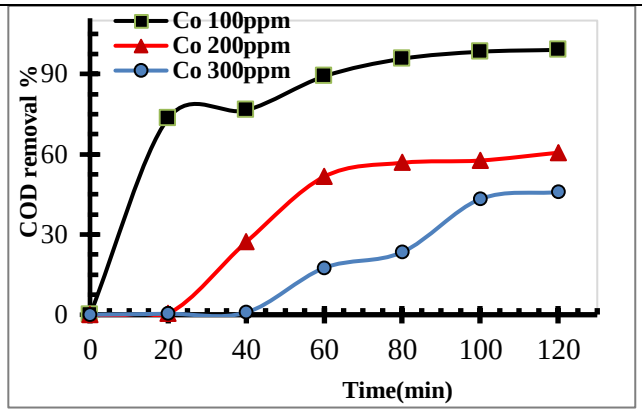

Figure (4-86) COD removal efficiency vs time with different O/W emulsion flow rates, **100 ppm** O/W. Al-Al electrodes, current density **20 mA/cm^2**.

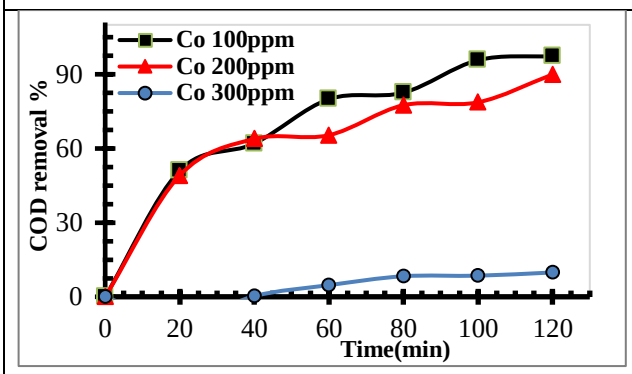

Figure **(4-87)** COD removal efficiency vs time with different O/W emulsion flow rates, **100** ppm O/W. Al-Al electrodes, current density **30** mA/cm^2.

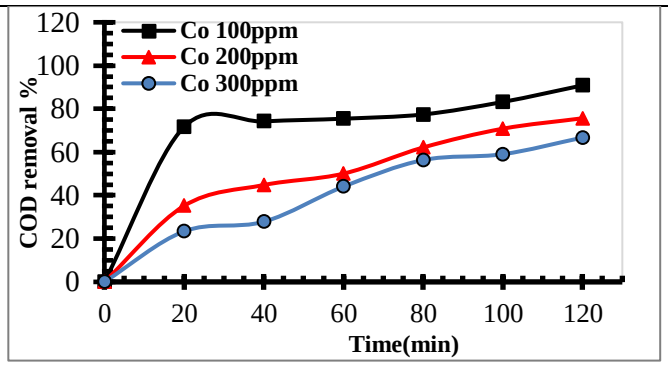

Figure (**4-88)** COD removal efficiency vs time with different O/W emulsion flow rates, **200** ppm O/W. Al-Al electrodes, current density **10** mA/cm^2.

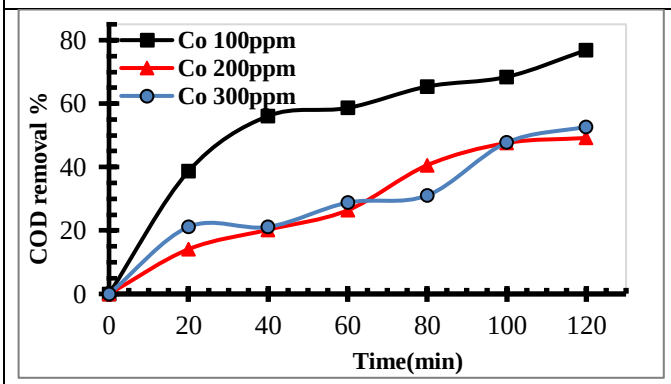

Figure (**4-89)** COD removal efficiency vs time with different O/W emulsion flow rates, **200** ppm O/W. Al-Al electrodes, current density **20** mA/cm^2.

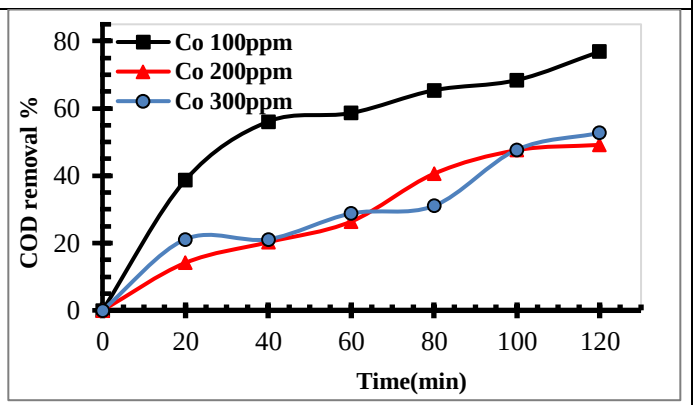

Figure (**4-90)** COD removal efficiency vs time with different O/W emulsion flow rates, **200** ppm O/W. Al-Al electrodes, current density **30** mA/cm^2.

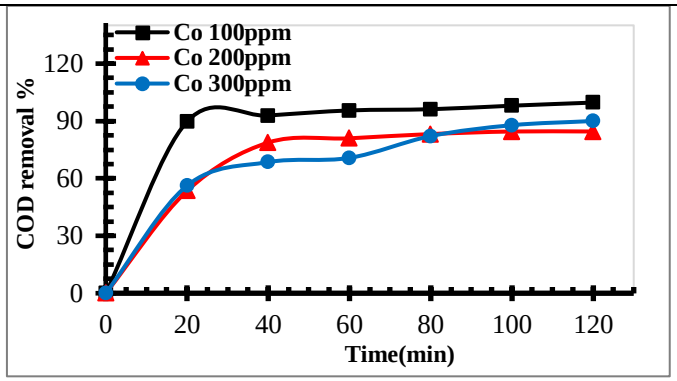

Figure (**4-91)** COD removal efficiency vs time with different O/W emulsion flow rates, **300** ppm O/W. Al-Al electrodes, current density **10** mA/cm^2.

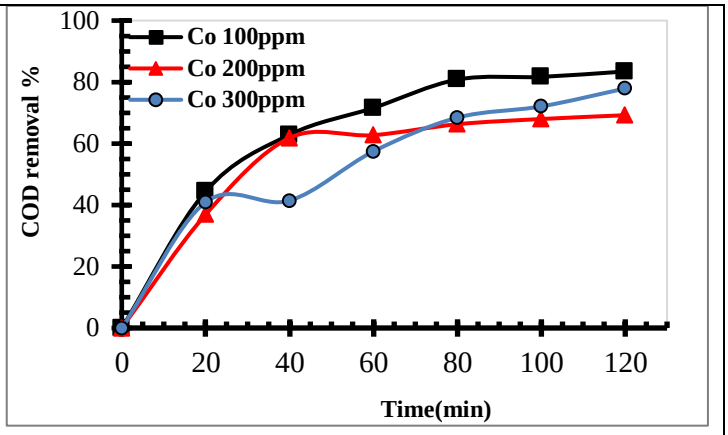

Figure **(4-92)** COD removal efficiency vs time with different O/W emulsion flow rates, **300** ppm O/W. Al-Al electrodes, current density **20** mA/cm2.

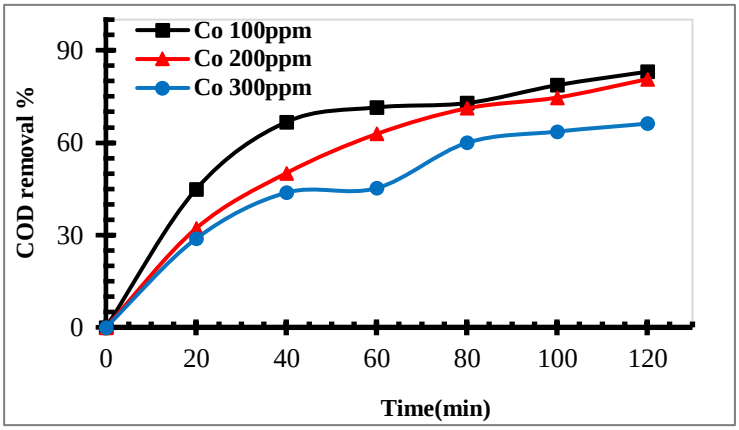

Figure (**4-93)** COD removal efficiency vs time with different O/W emulsion flow rates, **300** ppm O/W. Al-Al electrodes, current density **30** mA/cm^2.

4.3.4 Current Efficiency Variation(CE)

The results show the variance of current efficiency (CE) versus emulsion flow rate for demulsification using Al-Carbon felt electrodes for O/W treatment by the hybrid EC/EF method under conditions of different current densities, and initialO/W concentrations in Figures (4.94–4.99). It is clear that the increase in the current density led to a decrease in the current efficiency, and the process was said to be controlled by mass transfer. However, at a current densityas low as 10 mA/cm^2, it often exceeded 100%. The results data are given in appendix B

(Table B.8).

Figure (4.94–4.99), show the current efficiency (CE) variation against the O/W emulsion flow rate of EC/EF of petroleum refinery wastewater demulsification under different conditions of current densities (10,20, and 30 mA/cm^2), and different initial O/W concentration (100, 200, and 300 ppm).The difference in a current efficiency CE values against the increase in anO/W emulsion flow rate of 2.4, and 6 L/hr shown in Figure (4.94).

For 100 ppm initial O/W concentrations, applied current density was 10 mA/cm^2, it is illustrated in Figure (4.94), where the current efficiency (CE) was 142.8% at 2L/hr O/W emulsion flow rate ,113.1% at 4L/hr O/W emulsion flow rate, and150% at 6L/hr O/W emulsion flow rate respectively.When increase of 20 mA/cm^2 current density, the CE are illustrated in same Figure, were: 139.65%,127.5%, and 163.65%, for 2,4 and 6L/hr O/W emulsion flow rate respectively. For the current density of 30 mA/cm^2, the current efficiency were: 142.3%,136.2%, and 144.3, for 2,4 and 6L/hr O/W emulsion flow rate respectively.

Figure (4.95) shown the variation values of current efficiency with flow rate as a function of current density (10,20,30mA/cm^2) during EC/EF of O/W emulsion treatment at 200 ppm O/W concentration, were136.2%,150.9%, and117.6% for 2,4 and 6L/hr O/W emulsion flow rate, respectively. For 20 mA/cm^2 current density, CE value were: 161.4%,176.4%, and 144% for 2,4 and 6L/hr O/W emulsion flow rate, respectively. For 30 mA/cm^2 current density, CE value were,125.2%125.7%, and 121.7%, for 2,4 and 6L/hr O/W emulsion flow rate, respectively.

Figure (4.96) illustrated the variation values of current efficiency with flow rate as a function of current density (10,20,30mA/cm^2) during EC/EF of O/W emulsion treatment at 300 ppm O/W concentration, were126%,120%,

and131.4% for 2,4 and 6L/hr O/W emulsion flow rate, respectively. For 20 mA/cm^2 current density, CE value were: 140.7%,132.3%, and 146.7% for 2,4 and 6L/hr O/W emulsion flow rate, respectively. For 30 mA/cm^2 current density, CE value were,136.5%108.1%, and 140.8% for 2,4 and 6L/hr O/W emulsion flow rate, respectively

Similarly, Figure (4.97-4.99) shows the influence of current efficiency variation verses O/W emulsion flow rate under different initial O/W concentration under different current density (10,20, and 30 mA/cm^2).

Figure (4-97) shows the variation of current efficiency with volumetric flow rate as a function of 100,200,300ppm initial O/W concentration, and 10 mA/cm^2 current density during 120 minutes of EC/EF method of O/W emulsion demulsification.

For 100ppm initial O/W concentration, and 10 mA/cm^2, the current efficiency were; 142.8%,113.1%, and150% for 2,4 and 6L/hr O/W emulsion flow rate, respectively.

For 200ppm initial O/W concentration, and 10 mA/cm^{2,} the current efficiency were:136.2%,150.9%, and117.6% for 2,4 and 6L/hr O/W emulsion flow rate, respectively.

For 300ppm initial O/W concentration, and 10 mA/cm^2, the current efficiency were:126%,120%, and131.4% for 2,4 and 6L/hr O/W emulsion flow rate, respectively.

Figure (4-98) shows the variation of current efficiency with volumetric flow rate as a function of 100,200,300ppm initial O/W concentration, and 20 mA/cm^2 current density during 120 minutes of EC/EF method of O/W emulsion demulsification.

For 100ppm initial O/W concentration, and 20 mA/cm^2, the current efficiency were; 139.65%,127.5%, and 163.65%, for 2,4 and 6L/hr O/W emulsion flow

rate, respectively.

For 200ppm initial O/W concentration, and 20 mA/cm^2, the current efficiency were; 161.4%,176.4%, and 144%, for 2,4 and 6L/hr O/W emulsion flow rate, respectively.

For 300ppm initial O/W concentration, and 20 mA/cm^2, the current efficiency were; 140.7%,132.3%, and 146.7%. for 2,4 and 6L/hr O/W emulsion flow rate, respectively.

Figure (4-99) shows the variation of current efficiency with volumetric flow rate as a function of 100,200,300ppm initial O/W concentration, and 30 mA/cm^2 current density during 120 minutes of EC/EF method of O/W emulsion demulsification.

For 100ppm initial O/W concentration, and 30 mA/cm^2, the current efficiency were; 142.3%,136.2%, and 144.3, for 2,4 and 6L/hr O/W emulsion flow rate, respectively.

For 200ppm initial O/W concentration, and 30 mA/cm^2, the current efficiency were; 125.2%125.7%, and 121.7%, for 2,4 and 6L/hr O/W emulsion flow rate, respectively.

For 300ppm initial O/W concentration, and 30 mA/cm^2, the current efficiency were; 136.5%108.1%, and 140.8%, for 2,4 and 6L/hr O/W emulsion flow rate, respectively.

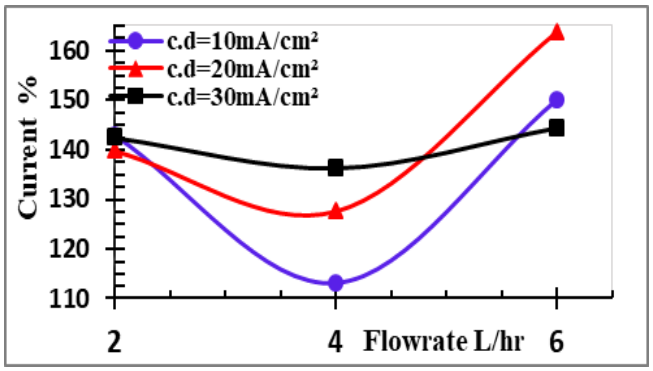

Figure (4-94) Variation of Current efficiency with O/W emulsion flow rate at different current densities, Al-C.felt electrode; initial O/W concentration 1**00** ppm

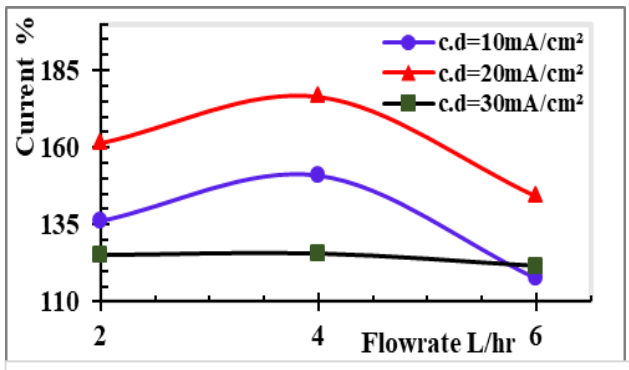

Figure (4-95) Variation of Current efficiency with O/W emulsion flow rate at different current densities, Al-C.felt electrode; initial O/W concentration 200 ppm

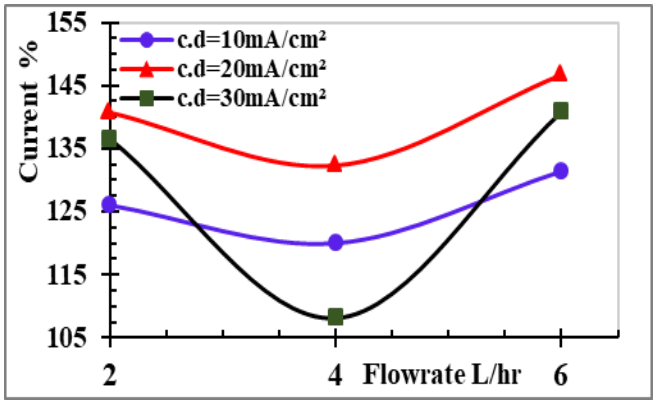

Figure (4-96) Variation of Current efficiency with O/W emulsion flow rate at different current densities, Al- C.felt electrode; initial O/W concentration **300** ppm

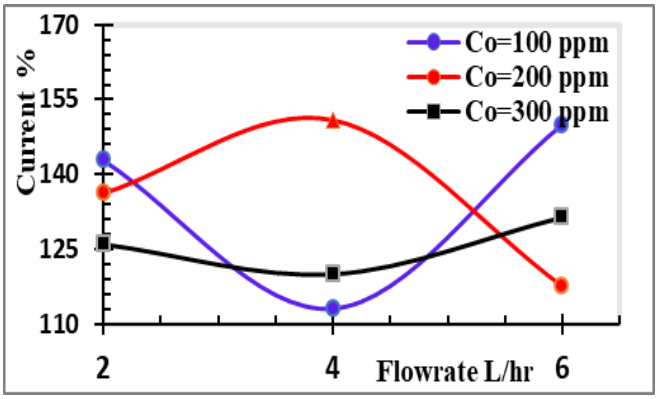

Figure (4-97) Variation of Current efficiency with O/W emulsion flowrate at different current densities, Al- C.felt electrode; **10** mA/cm^2 current density

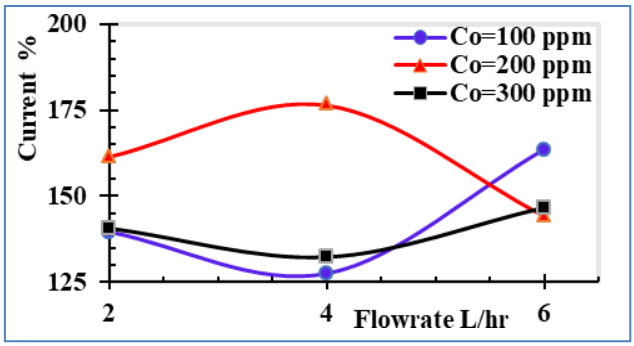

Figure (4-98) Variation of Current efficiency with O/W emulsion flowrate at different current densities, Al- C.felt electrode; **20** mA/cm^2 current density

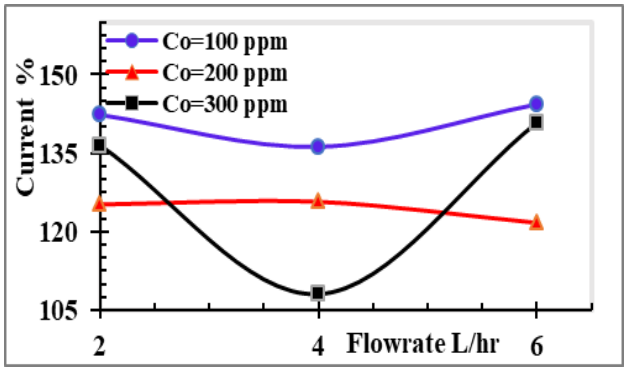

Figure (4-99) Variation of Current efficiency with O/W emulsion flowrate at different current densities, Al- C.felt electrode; **30** mA/cm^2 current density

Compared with aluminum-aluminum electrodes, the current efficiency values are higher (often exceeding 100%), although they decrease with the increase in current density, but they also decrease at flow rates of 4 L/hr, and rise again at higher flow rates, due to the increase of dissolved ions from the anode electrode. Because the electrode dissolution potential is higher than the voltage applied to the reactor, this work agrees with the researchers [Chen, 2004].

4.3.5 Specific Electrical Energy Consumption

Figure (4.100- 4.126) shown variation of the specific electrical energy consumption SEEC (kWh/m^3) with time at different condition of O/W emulsion flow rate, current density, initial O/W emulsion concentration.

The effect of SEEC is shown in Figure (4.100- 4.102), 100 ppm initial O/W concentration, and current density of 10, 20, 30 mA/cm^2, respectively. It can be seen that increasing the O/W emulsion flow rate from 2 ,4, and 6 L/hr leads to a decrease SEEC. All results data are shown in Appendix B.7 Table(B.7).

SEEC (kWh/m^3) variation during hybrid EC/EF treatment of oily wastewater treatment at 100 ppm initial O/W concentration ,10 mA/cm^2 current density, and different O/W flow rate (2,4, and 6L/hr) are shown in Figure (4.100). As seen the SEEC for 2L/hr O/W emulsion flow rate, was 1.125 kWh/m^3, 1.4kWh/m^3 at 4L/hr O/W emulsion flow, and1.008kWh/m^3 for 6L/hr O/W emulsion flow, respectively.

For 100 ppm initial O/W concentration,20 mA/cm^2 current density, and different O/W flow rate (2,4, and6L/hr) is shown in Figure (4.101). As seen the SEEC for 2L/hr O/W emulsion flow rate, was 6.2 kWh/m^3,3.25 kWh/m^3 at 4L/hr, and 2.3kWh/m^3 when flow rate rises to 6L/hr, respectively.

For 100 ppm initial O/W concentration ,30 mA/cm^2 current density, and

different O/W flow rate (2,4, and6L/hr) is shown in Figure (4.102). As seen the SEEC for 2L/hr O/W emulsion flow rate, was 11.85 kWh/m^3, 3.93 kWh/m^3 at 4L/hr, and 2.15kWh/m^3 when flow rate rises to 6L/hr, respectively.

Similarly, for 200 ppm initial O/W concentration ,10 mA/cm^2 current density, and different O/W flow rate (2,4, and 6L/hr), shown in Figure (4.103). As seen the SEEC for 2L/hr O/W emulsion flow rate, was 2.82 kWh/m^3,1.55 kWh/m^3 at 4L/hr, and1.5kWh/m^3 when flow rate rises to 6L/hr, respectively.

For 200 ppm initial O/W concentration ,20 mA/cm^2 current density, and different O/W flow rate (2,4, and 6 L/hr) shown in Figure (4.104). As seen the SEEC for 2L/hr O/W emulsion flow rate, was 1.2 kWh/m^3,5.65kWh/m^3 at 4L/hr, and 2.55kWh/m^3 when flow rate rises to 6L/hr, respectively.

For 200 ppm initial O/W concentration ,30 mA/cm^2 current density, and different O/W flow rate (2,4, and 6L/hr) is shown in Figure (4.105). As seen the SEEC for 2L/hr O/W emulsion flow rate, was 1.9kWh/m^3, 9kWh/m^3 at 4L/hr, and 3.82kWh/m^3, when flow rate rises to 6L/hr, respectively.

Also, For 300 ppm initial O/W concentration ,10 mA/cm^2 current density, and different O/W flow rate (2,4, and 6L/hr) is shown in Figure (4.106). As seen theSEEC for 2L/hr O/W emulsion flow rate, was2.42kWh/m^3, 1.25kWh/m^3 at 4L/hr, and 0.598kWh/m^3, when flow rate rises to 6L/hr, respectively.

For 300 ppm initial O/W concentration ,20 mA/cm^2 current density, and different O/W flow rate (2,4 , and 6L/hr) is shown in Figure (4.107). As seen the SEEC for 2L/hr O/W emulsion flow rate, was 0.35 kWh/m^3,3.62kWh/m^3 at 4L/hr, and to 2.72kWh/m^3 when flow rate rises to 6L/hr, respectively.

For 300 ppm initial O/W concentration ,30 mA/cm^2 current density, and different O/W flow rates shown in Figure (4.108). As seen theSEEC for 2L/hr O/W emulsion flow rate, was 1.75 kWh/m^3, 7.5kWh/m^3 at 4L/hr, and 4.16

kWh/m^3 at 6L/hr, respectively.

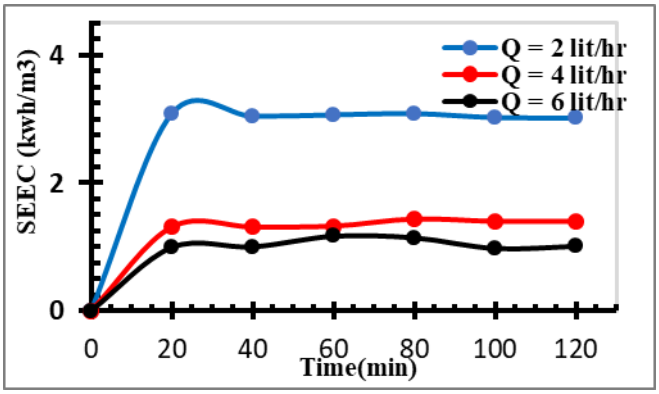

Figure **(4.100)** Variation of the specific electrical energy consumption SEEC (kwh/m3) with Time at different emulsion flow rates, **100 ppm** initial O/W emulsion conc., Al-Al electrode, and current density **10 mA/cm^2**

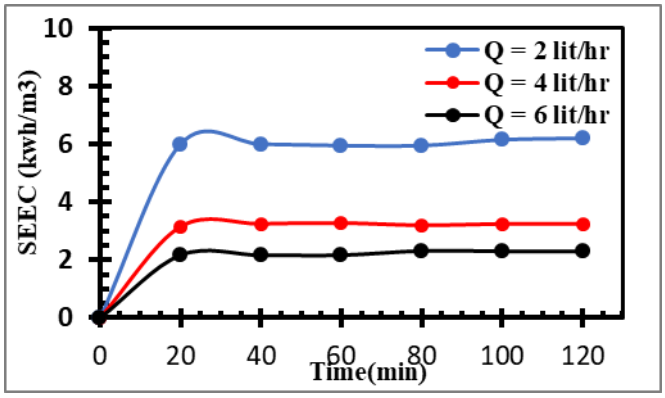

Figure **(4.101)** Variation of the specific electrical energy consumption SEEC (kwh/m3) vs Time during EC/EF treatment for **100 ppm** initial crude oil concentration of O/W emulsion, Al-Al electrode, and current density **20mA/cm^2**

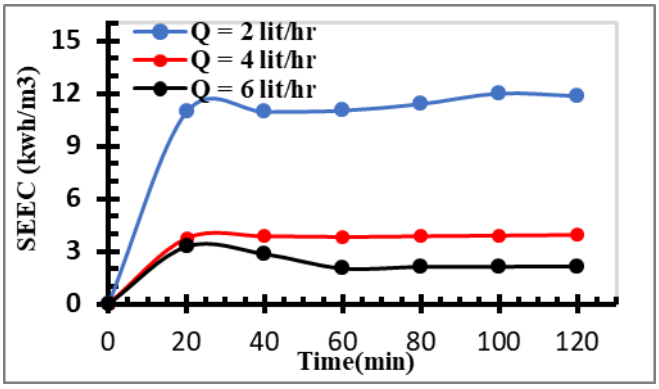

Fig **(4.102)** Variation of the specific electrical energy consumption SEEC (kwh/m3) vs Time during EC/EF treatment for **100 ppm** initial crude oil concentrationof O/W emulsion, Al-Al electrode, and current density **30mA/cm^2**

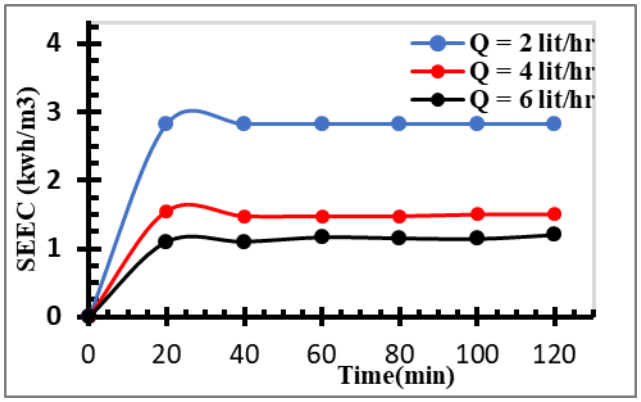

Fig **(4.103)** Variation of the specific electrical energy consumption SEEC (kwh/m3) vs Time during EC/EF treatment for 2**00 ppm** initial crude oil concentration of O/W emulsion, Al-Al electrode, and current density **10mA/cm^2**

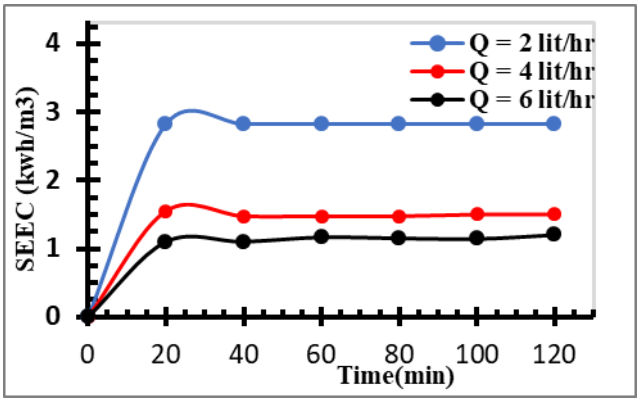

Fig **(4.104)** Variation of the specific electrical energy consumption SEEC (kwh/m3) vs Time during EC/EF treatment for **200 ppm** initial crude oil concentration of O/W emulsion, Al-Al electrode, and current density **20mA/cm^2**

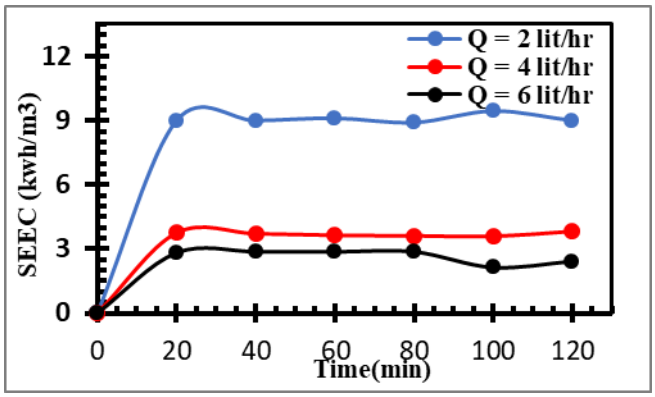

Fig **(4.105)** Variation of the specific electrical energy consumption SEEC (kwh/m3) vs Time during EC/EF treatment for 2**00 ppm** initial crude oil concentration of O/W emulsion, Al-Al electrode, and current density 3**0mA/cm^2**

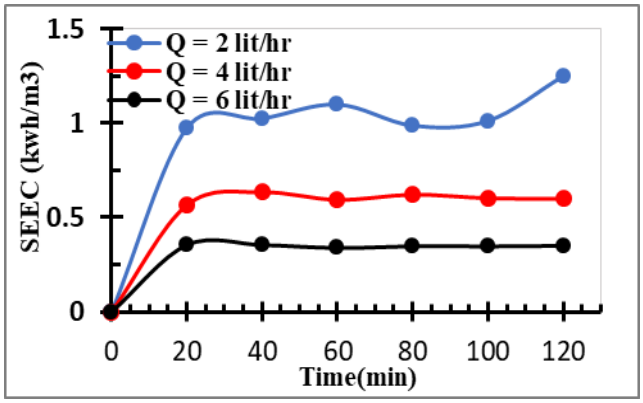

Figure **(4.106)** Variation of the specific electrical energy consumption SEEC (kwh/m3) vs Time during EC/EF treatment for 3**00 ppm** initial crude oil concentration of O/W emulsion, Al-Al electrode, and current density **10mA/cm^2**

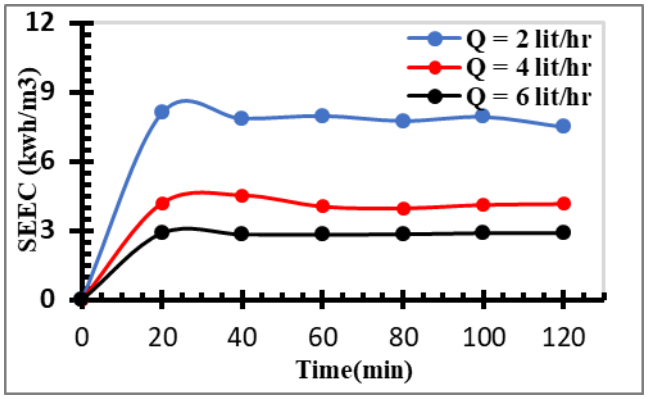

Figure **(4.107)** Variation of the specific electrical energy consumption SEEC (kwh/m3) vs Time during EC/EF treatment for 3**00 ppm** initial crude oil concentration of O/W emulsion, Al-Al electrode, and current density **20mA/cm^2**

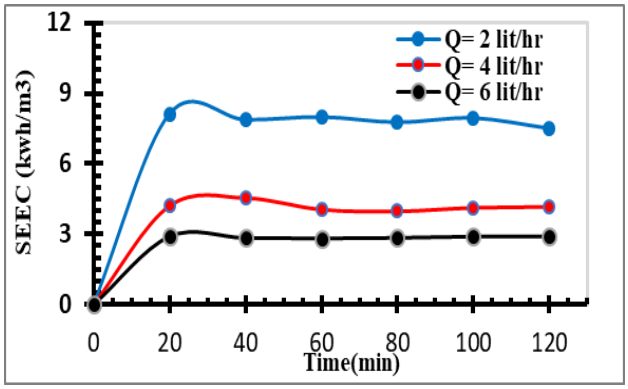

Figure **(4.108)** Variation of the specific electrical energy consumption SEEC (kwh/m3) vs Time during EC/EF treatment for 3**00 ppm** initial crude oil concentration of O/W emulsion, Al-Al electrode, and current density **30mA/cm^2**

Figure (4.109-4.117) illustrates the effect of SEEC with time at different current densities using O/W emulsion by hybrid EC/EF method with constant concentration, and flow rate, the results show with increasing current density, SEEC increases.

For 100 ppm initial O/W emulsion concentration, and O/W emulsion flow rate 2L/hr with different current density (10,20, and 30 mA/cm^2), shown in Figure

(4.109). As seen the SEEC were1.12kWh/m^3 at 10 mA/cm^2,6.2kWh/m^3 at 20mA/cm^2, and11.85kWh/m^3 when current density was 30mA/cm^2, respectively.

For 100 ppm initial O/W concentration, and O/W emulsion flow rate 4L/hr with different current density (10,20, and30 mA/cm^2), shown in Figure (4.110). As seen the SEEC were: 1.4kWh/m^3 at 10 mA/cm^2,3.25kWh/m^3 at 20mA/cm^2, and3.93kWh/m^3 when current density was 30mA/cm^2, respectively.

For 100 ppm initial O/W concentration, and O/W emulsion flow rate 6L/hr with different current density (10,20 , and30 mA/cm^2), shown in Figure (4.111). As seen the SEEC were: 1.008kWh/m^3 at 10 mA/cm^2,2.3kWh/m^3 at 20mA/cm^2, and2.15kWh/m^3 when current density was 30mA/cm^2, respectively.

Also, for 200 ppm initial O/W concentration, and O/W emulsion flow rate 2L/hr with different current density (10,20 , and30 mA/cm^2), shown in Figure (4.112). As seen the SEEC were 2.82kWh/m^3 at 10 mA/cm^2,5.65kWh/m^3 at 20mA/cm^2, and9kWh/m^3 when current density was 30mA/cm^2, respectively.

For 200 ppm initial O/W concentration, and O/W emulsion flow rate 4L/hr with different current density (10,20 , and30 mA/cm^2), shown in Figure (4.113).As seen the SEEC were:1.5 kWh/m^3 at 10 mA/cm^2, 2.55 kWh/m^3 at 20mA/cm^2, and3.82 kWh/m^3 when current density was 30mA/cm^2, respectively.

For 200 ppm initial O/W concentration, and O/W emulsion flow rate 6L/hr with different current density (10,20, and30 mA/cm2), shown in Figure (4.114). As seen the SEEC were:1.2 kWh/m3 at 10 mA/cm2, 1.9 kWh/m3 at 20mA/cm2, and2.42 kWh/m3 whenbcurrent density was 30mA/cm2, respectively.

Similarly, for 300 ppm initial O/W concentration, and O/W emulsion flow rate 2L/hr with different current density (10,20, and30 mA/cm2), shown in Figure (4.115). As seen the SEEC were: 1.25 kWh/m3 at 10 mA/cm2, 3.62

kWh/m^3 at 20mA/cm^2, and 7.5 kWh/m^3 when current density was 30mA/cm^2, respectively.

For 300 ppm initial O/W concentration, and O/W emulsion flow rate 4L/hr with different current density (10,20, and30 mA/cm^2), shown in Figure (4.116). As seen the SEEC were: 0.59 kWh/m^3 at 10 mA/cm^2, 2.72 kWh/m^3 at 20mA/cm^2, and4.16 kWh/m^3 when current density was 30mA/cm^2, respectively.

For 300 ppm initial O/W concentration, and O/W emulsion flow rate 6L/hr with different current density (10,20 , and30 mA/cm^2), shown in Figure (4.117). As seen the SEEC were: 0.35 kWh/m^3 at 10 mA/cm^2, 1.75 kWh/m^3 at 20mA/cm^2, and2.9 kWh/m^3 when current density was 30mA/cm^2, respectively.

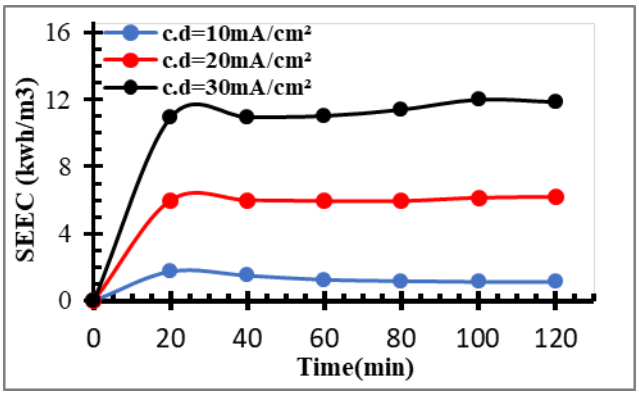

Figure. **(4.109)** Variation of specific electrical energy consumption SEEC (kWh/m^3) with Time at different current densities; Al- C.felt electrode,**100** ppm initial O/W concentration, volumetric flow rate **2** L/hr

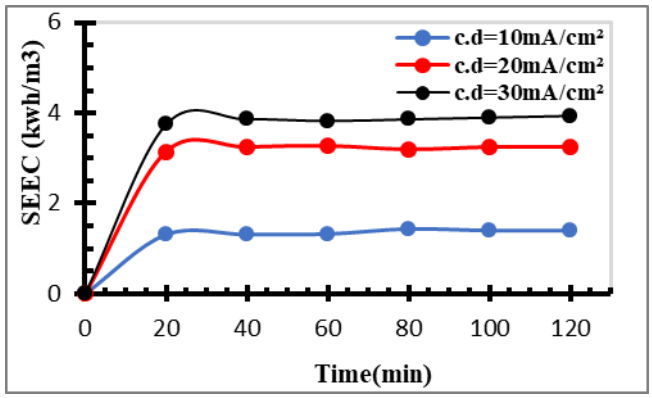

Figure. **(4.110)** Variation of specific electrical energy consumption SEEC (kWh/m^3) with Time for Al- C.felt electrode,**100** ppm initial O/W concentration, volumetric flow rate **4** L/hr

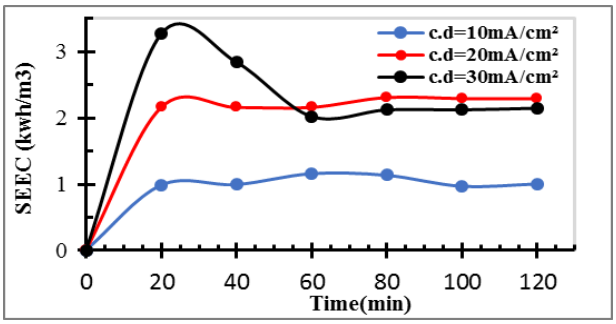

Figure. **(4.111)** Variation of specific electrical energy consumption SEEC (kWh/m^3) with Time for Al- C.felt electrode,**100** ppm initial O/W concentration, volumetric flow rate **6** L/hr

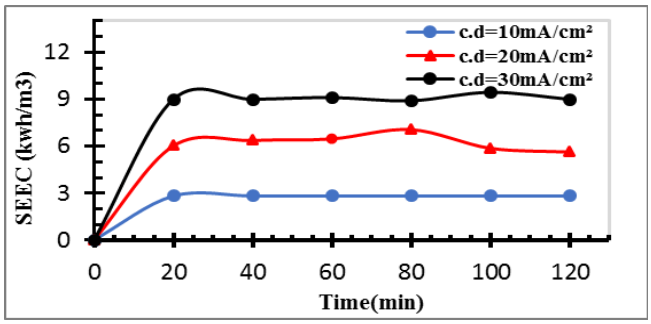

Figure. **(4.112)** Variation of specific electrical energy consumption SEEC (kWh/m^3) with Time for Al- C.felt electrode,**200** ppm initial O/W concentration, volumetric flow rate **2** L/hr

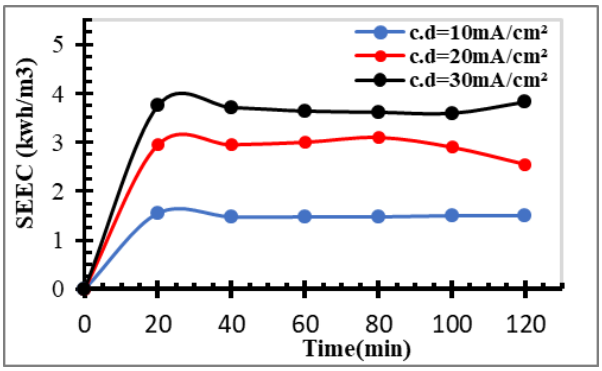

Figure. **(4.113)** Variation of specific electrical energy consumption SEEC (kWh/m^3) with Time for Al-C.felt electrode,2**00** ppm initial O/W concentration, volumetric flow rate **4** L/h

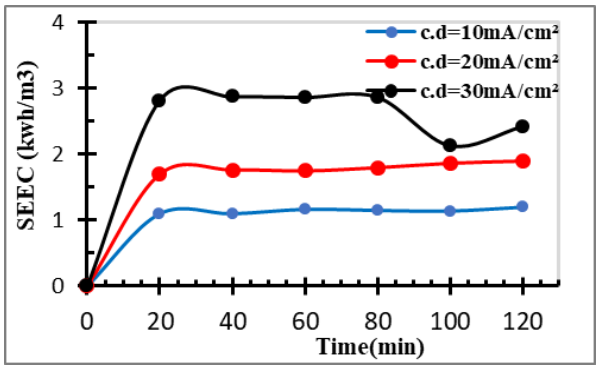

Figure. **(4.114)** Variation of specific electrical energy consumption SEEC (kWh/m^3) with Time for Al-C.felt electrode,2**00** ppm initial O/W concentration, volumetric flow rate **6** L/h

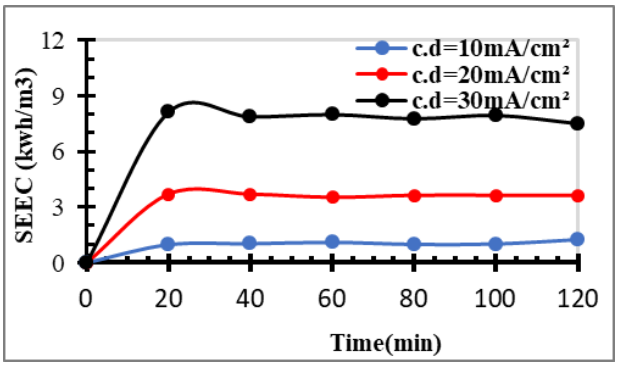

Figure. **(4.115)** Variation of specific electrical energy consumption SEEC (kWh/m^3) with Time for Al-C.felt electrode,**300** ppm initial O/W concentration, volumetric flow rate **2** L/h

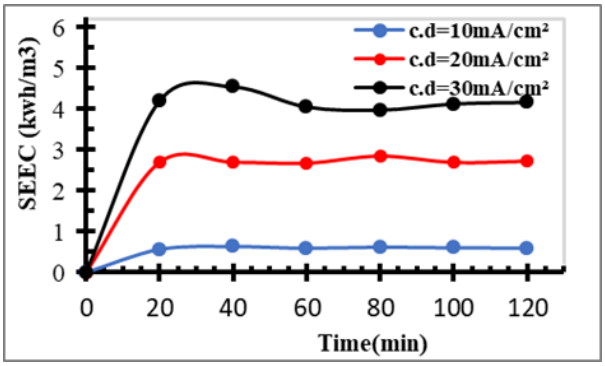

Figure. **(4.116)** Variation of specific electrical energy consumption SEEC (kWh/m^3) with Time for Al-C.felt electrode,**300** ppm initial O/W concentration, volumetric flow rate **4** L/h

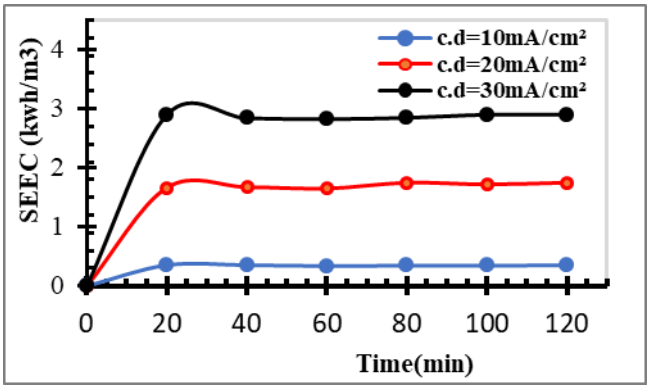

Figure. **(4.117)** Variation of specific electrical energy consumption SEEC (kWh/m^3) with Time for Al-C.felt electrode,**300** ppm initial O/W concentration, volumetric flow rate **6**L/h

The effect of increasing initial O/W concentration (C_o of O/W emulsion) on decay SEEC is shown in Figure (4.118-4.126), using Al-C-felt electrodes, different initial O/W concentration of O/W emulsion for each Figure (100,200, and 300 ppm), a current density of 10,20 , and 30 mA/cm^2 , and different O/W emulsion flow rate 2,4,6L/hr, respectively. It can be seen that increasing the O/W concentrations from 100 to 200 , and 300 ppm leads to a decrease SEEC in hybrid EC/EF at the end of treatment time (120 minutes).

For current density 10 mA/cm^2, O/W emulsion flow rate 2L/hr with different initial O/W concentration, shown in Figure (4.118). As seen the SEEC decreasing when increasing initial O/W concentration during treat by EC/EF.The specific electrical energy consumption were 1.12 kWh/m^3 at 2L/hr O/W emulsion flow rate, 2.82 kWh/m^{3}at 4L/hr, and1.25kWh/m^3 when O/W emulsion flow rate was 6L/hr, respectively.

For current density 10 mA/cm^2, O/W emulsion flow rate 4L/hr with different initial O/W concentration, shown in Figure (4.119). As seen the SEEC decreasing when increasing O/W emulsion concentration, the SEEC were: 1.4 kWh/m^3 at 2L/hr O/W emulsion flow rate, 1.5 kWh/m^3 at4L/hr, and0.59 kWh/m^3 when O/W emulsion flow rate was 6L/hr, respectively.

For current density 10 mA/cm^2, O/W emulsion flow rate 6L/hr with different initial O/W concentration, shown in Figure (4.120). As seen the SEEC decreasing when increasing initial O/W concentration, the SEEC were 1.008 kWh/m^3 at 2L/hr O/W emulsion flow rate, 1.2 kWh/m^{3}at 4L/hr, and 0.35kWh/m^3 when O/W emulsion flow rate was 6L/hr, respectively.

Also, for current density of 20 mA/cm^2, O/W emulsion flow rate 2L/hr with different initial O/W concentration, shown in Figure (4.121). As seen the SEEC decreasing when increasing initial O/W concentration, the SEEC were 6.2 kWh/m^3

at 2L/hr O/W emulsion flow rate, 5.65 kWh/m^3 at 4L/hr, and3.62 kWh/m^3 when O/W emulsion flow rate was 6L/hr, respectively.

For current density 20 mA/cm^2, O/W emulsion flow rate 4L/hr with different initial O/W concentration, shown in Figure (4.122). As seen the SEEC were: 3.25 kWh/m^3 at 2L/hr O/W emulsion flow rate, 2.55 kWh/m^3 at 4L/hr, , and2.72 kWh/m^3 when O/W emulsion flow rate was 6L/hr, respectively.

For current density 20 mA/cm^2, O/W emulsion flow rate 6L/hr with different initial O/W concentration, shown in Figure (4.123). As seen the SEEC were: 2.3 kWh/m^3 at 2L/hr O/W emulsion flow rate, 1.9 kWh/m^3 at4L/hr, and1.75 kWh/m^3 when O/W emulsion flow rate was 6L/hr, respectively.

Similarly, for current density 30 mA/cm^2, O/W emulsion flow rate 2L/hr with different initial O/W concentration, shown in Figure (4.124). As seen **t**he SEEC were: 11.85 kWh/m^3 at 2L/hr O/W emulsion flow rate, 9kWh/m^3 at 4L/hr, and7.5 kWh/m^3 when O/W emulsion flow rate was 6L/hr,respectively.

For current density 30 mA/cm^2, O/W emulsion flow rate 4L/hr with different initial O/W concentration, shown in Figure (4.125). As seen the SEEC were: 3.93 kWh/m^3 at 2L/hr O/W emulsion flow rate, 3.82kWh/m^3 at 4L/hr, and4.16 kWh/m^3 when O/W emulsion flow rate was 6L/hr, respectively.

For current density 30 mA/cm^2, O/W emulsion flow rate 6L/hr with different initial O/W concentration, shown in Figure (4.126). As seen the SEEC were 2.15kWh/m^3 at 2L/hr O/W emulsion flow rate, 2.42 kWh/m^3 at 4L/hr, and2.9 kWh/m^3 when O/W emulsion flow rate was 6L/hr, respectively.

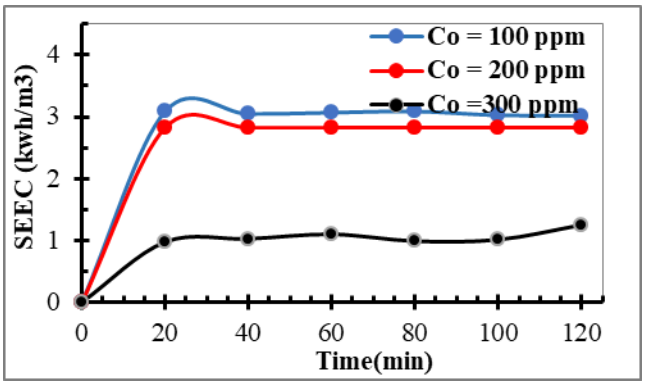

Figure. (**4.118**) Variation of specific electrical energy consumption SEEC (kWh/m^3) with Time during EC/EF method, with different O/W emulsion concentration, current density **10** mA/cm^2, volumetric flow rate **2** L/hr .

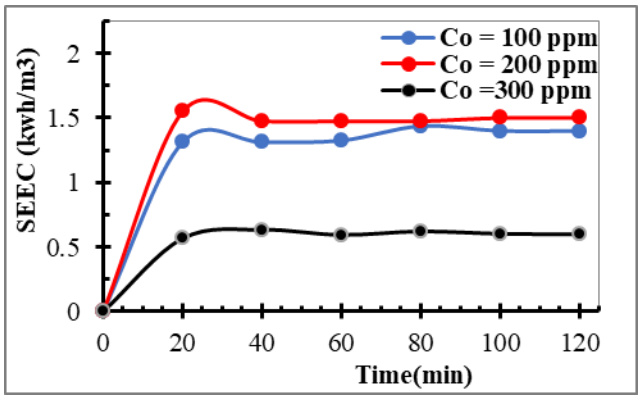

Figure. (**4.119**) Variation of specific electrical energy consumption SEEC (kWh/m^3) with Time during EC/EF method, with different O/W emulsion concentration, current density **10** mA/cm^2, volumetric flow rate **4** L/hr .

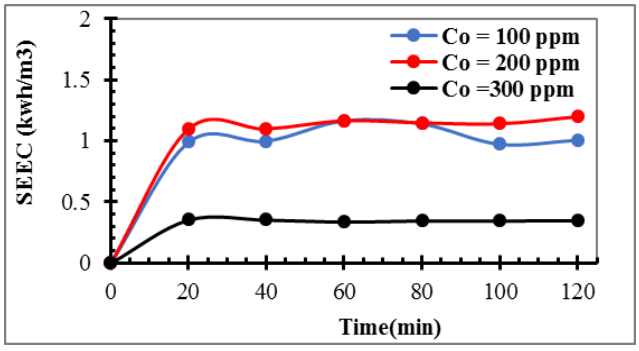

Figure. (**4.120**) Variation of specific electrical energy consumption SEEC (kWh/m^3) with Time during EC/EF method, with different O/W emulsion concentration, current density **10** mA/cm^2, volumetric flow rate 6 L/hr .

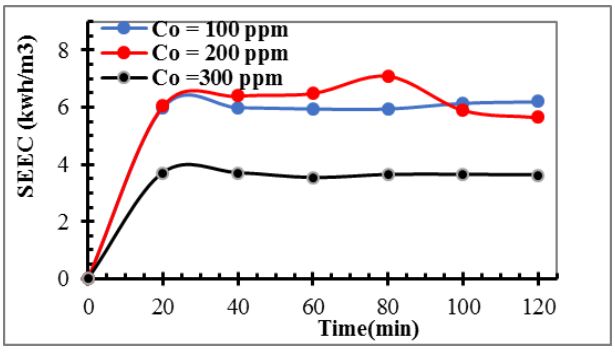

Figure. (**4.121**) Variation of specific electrical energy consumption SEEC (kWh/m^3) with Time during EC/EF method, with different O/W emulsion concentration, current density **20** mA/cm^2, volumetric flow rate **2** L/hr .

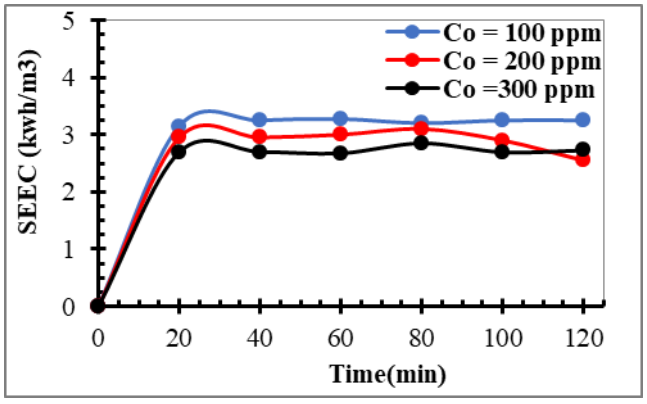

Figure. (**4.122**) Variation of specific electrical energy consumption SEEC (kWh/m^3) with Time during EC/EF method, with different O/W emulsion concentration, current density **20** mA/cm2, volumetric flow rate **4** L/hr.

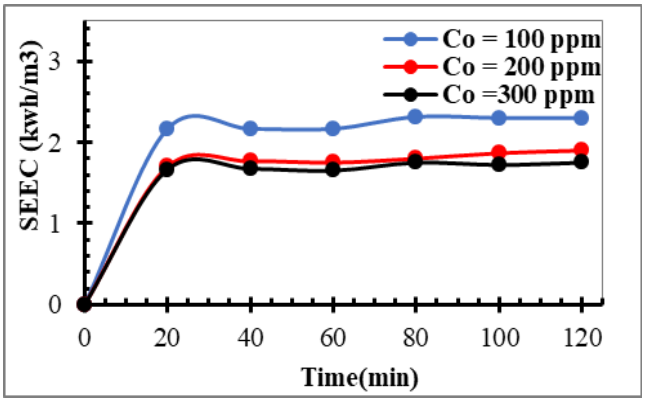

Figure. (**4.123**) Variation of specific electrical energy consumption SEEC (kWh/m^3) with Time during EC/EF method, with different O/W emulsion concentration, current density **20** mA/cm2, volumetric flow rate **6** L/hr.

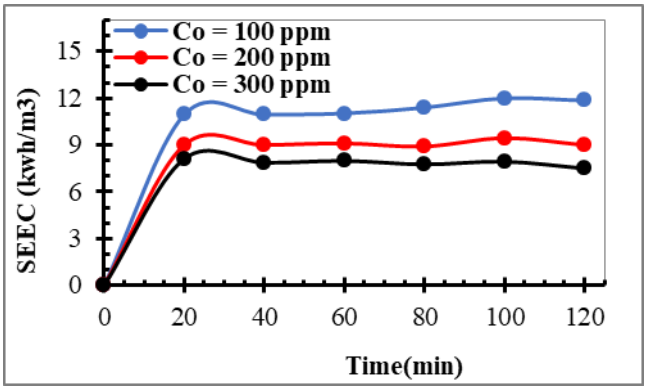

Figure. (**4.124**) Variation of specific electrical energy consumption SEEC (kWh/m^3) with Time during EC/EF method, with different O/W emulsion concentration, current density **30** mA/cm2, volumetric flow rate **2** L/hr.

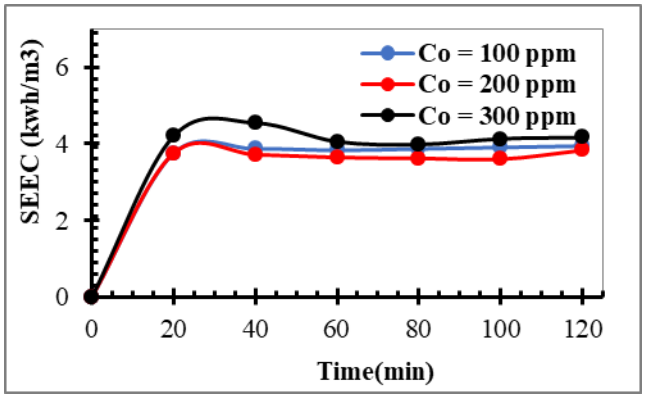

Figure. (**4.125**) Variation of specific electrical energy consumption SEEC (kWh/m^3) with Time during EC/EF method, with different O/W emulsion concentration, current density **30** mA/cm2, volumetric flow rate **4** L/hr.

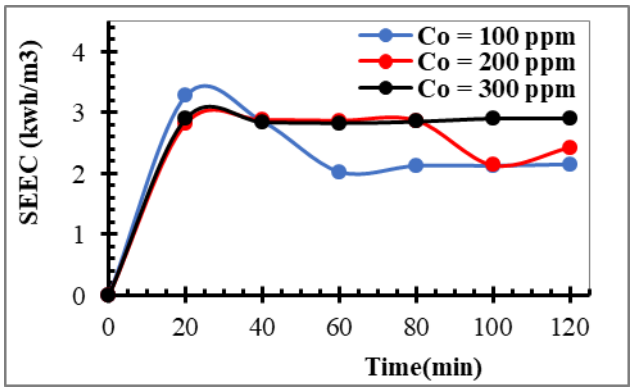

Figure. (**4.126**) The specific electrical energy consumptionSEEC (kwh/m^3) vs Time during EC/EF method, with different O/W emulsion concentration, current density 3**0** mA/cm^2, volumetric flow rate **6** L/hr.

Comparing the SEEC results for the aluminum-carbon field electrodes, founded lower with their counterpart when using aluminium-aluminum, and SEEC decreased as a function of the initial concentrations as well as current density, and flow rate, respectively.Its explanation seems to be an increase in the electroflotation, and thus an increase in the generation of bubbles at the cathode with a larger available surface area, thus higher efficiency, and lower energy required, Previous studieshave made similar observations [Un et al., 2009]; [Esfandiari et al., 2015]. [Paulista 2018].

4.3.6 pH Measurement

Figure (4.127- 4.129) shows the pH-time trend, as an optimum condition for 4L/hr O/W emulsion flow rate, studying the effect of increasing the applied current density on the pH when the initial O/W concentration (100, 200, and300 ppm), respectively. The results data shown in Appendix B, Table (B.9a).

For initial O/W concentration of 100 ppm, and current densities (10, 20, and30 mA/cm^2), the pH increased from its initial value of 7.1 to 8.3, from 7 to 8.3, and from 7.0 to 8.2, respectively, as shown in the Figure (4.127), and appendix B, Table (B.9a).

For 200 ppm initial O/W concentration, and current densities (10, 20, and30 mA/cm^2), the pH increased from its initial value of 6.8 to 7.8, from 6.7 to 7.6, and from 6.9 to 8.3, respectively, as shown in the Figure (4.128), appendix B, Table (B.9).

For 300 ppm initial O/W concentration, and current densities (10, 20, and 30 mA/cm2), pH increased from its initial value of 7.1 to 8.4, from 6.9to 8.2, and from 8.3 to 8.8, respectively, as shown in the Figure (4.63). The pH value increased as the operating time of EC process for both electrodes Was increased which was responsible for flocs production, agree with previous researchers [kobya et al., 2010].

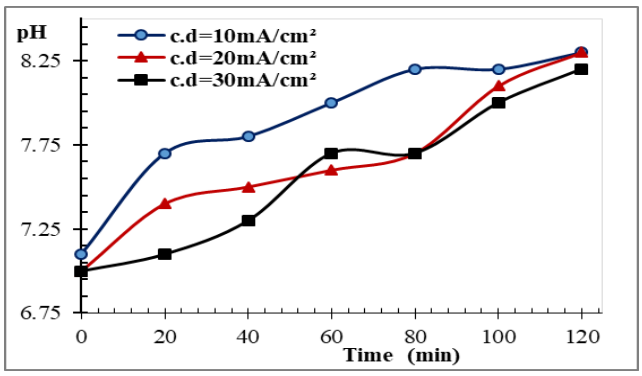

Figure (4.127) pH variation with time at different current densities; initial O/W emulsion conc.**100** ppm, Al-C.felt electrode, volumetric flow rate **4** L/hr

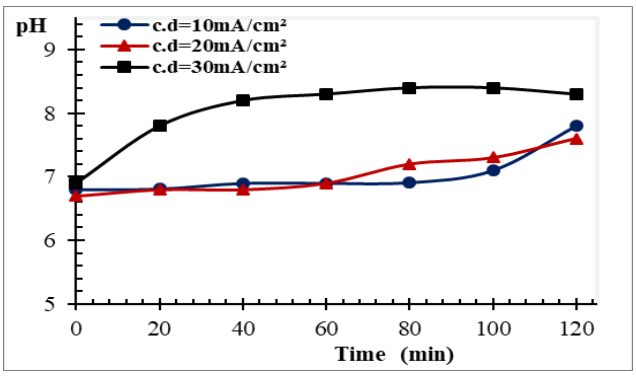

Figure (4.128) pH variation with time during EC/EF process for initial O/W concentration **200** ppm of O/W emulsion, Al-Al electrode, volumetric flow ate **4** L/hr**.**

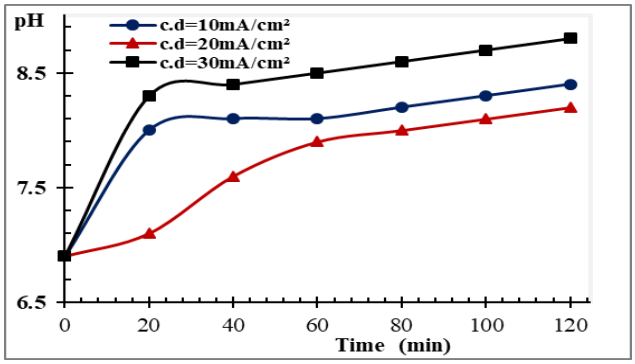

Figure. (4.129) pH variation with time during EC/EF process for initial crude oil concentration **300** ppm of O/W emulsion, Al-Al electrode, volumetric flow ate **4**

4.3.7 Zeta Potential Evaluations

Zeta potential is an effective indicator of the stability of the emulsion, it increases by adding ionic surfactants (SDS) as it has added a negative charge to the oil-water emulsion. On the other h, and, the data shows a decrease in the zeta potentialwith an increase in the concentration of the electrolyte, so increasing the zeta potential at lower concentrations leads to an increase in the stability of the emulsion. this is in agreement with [Kuo & Lee ,2010].

Figure (4.130)shown the best behavior of zeta potentials verses time for different initial O/W concentrations, during EC/EF of demulsification O/W emulsion at condition of current density 30 mA/cm² , and volumetric flow rate 4L/hr, It shows a positive behavior of the removal process of solutions with concentrations of 100, and 200 ppm O/W, in the form of oil effort at the points of intersection with the time axis, assuming that each solution behaves in a straight line during the analysis period. Moreover, the concentration curve approaches 300 ppm million,but at the end of the treatment (120 minutes).

Figure (4.130), and appendix D, Table (D.2) showed analysis of the most optimal samplesat optimal conditions (current density 30 mA/cm^2, emulsion flow rate 4 L/hr), and for the initial O/W concentrations (100, 200, and 300

ppm), for zeta potential.The results data are given in appendix D, Table (D.2)

The results give zeta potential -35.37 mV for initial O/Wemulsion analysis (time zero minutes), and gives the potential -11.18 mV at the end of the analysis (120 minutes), for the first concentration of 100 ppm.

In the case of increasing the initial concentration of O/W to 200 ppm, the results give zeta potential of -39.47mV at the beginning of the analysis, and 17.47mV at the end (120 minutes), respectively.

In the case of the initial O/W concentration of 300ppm, gives zeta potential -70 mV, and -19.04 mV at start, and end of the analysis, respectively.

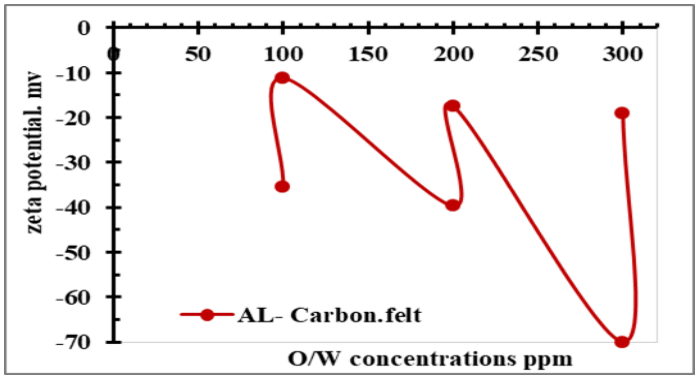

Figure (4.130) Behavior of zeta potentials (mv)) before and after treatment for different initial O/W concentrations during EC/EF of demulsification O/W emulsion, Al-C.felt electrodes, current density **30**mA/cm2, volumetric flow rate 4 L/hr

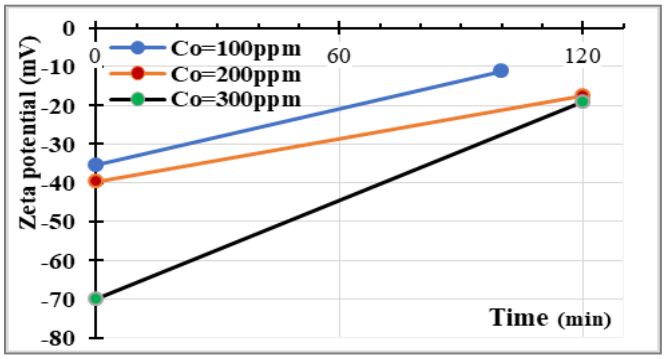

Figure (4.131) Best Behavior of zeta potentials (mv) Vs. Time(min) for different initial O/W concentrations, during EC/EF of demulsification O/W emulsion, Al-C.felt electrodes, current density **30** mA/cm² , volumetric flow rate **4** L/h

Figure (4.132), and (4.132) shows the comparison in the behavior of the zeta potential as a function of initial O/W concentration of the treated solution during the hybrid EC/EF. Curves that use aluminum-aluminum give approving results for the behavior of the zeta potential, as we note that cutting x-axis is evidence that it reached zero during the zeta analysis at the concentrations 200, and 300 ppm.

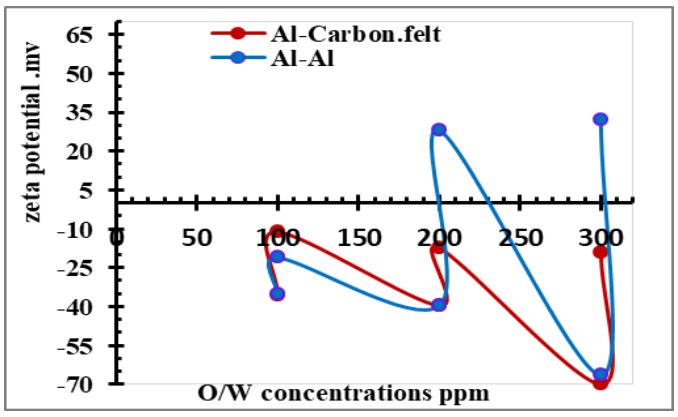

Figure (4.132) Behavior of zeta potentials (mv) before and after treatment for different initial crude oil concentrations during EC/EF of demulsification O/W emulsion, AL-Al, and Al-C.felt, current density **30**mA/cm^2, volumetric flow rate **4**L/hr.

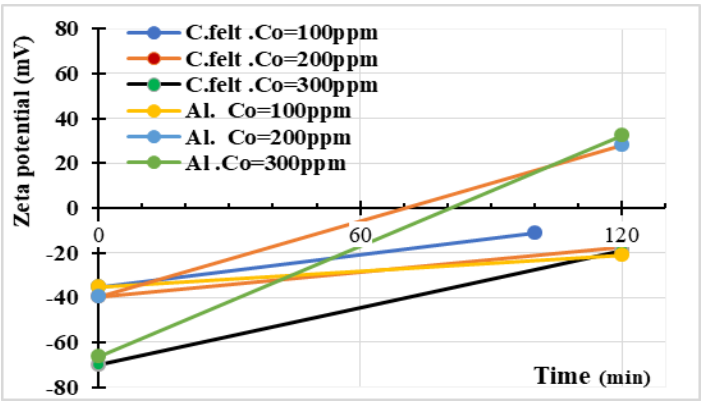

Figure (4.133) Best Behavior of zeta potentials (mv)) before and after treatment for different initial O/W concentration, during EC/EF of demulsification OWemlsion, both electrodes, current density **30** mA/cm², volumetric flow rate **4** L/hr.

4.3.8 Turbidity Evaluations

Appendix B, Table (B.10) shows the one of the optimum results of turbidity reduction duringelectrocoagulation/electroflotation test at the indicated times when the current density increased 10, 20, and 30 mA/cm^2 for the initial O/W concentration of100 ppm, 4 L/hr the volume flow rate of the emulsion O/W.

The results showed that the turbidity decreases with the increase in the current density, in other words removal efficiency of turbidity increases with an increasein the current density. Moreover, the turbidity increases with the increase in the concentration of pollutants in O/Wemulsion, that is, increase in initial O/W concentration the efficiency of removing turbidity decreases. The results data are given in appendix B, Table (B.10). The turbidity decreased sharply for 20 minutes of treatment at different current densities of 10,20,30 mA/cm^2 from 285,81.5, and 101 NTU to 84.4,38.94, and 41.5 NTU**,** respectively, followed by a small decrease at the end of the test as shown in appendix B, Table (B.10).

4.3.9 Total Dissolve Solid, Total Suspended Solid, and Total Solid Evaluation

The demulsification study enhances the removal efficiency of TDS, (TS, TSS). The results data are given in appendix B Table (B.9), (B.10), respectively.

Appendix B Table (B.9), (B.10) models show the results of TDS, (TSS, and TS), respectively,during hybrid EC/EF at optimum conditions, current, and fluorite density of initial O/W concentration of 200 ppm. The tables clearly show a decrease of total dissolved solid, total suspended solid, and total solid, evaluation against a timeof 20 minutes sharply, and then a slight decrease until the end of the analysis time.

4.4. Operational Cost of Hybrid EC/EF

Operational costs are one of the essential aspects of the EC/EF process because they influence the utilization of any wastewater treatment method. The total operation cost includes the direct and indirect costs. [Akarsu and Deniz, 2021], stated that the main parameters in the cost calculation of the EC/EF process are the energy consumption and electrode consumption. However, the operational cost involves cost of chemicals, electrodes and energy consumptions as well as labor, maintenance, flocs disposal, and fixed costs [Kobya et al., 2010].

In this study, the preliminary operational cost was determined using electrodes and electrical energy expenses and the labor cost, using the following formula [Yunksel et al.,2012]:

$$TOc = A_E E_x + B_{Al} E_y + \sum C_i E_i \quad \ldots\ldots\ldots (4.1)$$

Where, *TO*c is the total operational cost in ($/m^3 of treated wastewater)

A_E is the unit price of electricity $/kWh

E_x is the energy consumption/m^3 of solution (SEEC) for EC/EF in kWh

B_{Al} is the unit price of aluminum metal used as electrode for EC/EF

E_y is the electrode consumption per m^3 of solution

C_i is the unit price of chemicals

E_i is the cost of laboratory test used per m^3 of wastewater

The expenses of the included parameters in equation (4.1) according to the Iraqi markets for the first quarter of 2021 are explained in table 4-1.

Table 4-1. Direct and indirect cost parameters for hybrid EC/EF treatment.

Material and Formula	Price ($)	Consumption	
		Al-Al	Al-C felt
Electrical Energy	0.024 $/kWh	9 kWh/m^3	11.3 kWh/m^3
Aluminum	1.9 $/kg	0.0012696kg	0.001423kg
Potassium Dichromate ($K_2Cr_2O_7$)	200 $/kg	0.0000153kg	0.0000153kg
Sulfuric Acid (H_2SO_4)	7 $/kg	0.00046 kg	0.00046 kg
Mercury Sulfate ($HgSO_4$)	450 $/kg	0.00005kg	0.00005kg
Silver Sulfate (Ag_2SO_4)	2000$/kg	0.0000346kg	0.0064kg
Sulfuric Acid (H_2SO_4)	7 $/kg	0.0000064kg	0.0000064kg
Deionized water	0.25 $/kg	0.00027kg	0.00027kg
Sodium Dodecyl Sulphate (SDS)	250 $/kg		
Potassium Hydrogen Phthalate ($C_8H_5KO_4$)	700 $/kg		
Sodium Chloride (NaCl)	20 $/kg		

Since A= 0.024 $/kWh , E_x = 9 kWh/m^3, and B= 1.848 $/kg for Al

$E_y = \Delta m$ (kg)= 7.828g - 6.5584g = 0.0012696 kg Al (for 120 Min. treatment)

$\sum CE = (CE)_1 + (CE)_2 + (CE)_3 + (CE)_4 + (CE)_5$

$\sum CE$ = (200$/kg) (0.00153kg) +(7$/kg) (0.00046 kg) + (450 $/kg) (0.00005kg)
+(2000$/kg) (0.0000346kg) + (7$/kg) (0.00046 kg)
= 0.38 $

1. **Al-Al electrode pair:**

By applying equation 4.1, the total operational cost:

$TOc=(0.024\ \$/kWh)\ (9\ kWh/m^3)+(\ 1.848\ \$/kgAl)(0.5033\ \ kgAl/m^3)+(0.38\$/m^3)$

$= 1.5255\ US\$/m^3$ of treated oily wastewater.

2. **Al-Carbon felt electrode pair:**

By applying equation 4.1, the total operational cost:

$TOc=(0.024\ \$/kWh)(11.3\ kWh/m^3)+(1.848\ \$/kgAl)(0.001423kgAl)+(0.38\ \ \$/m^3)$

$= 0.65383\ US\$/m^3$ of treated oily wastewater.

5 Chapter Five

CONCLUSIONS AND RECOMMENDATIONS

Aqeel Talib

CHAPTER FIVE

CONCLUSIONS AND RECOMMENDATIONS

5.1 Conclusions

From the current study, the following conclusions may be drawn.

1. The findings revealed that increasing current density increased COD removal efficiency, however increasing initial O/W concentration and volumetric flow rate decreased COD removal efficiency.
2. The hight EC/EF conditions for COD removal percent were found to be a current density of 20 and 30mA/cm^2, initial O/W emulsion concentration 100ppm, and 2L/hr volumetric O/W emulsion flowrate with active treatment time (20-40 minutes) for both cases, with a maximum COD removal efficiency of 96.93 %, 99.8 % for Aluminium - Aluminum and Aluminium -Carbon. felt electrodes, respectively.
3. The active and effective treatment time ranges from 20 to 60 minutes, and when the time is extended to 2 hours, a stable state of % removal is achieved.
4. The two pairs of electrodes result revealed of pH=8,7.9, turbidity =16.3 ,119NTU, Ec=2960,2960 µS, TDS =1530,1520ppm, TSS =140, 548ppm, and TS =1670, 2068 ppm, respectively.
5. The Carbon.felt electrode's high surface area and porous form aid in the production of additional hydrogen gas, which improves COD removal efficiency and elevating sludge masses to the top of the reactor.
6. The experiments reveal that the performance and the energy consumption of the EC/EF process were highly affected by the current density. It was found that 30 mA/cm^2, 6L/hr volumetric O/W emulsion flow rate,300 ppm O/W emulsion concentration and 60 min of Al-C. felt treatment offered the best overall performance for the EC/EF process with more

than 89.13% of COD and 81% of turbidity removal, and moderate energy consumption with 0.354 kWh/m^3 of O/W emulsion demulsified.

7. For optimal conditions for Al-Al and Al-C. felt electrodes, the values of current efficiency(Ø) for the two cases 126.96 % and 142.3 %.
8. The results of the zeta potential using aluminum electrodes were better than the results of the aluminum - carbon field at a concentrations of O/W 200, 300 ppm, were, -39.73,27.98mv and -66.41,32.32 mv, respectively. Intersection occurs to x axis which zeta reached to zero as an indication of the stability of the emulsion.
9. XRD diffraction results characterize aluminum hydroxide compounds in sludge generated by electrochemical treatment process according to standard patterns International Center for Diffraction Data (ICDD).
10. The total operating cost (TOc) at optimum condition and best demulsification of the process was estimated at 1.5255 and 0.65383 US$/$m^3$ of treated oily wastewater for the Al electrodes and Al-Carbon-felt electrodes, respectively

5.2 Recommendations

1 / Using several sources of effluent from a different refinery and comparing the outcomes to the present ones.

2 / Study of the effect of pH and the effect of temperature as two main factors.

3 / Use of metals that are cheaper than Al and comparison with the results of the current work.

4 / Combining the EC/EF process with one of the advanced processes such as electrocoagulation / electrochemical oxidation processes.

5/ The use of an ultrasonic separation method for oil-in-water emulsions paired with simultaneous electrolysis may be able to remove up to 100% of grease from the oily wastewater treated.

References

[1]. Abbas, H. K. (2011,). Demulsification of oily water. Department of Chemical Engineering, College of Engineering, Tikrit University, *master's thesis*. & *ref. Malvern Instruments Ltd, Enigma Business Park, GrovewoodRoad, Malvern, Worcestershire, UK ,WR14 1XZ, Tel: +44(0)1684 892456 , Fax: +44 (0)1684 892789.*

[2]. Abd, M. F., Jasim, F. T., & Ahmed, L. S. (2013). Removal of Phenols from Refinery Wastewater Using Trickle Bed Reactor. *Engineering and Technology Journal, 31(18 Part (A) Engineering).*

[3]. Abed, S. M., Abdurahman, N. H., Yunus, R. M., Abdulbari, H. A., & Akbari, S. (2019). Oil emulsions and the different recent demulsification techniques in the petroleum industry-A review. *In IOP Conference Series: Materials Science and Engineering. IOP Publishing (Vol. 702, No. 1, p. 012060).*

[4]. Akarsu, C., & Deniz, F. (2021). Electrocoagulation/electroflotation process for removal of organics and microplastics in laundry wastewater. *Clean–Soil, Air, Water, 49(1), 2000146.*

[5]. Al-Malack, M. H., & Siddiqui, M. (2013). Treatment of synthetic petroleum refinery wastewater in a continuous electro-oxidation process. *Desalination and Water Treatment*, *51*(34-36), *pp.1-12, 6580-6591*.

[6]. Al-Shamrani, A. A., James, A., & Xiao, H. (2002). Separation of oil from water by dissolved air flotation. *Colloids and Surfaces A: Physicochemical and Engineering Aspects*, *209(1), 15-26.*

[7]. Ammar, S. H., Ali, F. D., Shafi, R. F., & Elaibi, A. I. (2018). Zn (II) Removal from wastewater by electrocoagulation/flotation method using new configuration of a split-plate airlift electrochemical reactor. *Journal of Engineering, 24(1), 97-110.*

References

[8]. An, C., Huang, G., Yao, Y., & Zhao, S. (2017). Emerging usage of electrocoagulation technology for oil removal from wastewater: A review. *Science of the Total Environment*, *579*, *537-556*.

[9]. Anglada, A., Urtiaga, A., & Ortiz, I. (2009). Contributions of electrochemical oxidation to waste-water treatment: fundamentals and review of applications. *Journal of Chemical Technology &Biotechnology*, *84(12), 1747–1755.*

[10].Aoudj, S., Khelifa, A., & Drouiche, N. (2017). Removal of fluoride, SDS, ammonia and turbidity from semiconductor wastewater by combined electrocoagulation– electroflotation. *Chemosphere*, *180*, 379-387.

[11].Auflem, I. H, 2002 (Doktor Ingenior Thesis), *Influence of asphaltene aggregation and pressure on crude oil emulsion stability Norwegian University of Science and Technology.*

[12].Cañizares, P., Martínez, F., Lobato, J., & Rodrigo, M. A. (2007). Break-up of oil-in-water emulsions by electrochemical techniques. *Journal of hazardous materials*, *145(1-2), 233-240.*

[13].Changmai, M., Pasawan, M., & Purkait, M. K. (2019). Treatment of oily wastewater from drilling site using electrocoagulation followed by microfiltration. *Separation and purification Technology*, *210*, *463-472.*

[14].Chaturvedi, S. I. (2013). Electrocoagulation: a novel waste water treatment method. *International journal of modern engineering research*, *3(1), 93-100.*

[15].Chen, G. (2004). Electrochemical technologies in wastewater treatment. *Separation and purification Technology*, *38(1), 11-41*.

[16]. Chen, G., Chen, X., & Yue, P. L. (2000). Electrocoagulation and electroflotation of restaurant wastewater. *Journal.*

References

[17].Chen, J. P., Chang, S. Y., & Hung, Y. T. (2005). Electrolysis. In Physicochemical Treatment Processes *(pp. 359-378). Humana Press*.

[18].Chen, X., Chen, G., & Yue, P. L. (2000). Separation of pollutants from restaurant wastewater by electrocoagulation. *Separation and purification technology, 19(1-2), 65-76.*

[19].Chen, X., Chen, G., & Yue, P. L. (2003). Anodic oxidation of dyes at novel Ti/B-diamond electrodes. *Chemical Engineering Science, 58(3-6), 995-1001.*

[20].Coca J., Gutierrez G., And Benito J., (2011)," Treatment of Oily Wastewater", in: J. Coca-Prados and G. Gutiérrez-Cervelló (eds.), Water Purification and Management, *Springer Science+Business Media B.V.*

[21].da Mota, I. D. O., de Castro, J. A., de Góes Casqueira, R., & de Oliveira Junior, A. G. (2015). Study of electroflotation method for treatment of wastewater from washing soil contaminated by heavy metals. *Journal of Materials Research and Technology, 4(2), 109-113.*

[22].Davarnejad, R., Pirhadi, M., Mohammadi, M., & Arpanahzadeh, S. (2015). Numerical analysis of petroleum refinery wastewater treatment using electro-Fenton process. *Chemical Product and Process Modeling, 10(1), 11-16.*

[23].Derjaguin, B. V., & Dukhin, S. S. (1993). Theory of flotation of small and medium-size particles. *Progress in Surface Science, 43(1-4), 241-266.*

[24].Dermentzis, K., Marmanis, D., Christoforidis, A., & Ouzounis, K. (2014). Electrochemical reclamation of wastewater resulted from petroleum tanker truck cleaning. *Environmental Engineering & Management Journal (EEMJ), 13*(9).

[25].Dimoglo, A., Akbulut, H. Y., Cihan, F., & Karpuzcu, M. (2004). Petrochemical wastewater treatment by means of clean electrochemical technologies. *Clean Technologies and Environmental Policy*, 6(4), 288-295.

References

[26].Diya'uddeen, B. H., Daud, W. M. A. W., & Aziz, A. A. (2011). Treatment technologies for petroleum refinery effluents: A review. *Process safety and environmental protection, 89(2), 95-105.*

[27].Do, J. S. & Chen, M. L. (1994). Decolorization of dye-containing solutions by electrocoagulation. Journal of Applied Electrochemistry, *24, 8:785-790.*

[28].Emamjomeh, M. M., & Sivakumar, M. (2009). Review of pollutants removed by electrocoagulation and electrocoagulation/flotation processes. *Journal of environmental management, 90(5), 1663-1679.*

[29].Esfandyari, Y., Mahdavi, Y., Seyedsalehi, M., Hoseini, M., Safari, G. H., Ghozikali, M. G & Jaafari, J. (2015). Degradation and biodegradability improvement of the olive mill wastewater by peroxi-electrocoagulation/electrooxidation-electroflotation process with bipolar aluminum electrodes. *Environmental Science and Pollution Research*, 22(8), 6288-6297.

[30].Eskandarloo, H., Selig, M. J., & Abbaspourrad, A. (2018). In situ H2O2 generation for de-emulsification of fine stable bilge water emulsions. Chemical Engineering Journal, 335, 434-442.

[31].Essadki, A. H., Gourich, B., Vial, C., Delmas, H., & Bennajah, M. (2009). Defluoridation of drinking water by electrocoagulation/electroflotation in a stirred tank reactor with a comparative performance to an external-loop airlift reactor. *Journal of hazardous materials*, *168(2-3), 1325-1333.*

[32].Evdokimov, I. N., & Losev, A. P. (2014). Microwave treatment of crude oil emulsions: Effects of water content. *Journal of Petroleum Science and Engineering*, *115, 24-30*.

[33].Fahim, S. A. (2020, July 1). Comparative study for degradation of effluents in Al-Diwaniya oil refinery wastewater by electrochemical advanced oxidation

processes. Chemical Engineering Department, Faculty of Engineering, Al-Qadisiya University, master's thesis. By Ahmad Salah Fahim *Supervised by (Asst. Prof. Dr.) Ali Hussein Abbar.*

[34].Gao, P., Chen, X., Shen, F., & Chen, G. (2005). Removal of chromium (VI) from wastewater by combined electrocoagulation–electroflotation without a filter. *Separation and purification technology*, *43(2), 117-123.*

[35].Gargouri, B., Gargouri, O. D., Gargouri, B., Trabelsi, S. K., Abdelhedi, R., & Bouaziz, M. (2014). Application of electrochemical technology for removing petroleum hydrocarbons from produced water using lead dioxide and boron-doped diamond electrodes. *Chemosphere*, *117, 309-315.*

[36].Ghernaout, D., Naceur, M. W., & Ghernaout, B. (2011). A review of electrocoagulation as a promising coagulation process for improved organic and inorganic matters removal by electrophoresis and electroflotation. *Desalination and Water Treatment*, *28(1-3), 287-320.*

[37]. Guinea, E., Garrido, J. A., Rodríguez, R. M., Cabot, P. L., Arias, C., Centellas, F., & Brillas, E. (2010). Degradation of the fluoroquinolone enrofloxacin by electrochemical advanced oxidation processes based on hydrogen peroxide electrogeneration. *Electrochimica Acta*, *55*(6), 2101-2115.

[38].Hakizimana, J. N., Najid, N., Gourich, B., Vial, C., Stiriba, Y., & Naja, J. (2017). Hybrid electrocoagulation/electroflotation/electrodisinfection process as a pretreatment for seawater desalination. *Chemical Engineering Science*, *170, 530-541*.

[39].Hami, M. L., Al-Hashimi, M. A., & Al-Doori, M. M. (2007). Effect of activated carbon on BOD and COD removal in a dissolved air flotation unit treating refinery wastewater. *Desalination, 216(1-3), 116-122.*

[40]. Han, M., Zhang, J., Chu, W., Chen, J., & Zhou, G. (2019). Research progress

and prospects of marine oily wastewater treatment: A review. *Water*, *11*(12), 2517.

[41].Hassan, A. K., Hassan, M. M. A., & Hasan, A. F. (2020, November). Treatment of Iraqi Petroleum Refinery Wastewater by Advanced Oxidation Processes. In *Journal of Physics: Conference Series* (Vol. 1660, No. 1, p. 012071). *IOP Publishing.*

[42].Hu, C. Y., Lo, S. L., & Kuan, W. H. (2003). Effects of co-existing anions on fluoride removal in electrocoagulation (EC) process using aluminum electrodes. *Water research, 37(18), 4513-4523.*

[43].İrdemez, Ş., Yildiz, Y. Ş., & Tosunoğlu, V. (2006). Optimization of phosphate removal from wastewater by electrocoagulation with aluminum plate electrodes. *Separation and purification Technology, 52(2), 394-401.*

[44].Issaka, S. A., Nour, A. H., & Yunus, R. M. (2015). Review on the fundamental aspects of petroleum oil emulsions and techniques of demulsification. *Journal of Petroleum & Environmental Biotechnology, 6(2), 1.*

[45].J. Ge, J. Qu, P. Lei, H. Liu, New bipolar electrocoagulation-electroflotation process for the treatment of laundry wastewater, *Sep. Purif. Technol. 36 (2004)33–39.*

[46].Jiang, J., Wu, H., Lu, Y., Ma, T., Li, Z., Xu, D., ... & Bai, B. (2018). Application of α-amylase as a novel biodemulsifier for destabilizing amphiphilic polymer-flooding produced liquid treatment. *Bioresource technology, 259, 349-356.*

[47].Jiang, T. (2010). (Doktor Ingenior Thesis), *Diluted bitumen emulsion characterization and separation*. Rice University. Houston, Texas, USA.

[48].Jiménez, C., Sáez, C., Cañizares, P., & Rodrigo, M. A. (2016). Optimization of a combined electrocoagulation-electroflotation reactor. *Environmental Science and Pollution Research, 23(10), 9700-9711.*

References

[49].Kobya, M., Demirbas, E., Dedeli, A., & Sensoy, M. T. (2010). Treatment of rinse water from zinc phosphate coating by batch and continuous electrocoagulation processes. *Journal of Hazardous Materials, 173(1-3), 326-334.*

[50].Kokal, S., & Al-Juraid, J. (1998, September). Reducing emulsion problems by controlling asphaltene solubility and precipitation. In *SPE Annual Technical Conference and Exhibition*. *OnePetro.*

[51].Kumar, P. R., Chaudhari, S., Khilar, K. C., & Mahajan, S. P. (2004). Removal of arsenic from water by electrocoagulation. *Chemosphere, 55(9), 1245-1252.*

[52].Kuo, C. H., & Lee, C. L. (2010). Treatment of oil/water emulsions using seawater-assisted microwave irradiation. *Separation and Purification Technology*, *74(3), 288-293.*

[53]. Larue, O., Vorobiev, E., Vu, C., & Durand, B. (2003). Electrocoagulation and coagulation by iron of latex particles in aqueous suspensions. *Separation and purification technology*, *31(2), 177-192.*

[54].Le Follotec, A., Pezron, I., Noik, C., Dalmazzone, C., & Metlas-Komunjer, L. (2010). Triblock copolymers as destabilizers of water-in-crude oil emulsions. *Colloids and Surfaces A: Physicochemical and Engineering Aspects*, *365*(1-3), 162-170.

[55].Less, S., Hannisdal, A., Bjørklund, E., & Sjöblom, J. (2008). Electrostatic destabilization of water-in-crude oil emulsions: Application to a real case and evaluation of the Aibel VIEC technology. *Fuel, 87(12), 2572-2581*.

[56].Lin, S. H., Shyu, C. T., & Sun, M. C. (1998). Saline wastewater treatment by electrochemical method. *Water Research*, *32(4), 1059-1066*.

References

[57].Liu, J., Wang, H., Li, X., Jia, W., Zhao, Y., & Ren, S. (2017). Recyclable magnetic graphene oxide for rapid and efficient demulsification of crude oil-in-water emulsion. *Fuel, 189, 79-87.*

[58].Liu, Q. Y., Zhang, Y. B., and Zhao, C. C. (2014). The isolation of bioflocculant producing strains and the application in the oily wastewater treatment process. *Petrol. Sci. Technol. 32:2807–2814.*

[59]. Lundgaard, L. E., Berg, G., Ingebrigtsen, S., & Atten, P. (2005). Electrocoalescence for oil–water separation: fundamental aspects. In *Emulsions and Emulsion stability (pp. 569-612). CRC Press.*

[60].Maiti, S., Mishra, I. M., Bhattacharya, S. D., & Joshi, J. K. (2011). Removal of oil from oil-in-water emulsion using a packed bed of commercial resin. Colloids and surfaces a: physicochemical and engineering aspects, 389(1-3), 291-298.

[61].Majlesi, M., Mohseny, S. M., Sardar, M., Golmohammadi, S., & Sheikhmohammadi, A. (2016). Improvement of aqueous nitrate removal by using continuous electrocoagulation/electroflotation unit with vertical monopolar electrodes. *Sustainable Environment Research, 26(6), 287-290.*

[62].Mazumder, A., Chowdhury, Z., Sen, D., & Bhattacharjee, C. (2020). Electric field assisted membrane separation for oily wastewater with a novel and cost-effective electrocoagulation and electroflotation enhanced membrane module (ECEFMM). *Chemical Engineering and Processing-Process Intensification, 151, 107918.*

[63].Mikula, R. J., & Munoz, V. A. (2000). Characterization of Demulsifiers in Surfactants, Fundamentals and Applications in the Petroleum Industry, *Schramm, LL., Cambridge University Press: Cambridge, UK, PP.51-78.*

[64].Mohammed, T. J., Mohammed, S. S., & Khalaf, Z. (2013). Treatment of oily wastewater by induced air flotation. *Engineering and Technology Journal*, *31(18 Part (A) Engineering*).

[65].Mohora, E., Rončević, S., Dalmacija, B., Agbaba, J., Watson, M., Karlović, E., & Dalmacija, M. (2012). Removal of natural organic matter and arsenic from water by electrocoagulation/flotation continuous flow reactor. *Journal of hazardous materials*, *235*, *257-264.*

[66].Mollah, M. Y., Morkovsky, P., Gomes, J. A., Kesmez, M., Parga, J., & Cocke, D. L. (2004). Fundamentals, present and future perspectives of electrocoagulation. *Journal of hazardous materials*, *114(1-3)*, *199-210.*

[67].Moreno-Casillas, H. A., Cocke, D. L., Gomes, J. A., Morkovsky, P., Parga, J. R., & Peterson, E. (2007). Electrocoagulation mechanism for COD removal. *Separation and purification Technology*, *56(2)*, *204-211*.

[68].Nour, A. H., Abu Hassan, M. A., & Yunus, R. M. (2007). Characterization and demulsification of water-in-crude oil emulsions. *Journal of Applied Sciences*, *7(10)*, *1437-1441.*

[69].Nour, A. H., Yunus, R. M., & Nour, A. H. (2010). Demulsification of water-in-oil emulsions by microwave heating technology. *World Academy of Science, Engineering and Technology*, *4*.

[70].O'Dell, J. W. (1993). Method 410.4, revision 2.0: the determination of chemical oxygen demand by semi-automated colorimetry. *US Environmental Protection Agency (EPA), Office of Research and Development, Environmental Monitoring Systems Laboratory: Cincinnati, Ohio, USA) Available at [verified 2 July 2019]*.

[71].Panizza, M., & Cerisola, G. (2010). Applicability of electrochemical methods to carwash wastewaters for reuse. Part 2: Electrocoagulation and anodic oxidation integrated process. *Journal of Electroanalytical Chemistry*, *638*(2), 236-240.

References

[72]. Paulista. O., Presumido, P. H., Theodoro, J. D. P., & Pinheiro, A. L. N. (2018). Efficiency analysis of the electrocoagulation and electroflotation treatment of poultry slaughterhouse wastewater using aluminum and graphite anodes. *Environmental Science and Pollution Research*, *25*(20), 19790-19800.

[73]. Pisal, A. (2009). Determination of Oil and Grease in Water with a Mid-Infrared Spectrometer. *PerkinElmer, Inc., United States*, 1-4.

[74].Rauckyte, T., Żak, S., Pawlak, Z., & Oloyede, A. (2010). Determination of oil and grease, total petroleum hydrocarbons and volatile aromatic compounds in soil and sediment samples. *Journal of Environmental Engineering and Landscape Management, 18(3), 163-169.*

[75].Redah, M. A. (2016). *Wastewater Treatment Using Successive Electrochemical Approaches (Doctoral dissertation, PH. D. thesis).*

[76].Rincon, G. J., & La Motta, E. J. (2014). Simultaneous removal of oil and grease, and heavy metals from artificial bilge water using electro-coagulation/flotation. *Journal of Environmental Management, 144, 42-50.*

[77].Rocha, J. H. B., Gomes, M. M. S., Fernandes, N. S., da Silva, D. R., & Martínez-Huitle, C. A. (2012). Application of electrochemical oxidation as alternative treatment of produced water generated by Brazilian petrochemical industry. *Fuel Processing Technology*, *96*, 80-87.

[78].Rodrigo, M. A., Michaud, P. A., Duo, I., Panizza, M., Cerisola, G., & Comninellis, C. (2001). Oxidation of 4-chlorophenol at boron-doped diamond electrode for wastewater treatment. *Journal of the Electrochemical Society, 148(5), D60.*

[79].Safari, S., Azadi Aghdam, M., & Kariminia, H. R. (2016). Electrocoagulation for COD and diesel removal from oily wastewater. *International Journal of Environmental Science and Technology, 13(1), 231-242.*

References

[80].Safwat, S. M., Hamed, A., & Rozaik, E. (2019). Electrocoagulation/electroflotation of real printing wastewater using copper electrodes: a comparative study with aluminum electrodes. *Separation science and technology*, *54*(1), 183-194.

[81].Sangal, V. K., Mishra, I. M., & Kushwaha, J. P. (2013). Electrocoagulation of soluble oil wastewater: parametric and kinetic study. *Separation Science and Technology, 48(7), 1062-1072.*

[82].Santos, G. D. O. S., de Salles Pupo, M. M., Vasconcelos, V. M., Eguiluz, K. I. B., & Banda, G. R. S. (2018). Electroflotation. In *Electrochemical Water and Wastewater Treatment. Butterworth-Heinemann. (pp. 77-118).*

[83].Shonza, N. S., Andreatta, D., Muniz, E. P., Dalmaschio, C. J., de Freitas, R. R., & Porto, P. S. D. S. (2020). Crude oil wastewater treatment by electrocoagulation in a continuous process with polarity switch. *Environmental Technology*, 1-9.

[84].Sobreira, S., Pacheco, M. J., Ciríaco, L., & Lopes, A. (2011). Effect of the Hydrodynamic Conditions on the Electrochemical Degradation of Phenol on a BDD Anode. *Portugaliae Electrochimica Acta*, *29(5), 343-348.*

[85].Song, S., Yao, J., He, Z., Qiu, J., & Chen, J. (2008). Effect of operational parameters on the decolorization of CI Reactive Blue 19 in aqueous solution by ozone-enhanced electrocoagulation. *Journal of hazardous materials*, *152*(1), 204-210.

[86].Stack, L. J., Carney, P. A., Malone, H. B., & Wessels, T. K. (2005). Factors influencing the ultrasonic separation of oil-in-water emulsions. *Ultrasonics sonochemistry, 12(3), 153-160.*

[87].Sun, C., Leiknes, T., Weitzenböck, J., & Thorstensen, B. (2009). The effect of bilge water on a Biofilm—MBR process in an integrated shipboard wastewater treatment system. Desalination, 236(1-3), 56-64.

References

[88].Sztukowski, 2005, PhD Thesis, Asphaltene and Solids-Stabilized Water-In-Oil Emulsions, Department of Chemical and Petroleum Engineering, Faculty of Grad University of Calgary, *Alberta://www.elibrary.ru/item.asp, id=9357297.*

[89].Tasic, Z., Gupta, V. K., & Antonijevic, M. M. (2014). The mechanism and kinetics of degradation of phenolics in wastewaters using electrochemical oxidation. *Int. J. Electrochem. Sci, 9(7), 3473-3490.*

[90].Tir, M., & Moulai-Mostefa, N. (2008). Optimization of oil removal from oily wastewater by electrocoagulation using response surface method. *Journal of hazardous materials*, *158(1), 107-115.*

[91].Ulucan, K., & Kurt, U. (2015). Comparative study of electrochemical wastewater treatment processes for bilge water as oily wastewater: a kinetic approach. Journal of Electroanalytical Chemistry, 747, 104-111.

[92].Ulucan, K., & Kurt, U. (2015). Comparative study of electrochemical wastewater treatment processes for bilge water as oily wastewater: a kinetic approach. Journal of Electroanalytical Chemistry, 747, 104-111.s for bilge water as oily wastewater: a kinetic approach. *Journal of Electroanalytical Chemistry*, *747, 104-111*.

[93].Un, U. T., Koparal, A. S., & Ogutveren, U. B. (2009). Electrocoagulation of vegetable oil refinery wastewater using aluminum electrodes. *Journal of environmental management*, *90(1), 428-433.*

[94].Wang, C. T., Chou, W. L., & Kuo, Y. M. (2009). Removal of COD from laundry wastewater by electrocoagulation/electroflotation. *Journal of hazardous materials*, *164*(1), 81-86.

[95]. Wang, D., Yang, D., Huang, C., Huang, Y., Yang, D., Zhang, H., ... & Zeng, H. (2021). Stabilization mechanism and chemical demulsification of water-in-oil and oil-in-water emulsions in petroleum industry: A review. *Fuel*, *286*, 119390.

References

[96].Wang, L. K., Shammas, N. K., & Wu, B. C. (2010). Electroflotation. In Flotation technology, *(pp. 165-197). Humana Press, Totowa, NJ*.

[97].Wolf, N. O. (1986). Use of microwave radiation in separating emulsions and dispersions of hydrocarbons and water ed: *Google Patents. Washington, DC: U.S. Patent and Trademark Office. U.S. Patent No. 4,582,629.*

[98].Xu, X., & Zhu, X. (2004). Treatment of refectory oily wastewater by electro-coagulation process. *Chemosphere, 56(10), 889-894.*

[99].Yang, C. L. (2007). Electrochemical coagulation for oily water demulsification. *Separation and purification technology, 54(3), 388-395.*

[100]. Yang, Y., Li, Y., Cao, L., Wang, Y., Li, L., & Li, W. (2021). Electrospun PVDF-SiO2 nanofibrous membranes with enhanced surface roughness for oil-water coalescence separation. *Separation and Purification Technology, 269, 118726.*

[101]. Yavuz, Y., Koparal, A. S., & Öğütveren, Ü. B. (2010). Treatment of petroleum refinery wastewater by electrochemical methods. *Desalination, 258(1-3), 201-205.*

[102]. Yu, L., Han, M., & He, F. (2017). A review of treating oily wastewater. *Arabian journal of chemistry, 10, S1913-S1922.*

[103]. Yunksel, E.; Gurbulak, E.; Eyvaz, M., 2012, Decolorization of a reactive dyes solutions and treatment of a textile wastewater by electrocoagulation and chemical coagulation: Techno-economic comparison. *Environ. Prog. Sustain. Energy, 31, 524-535.*

[104]. Zhang, H., Bukosky, S. C., & Ristenpart, W. D. (2018). Low-voltage electrical demulsification of oily wastewater. *Industrial & Engineering Chemistry Research, 57(24), 8341-8347.*

References

[105]. Zhang, H., Bukosky, S. C., & Ristenpart, W. D. (2018). Low-voltage electrical demulsification of oily wastewater. *Industrial & Engineering Chemistry Research, 57(24), 8341-8347.*

[106]. Zolfaghari, R., Fakhru'l-Razi, A., Abdullah, L. C., Elnashaie, S. S., & Pendashteh, A. (2016). Demulsification techniques of water-in-oil and oil-in-water emulsions in petroleum industry. *Separation and Purification Technology, 170, 377-407.*

[107]. Zongo, I., Maiga, A. H., Wethe, J., Valentin, G., Leclerc, J. P., Paternotte, G., & Lapicque, F. (2009). Electrocoagulation for the treatment of textile wastewaters with Al or Fe electrodes: Compared variations of COD levels, turbidity and absorbance. *Journal of Hazardous Materials, 169(1-3), 70-76.*

Appendix A
Calibration Curve for Standards Solutions

Table A.1: Calibration Curve for Standards Solutions

	KPH sol. in 50ml Vol. flaks	COD ppm	Abs.
Blank	...	0	0.14
Reference 1	1 mL	20	0.17
Reference 2	2.5 mL	50	0.153
Reference 3	5 mL	100	0.166
Reference 4	10 mL	200	0.196
Reference 5	20 mL	400	0.225
Reference 6	30 mL	600	0.231
Reference 7	45mL	900	0.323

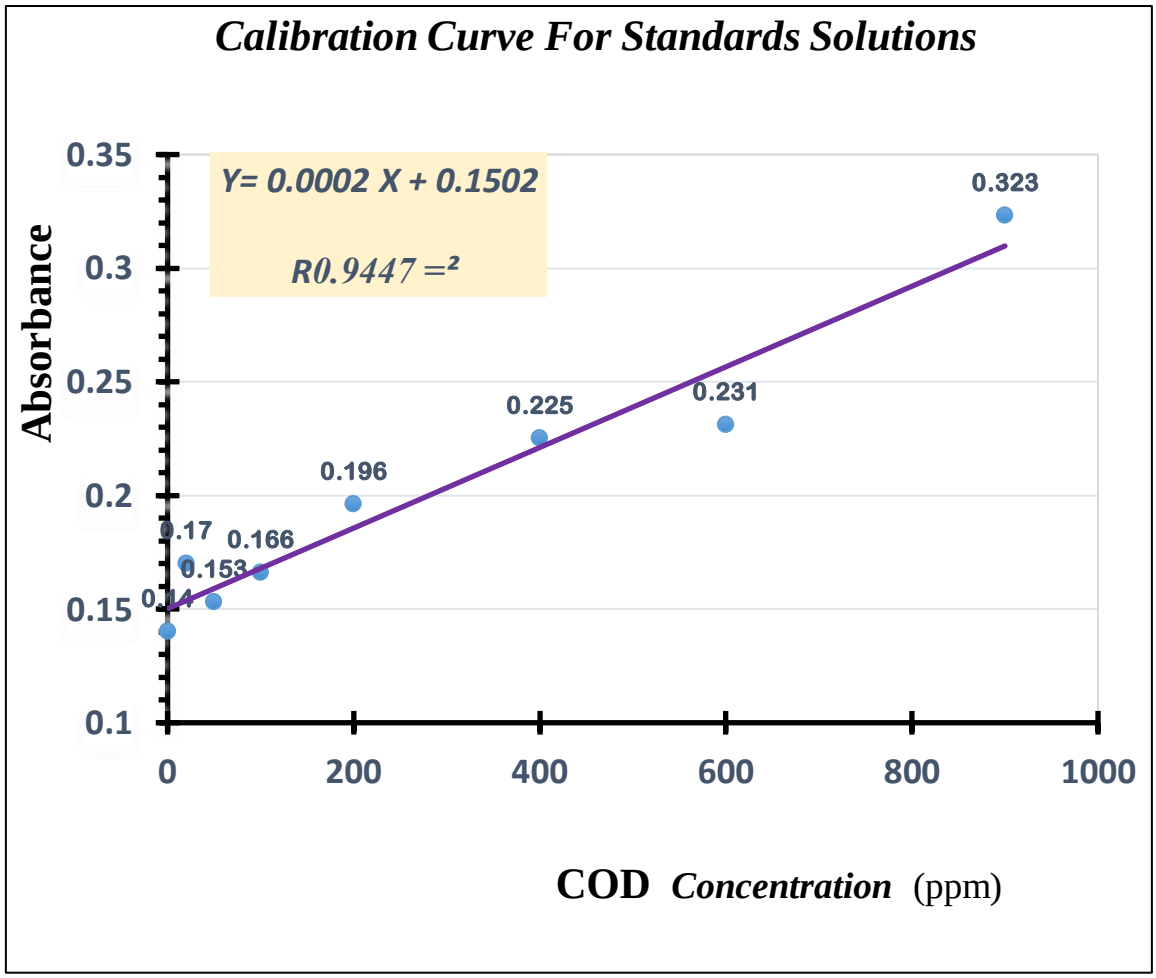

ABS vs. Conc. Standard Curve 30/3/2021 600 nm wave length

Appendix B

Experimental data :- B.1. *COD Removal %*

1. Aluminum- Aluminum Electrode

The COD removal % = $((C_o-Ct)/C_o)$ x100

Table B.1: The COD removal % variation of O/W emulsion with different operating condition

Parameter		*COD Removal %*								
		C_o = 100 ppm			C_o = 200 ppm			C_o = 300 ppm		
c.d. ($mAcm^{-2}$)		10	20	30	10	20	30	10	20	30
Q (L/hr)	**t** (min)									
2	0	0	0	0	0	0	0	0	0	0
	20	50.36	63.89	79.96	37.36	50.08	67.17	37.51	47.41	62.31
	40	50.45	66.33	87.36	44.03	65.39	71.61	43.55	56.17	64.85
	60	52.70	70.30	87.99	55.16	65.39	72.50	48.90	64.94	68.44
	80	57.22	73.01	90.34	60.05	76.06	75.17	63.97	73.70	71.77
	100	60.83	77.43	94.22	73.84	78.64	77.84	71.16	75.46	73.88
	120	69.40	78.97	96.93	79.00	79.53	80.24	75.28	78.26	76.51
4	0	0	0	0	0	0	0	0	0	0
	20	39.16	52.88	75.63	17.79	43.59	56.93	33.21	51.00	61.60
	40	40.52	55.05	85.01	42.25	55.60	62.72	41.98	58.23	78.61
	60	41.87	62.99	86.01	44.92	56.49	65.39	53.46	65.46	83.87
	80	45.94	68.05	88.08	49.15	67.61	69.30	61.26	71.16	85.18
	100	48.19	71.93	88.44	53.38	69.75	71.26	66.69	75.76	86.50
	120	55.4	73.10	89.07	57.60	73.30	74.19	73.70	80.36	87.81
6	0	0	0	0	0	0	0	0	0	0
	20	36.55	47.78	71.11	5.33	16.03	47.46	1.051	11.12	38.51
	40	38.26	50.67	79.33	9.78	34.83	53.82	11.13	34.25	54.82
	60	38.26	54.46	79.78	33.8	48.81	58.05	21.20	48.04	67.17
	80	45.93	56.45	81.04	36.0	55.65	59.96	26.90	51.15	68.22
	100	45.03	59.34	82.94	39.5	62.48	63.34	31.72	54.27	69.28
	120	45.93	62.22	84.11	43.5	63.43	66.37	40.49	60.49	80.54

B.2. *The Specific Electric Energy Consumption. (SEEC)*

SEEC (kWh/m^3) = VI/Q

Table B.2: Specific electrical energy conception (SEEC) for The COD removal % variation of O/W emulsion with different operating condition.

Parameter		SEEC (kWh/m^3)								
		C_o = 100 ppm			C_o = 200 ppm			C_o = 300 ppm		
c.d. (mAcm^{-2})		10	20	30	10	20	30	10	20	30
Q (L/hr.)	**t** (min)									
2	0	0	0	0	0	0	0	0	0	0
	20	6.7	13.5	9.3	2.9	6.12	9.02	3	5	9.17
	40	6.2	13.25	9.45	2.84	6.06	9.02	3.06	5.2	9.48
	60	6.5	13.5	9.3	2.84	6.05	9.02	3	5.58	9.41
	80	6.5	12	9.37	2.84	5.93	9.02	3.12	5.8	9.34
	100	6.5	14	9.22	2.9	5.88	9.02	3	5.8	9.36
	120	6.4	12.7	9	2.8	5.94	9.02	3	5.9	9.22
4	0	0	0	0	0	0	0	0	0	0
	20	3.5	7.2	4.61	1.5	3.17	4.71	1.5	3	4.63
	40	3.4	6	4.65	1.5	3.26	4.46	1.5	2.9	4.5
	60	3.4	6.25	4.97	1.53	3.18	4.23	1.4	2.9	4.6
	80	3.27	6.5	4.76	1.5	3	4.72	1.4	3	4.6
	100	3.27	6.75	4.8	1.47	2.95	4.66	1.56	3	4.5
	120	3.5	6	4.76	1.46	3.12	4.23	1.6	2.9	4.5
6	0	0	0	0	0	0	0	0	0	0
	20	2.28	1.76	2.97	1	2	2.97	0.98	2.02	3.08
	40	2.38	1.76	3	1	1.96	2.93	0.32	2.1	3.04
	60	2.27	1.68	3	1	1.99	2.87	0.31	2.1	3.6
	80	2.3	1.68	3	1	1.95	2.95	1	2.1	3.08
	100	2.2	1.73	3	1	1.95	2.97	1.04	2.1	3.02
	120	2.3	1.68	3	0.86	1.9	2.97	1	2.14	3.02

B.3. The Currant Efficiency (Ø%)

$$Ø\% = \frac{C\ exp}{C\ Theory} \times 100\% \qquad C\ exp = (\Delta m/Q)\ ,\ C_{Theory} = (26.80148 \times I)/(80.40444 \times Q)$$

Table B.3: The current efficiency (CE) variation of O/W emulsion with different volumetric flowrate.

Parameter	Ø %								
	C_o = 100 ppm			**C_o = 200 ppm**			**C_o = 300 ppm**		
c.d. (mAcm^{-2})	10	20	30	10	20	30	10	20	30
Q (L/hr)									
2	126	120.75	126.96	114	120.06	119.88	48.69	85.26	124.22
4	126.48	120.15	147.24	285	116.4	125.22	131.88	164.97	117.5
6	135.72	205.5	143	27	183.6	117.06	170.52	64.2	117.5

B.4 a. Power of Hydrogen, pH

Table B.4a: The pH during EC/EF

Parameter		pH								
		C_o = 100 ppm			**C_o = 200 ppm**			**C_o = 300 ppm**		
c.d. (mAcm^{-2})		10	20	30	10	20	30	10	20	30
Q (L/hr)	**t** (min)									
2	0	7.8	6.8	6.4	7.5	7.2	7.8	7.2	6.4	8.1
	20	8.2	8.4	8	8.2	7.4	8.9	6	5.8	7.2
	40	8.3	8.4	8.2	8.1	7.4	8.8	6	6.1	7.9
	60	8.4	8.5	8.3	8.1	7.5	8.7	6.1	6.3	8.1
	80	8.4	8.6	8.3	8.1	7.9	8.6	6.3	6.9	8.2
	100	8.4	8.6	8.3	8.1	7.9	8.6	6.1	7.1	8
	120	8.4	8.6	8.1	8.6	8.4	8.6	6	7.7	8
4	0	7.8	7.2	6.8	7.3	7.8	7.4	6	5.9	7.1
	20	8	8.8	7.1	8.2	8.8	8	6.2	7.4	7.5
	40	8.2	8.7	8.3	8.2	8.6	8.2	6.3	8.1	7.7
	60	8.3	8.4	8.3	8	8.4	8.2	6.3	8.5	7.8
	80	8.3	8.4	8.5	8.2	7.9	8.3	6.3	8.7	7.8
	100	8.3	8.5	8.5	8.2	8	8.3	6.4	8.7	8
	120	8.3	8.5	8.6	8.4	8.3	8.4	6.4	8.8	8.1
6	0	8	7.3	8.2	7.2	7.6	7.5	6.5	6.3	7.3
	20	8.4	7.3	8.6	7.4	8.1	8.4	6	6.4	7.5
	40	8.3	7	8.7	7.4	8.1	8.3	6.1	6.8	7
	60	8.2	7.8	8	8.2	8.1	8	6.3	6.8	7.8
	80	8.1	8.1	8.4	8.3	8.1	7.9	6.4	6.8	7.9
	100	8.1	8.2	8.4	8.3	8.1	7.8	6.4	6.8	8
	120	8.1	7.8	8.7	8.3	7.9	7.7	6.8	7.7	8.2

B.4 b. Total Dissolved Solid (TDS)

Table B.4b: Total Dissolved Solid (TDS) evolution.

Table B.4b : Total Dissolved Solid (TDS) during EC/EF

Parameter		*TDS ppm*								
		C_o = 100 ppm			**C_o = 200 ppm**			**C_o = 300 ppm**		
c.d. (mAcm-2)		**10**	**20**	**30**	**10**	**20**	**30**	**10**	**20**	**30**
Q (L/hr)	t (min)									
2	0	**1730**	**1730**	**1500**	**2223**	**2223**	**2223**	**2964**	**1664**	**2323**
	20	**149**	**738**	**1530**	**2197**	**990**	**2093**	**2080**	**1436**	**2281**
	40	**147**	**408**	**1540**	**2171**	**815**	**2093**	**1860**	**1345**	**2028**
	60	**144**	**385**	**1440**	**2140**	**826**	**2067**	**1815**	**1339**	**1985**
	80	**144**	**390**	**1555**	**2119**	**877**	**2028**	**1742**	**975**	**1985**
	100	**143**	**310**	**1500**	**2093**	**870**	**2028**	**1683**	**871**	**1985**
	120	**142**	**345**	**1570**	**2067**	**980**	**1690**	**1618**	**8644**	**1905**
4	0	**1730**	**1730**	**1570**	**2223**	**2440**	**2223**	**2158**	**1709**	**2294**
	20	**144**	**327**	**1580**	**2226**	**2400**	**1730**	**1742**	**806**	**2267**
	40	**139**	**330**	**1570**	**1235**	**1670**	**1610**	**1774**	**968**	**2112**
	60	**137**	**277**	**1420**	**1410**	**16660**	**1670**	**1326**	**1040**	**2028**
	80	**144**	**360**	**1520**	**1397**	**1620**	**1665**	**1443**	**942**	**1521**
	100	**142**	**338**	**1560**	**1413**	**1650**	**1660**	**1565**	**845**	**2112**
	120	**140**	**330**	**1580**	**2216**	**1590**	**1650**	**1501**	**773**	**2250**
6	0	**1730**	**1430**	**1580**	**2223**	**2223**	**2223**	**1794**	**1680**	**1394**
	20	**139**	**1450**	**1570**	**830**	**1620**	**1690**	**1560**	**981**	**259**
	40	**135**	**1500**	**1540**	**400**	**1580**	**1660**	**1527**	**767**	**248**
	60	**136**	**1420**	**1540**	**490**	**1620**	**1650**	**1417**	**708**	**247**
	80	**135**	**1520**	**1460**	**560**	**1600**	**1650**	**1358**	**585**	**246**
	100	**134**	**1490**	**1440**	**630**	**1630**	**1640**	**1345**	**526**	**245**
	120	**134**	**1500**	**1530**	**890**	**1650**	**1445**	**1261**	**476**	**241**

B.5. Turbidity(NTU), Total Suspended Solid (TSS ppm) and Total Solid (TS ppm) Evaluation.

Table B.5: Turbidity(NTU), Total Suspended Solid (TSS ppm) and Total Solid (TS ppm) Evaluation for different initial O/W emulsion concentration

C_o = 100 ppm		*Turbidity NTU*			*TSS ppm*			*TS ppm*		
c.d. ($mAcm^{-2}$)		10	20	30	10	20	30	10	20	30
Q (L/hr)	**t** (min)									
2	0	28.4	28.4	28.4	320	320	320	2050	2050	1820
	20	15	6.14	16	144	200	140	293	938	1670
	120	11	4.5	6.3	132	100	48	274	445	1618
4	0	28.4	28.4	28.4	320	320	320	2050	2050	1890
	20	14.3	17	5.8	52	152	316	196	479	1886
	120	7.8	15	3.32	12	12	144	152	342	1704
6	0	28.4	28.4	28.4	320	320	320	2050	348.4	3160
	20	18	11.9	4.96	132	120	148	271	132	1718
	120	17	9.3	2.98	100	28	144	234	37.3	1674
C_o = 200 ppm		*Turbidity NTU*			*TSS ppm*			*TS ppm*		
c.d. ($mAcm^{-2}$)		10	20	30	10	20	30	10	20	30
Q (L/hr)	**t** (min)									
2	0	55	55	55	216	216	216	2439	2439	2439
	20	8.5	38	22	128	212	44	2325	1202	2137
	120	2.5	25	12	116	16	40	2183	996	1730
4	0	55	55	55	216	216	216	2439	2656	2439
	20	14	38	60	148	212	208	2384	2612	1938
	120	8.5	11	10	100	16	4	2316	1606	1654
6	0	55	55	55	216	216	216	2439	2439	2439
	20	25	51	16.4	136	156	16	1166	1776	1706
	120	17	41	12.6	212	96	28	1102	1746	1473
C_o = 300 ppm		*Turbidity NTU*			*TSS ppm*			*TS ppm*		
c.d. ($mAcm^{-2}$)		10	20	30	10	20	30	10	20	30
Q (L/hr)	**t** (min)									
2	0	687	687	687	429	1308	429	3393	2972	2752
	20	5	3.25	44	304	1240	333	2384	2676	2600
	120	3.3	1.76	32	276	529	281	1894	1293	2450
4	0	687	687	687	5366	512	429	2693	2222	2132
	20	49	92	25	476	512	198	2218	1318	1800
	120	46	45	11	429	220	178	2037	993.5	1100
6	0	687	687	687	429	429	429	2223	2109	1950
	20	110	70.3	200	428	148	300	1988	1129	1840
	120	30.7	41	120	344	16	240	1605	492	1830

Appendix B

Experimental data:- B.6. *COD Removal %*

2. Aluminum- Carbon.felt Electrode

The COD removal % = $((C_o-Ct)/C_o)$ x100

Table B.6: The COD removal % variation of O/W emulsion with different operating condition.

Parameter		***COD Removal %***								
		C_o = 100 ppm			**C_o** = 200 ppm			**C_o** = 300 ppm		
c.d. (mAcm^{-2})		**10**	**20**	**30**	**10**	**20**	**30**	**10**	**20**	**30**
Q (L/hr)	**t** (min)									
2	0	0	0	0	0	0	0	0	0	0
	20	0.3	21.1	71.6	47.28	53.4	38.7	81.6	35.2	32.1
	40	12.9	21.1	71.6	53.6	56	78.7	85.6	54	68.5
	60	20.2	28.7	72.5	58.6	56.8	80.9	95.7	58.4	68.9
	80	22	56.3	77.4	64	56.8	83.1	95.8	62.8	71.1
	100	43.2	59	83.1	64.4	57.6	84.5	98.4	73.3	64.6
	120	82	66.6	99.8	72.6	60.5	84.5	99.5	99.9	83.4
4	0	0	0	0	0	0	0	0	0	0
	20	0.18	23.3	40.9	0.44	15.5	36.9	37.3	7.1	44.4
	40	4.69	23.3	41.4	62.98	27.1	61.3	76.4	8.9	50.1
	60	8.3	25.6	57.4	67.21	51.6	62.7	79.9	18.1	62.8
	80	8.5	28.7	68.4	67.7	65.3	66.2	82.5	80.8	73.3
	100	9.8	32.4	72.06	67.9	74.2	90.3	95.7	81.6	78.1
	120	36.9	43.6	98	75.8	90.3	93.4	98.7	83.4	79
6	0	0	0	0	0	0	0	0	0	0
	20	3.06	0.36	44.9	49	27.7	89.8	51.0	2.8	21.6
	40	5.32	0.8	66.7	63.8	42.9	92.9	61.9	4.1	62.8
	60	17.5	21.1	71.48	65.3	44.4	95.5	89.1	24.2	70.7
	80	23.3	31	72.87	7.4	62.3	96.2	95.7	82.1	75.5
	100	45.9	47.7	78.7	78.6	69.6	98	98.3	87.8	67.8
	120	45.9	52.7	83.73	89.9	73.7	99.1	99.9	90	78.1

B.7. The Specific Electric Energy Consumption. (SEEC)

SEEC (kWh/m^3) = VI/Q

Table B.7: Specific electrical energy conception (SEEC) for The COD removal % variation of O/W emulsion with different operating condition.

Parameter		***SEEC (kWh/m^3)***								
		C_o = 100 ppm			**C_o = 200 ppm**			**C_o = 300 ppm**		
c.d. (mAcm^{-2})		10	20	30	10	20	30	10	20	30
Q (L/hr.)	**t** (min)									
2	0	0	0	0	0	0	0	0	0	0
	20	1.75	6	10.95	2.82	6.05	9	0.97	3.705	8.1
	40	1.5	6	10.95	2.82	6.4	9	1.02	3.7	7.86
	60	1.25	5.95	11.02	2.82	6.5	9.1	1.1	3.53	7.98
	80	1.175	5.95	11.4	2.82	7.1	8.9	0.98	3.64	7.76
	100	1.125	6.15	12	2.82	5.9	9.45	1.01	3.64	7.94
	120	1.125	6.2	11.85	2.82	5.65	9	1.25	3.62	7.5
4	0	0	0	0	0	0	0	0	0	0
	20	1.31	3.15	3.75	1.55	2.95	3.75	0.56	2.69	4.2
	40	1.31	3.25	3.86	1.47	2.95	3.7	0.63	2.7	4.54
	60	1.32	3.27	3.82	1.47	3	3.6	0.59	2.67	4.05
	80	1.43	3.2	3.86	1.47	3.1	3.6	0.62	2.85	3.97
	100	1.4	3.25	3.9	1.5	2.9	3.59	0.6	2.69	4.12
	120	1.4	3.25	3.93	1.5	2.55	3.82	0.59	2.7	4.16
6	0	0	0	0	0	0	0	0	0	0
	20	0.99	2.16	3.27	1.1	1.7	2.82	0.35	1.66	2.9
	40	1	2.16	2.85	1.1	1.76	2.87	0.35	1.67	2.84
	60	1.16	2.16	2.02	1.16	1.75	2.86	0.33	1.65	2.82
	80	1.14	2.31	2.12	1.15	1.8	2.86	0.34	1.75	2.84
	100	0.97	2.3	2.12	1.14	1.86	2.13	0.34	1.72	2.9
	120	1.008	2.3	2.15	1.2	1.9	2.42	0.35	1.75	2.9

B.8. The Currant Efficiency (Ø%)

$$Ø\% = \frac{C\ exp}{C\ Theory} \text{ x } 100\%$$

$$C\ exp = (\Delta m/Q) \quad , \quad C_{Theory} = (26.80148 \text{ x } I)/ (80.40444 \text{xQ})$$

Table B.8: The current efficiency (CE) variation of O/W emulsion with different volumetric flowrate.

Parameter	Ø %								
	C_o = 100 ppm			C_o = 200 ppm			C_o = 300 ppm		
c.d. ($mAcm^{-2}$)	10	20	30	10	20	30	10	20	30
Q (L/hr)									
2	142.8	139.65	142.3	136.2	161.4	125.2	126	140.7	136.5
4	113.1	127.5	136.2	150.9	176.4	125.7	120	132.3	108.1
6	150	163.65	144.3	117.6	144.15	121.7	131.4	146.7	140.8

B.9a. Power of Hydrogen, pH

Table B.9a: The pH during EC/EF

Parameter		pH								
		C_o = 100 ppm			C_o = 200 ppm			C_o = 300 ppm		
c.d. ($mAcm^{-2}$)		10	20	30	10	20	30	10	20	30
Q (L/hr)	t (min)									
2	0	6.3	8	7.4	6.6	6.9	7.5	8.2	7.2	7.7
	20	6.3	8.1	7.9	5.5	7.3	7.6	7.7	7.2	7.8
	40	6.7	8.4	8	4.9	7.8	8	7.9	7.4	8.3
	60	7.2	8.5	8	4.6	8	8.5	8.1	7.5	8.4
	80	7.5	8.6	8.1	5	8.2	8.5	8.1	7.6	7.9
	100	7.7	8.6	8.2	4.7	8.3	8.5	8.1	8.2	8.3
	120	7.8	8.7	8.3	7.3	8.5	8.5	8.2	8.2	8.5
4	0	7.6	7	7.3	7.8	6.7	6.9	8.6	7.1	8.3
	20	7.7	7.4	7.7	7.1	6.8	7.8	8.7	6.9	8.2
	40	7.8	7.5	8	5.8	6.8	8.2	8.1	7.6	8.4
	60	8	7.6	4.5	5.3	6.9	8.3	8.1	7.9	8.5
	80	8.2	7.7	8.2	6.1	7.2	8.4	8.2	8	8.6
	100	8.2	8.1	7.7	6.2	7.3	8.4	8.3	8.1	8.7
	120	8.3	8.3	7.1	6	7.6	8.3	8.4	8.2	8.8
6	0	7.5	8.7	6.5	6.4	7.2	8.1	7.4	8.1	8.8
	20	7.5	8.3	6.6	6.5	7.2	8.2	7.5	8.2	8.8
	40	7.7	8.3	7.4	6.6	7.6	8.2	7.7	8.2	8.8
	60	7.8	8.3	7.4	7.1	7.7	8.3	7.9	8.3	8.5
	80	7.8	8.3	7.5	7.2	7.9	8.1	7.9	8.3	8.5
	100	8	8.3	7.6	7.3	7.9	8.4	8.1	8.4	8.5
	120	8.1	8.3	7.7	7.5	8.1	8.5	8.1	8.4	8.6

B.9b. Total Dissolved Solid (TDS)

Table B.9b: Total Dissolved Solid (TDS) during EC/EF

Parameter		TDS ppm								
		C_o = 100 ppm			C_o = 200 ppm			C_o = 300 ppm		
c.d. (mAcm-2)		10	20	30	10	20	30	10	20	30
Q (L/hr)	t (min)									
2	0	1540	1550	1450	1340	1330	1150	1200	1220	1250
	20	1470	1250	1520	1440	1270	1200	1230	1230	1250
	40	1560	1650	1470	1450	1280	1270	1270	1230	1240
	60	1630	1580	1525	1450	1310	1210	1260	1220	1220
	80	1560	1590	1570	1370	1320	1270	1270	1260	1220
	100	1600	1595	1550	1455	1030	1280	1250	1260	1250
	120	1610	1575	1570	1390	1340	1300	1270	1250	1240
4	0	1540	1340	1550	1530	1220	1020	12300	1240	1210
	20	1550	1620	1570	1310	1330	1240	1280	1210	1070
	40	1530	1580	1540	1340	1380	1280	1230	1230	1230
	60	1550	1630	1570	1340	1360	1270	1250	1240	1240
	80	1530	1620	1580	1340	1390	1275	1255	1240	1270
	100	1560	1630	1560	1340	1430	1280	1250	1260	1270
	120	1600	1590	1520	1130	1490	1260	1240	1240	1260
6	0	1510	1160	1482	1310	1210	1270	1240	1080	1270
	20	1480	1410	2000	1380	1270	1300	1250	1260	1250
	40	1490	1490	2030	1330	1280	1290	1230	1220	1230
	60	1430	1440	2035	1330	1310	1280	1240	1260	1250
	80	1550	1450	2020	1340	1310	1270	1250	1250	1240
	100	1420	1360	2027	1360	1320	1280	1230	1250	1210
	120	1500	1380	2028	1380	1000	1260	1250	1220	1250

B.10. Turbidity (NTU), Total Suspended Solid (TSS ppm) and Total Solid (TS ppm) Evaluation.

Table B.10: Turbidity (NTU), Total Suspended Solid (TSS ppm) and Total Solid (TS ppm) evaluation for different initial O/W emulsion concentration.

C_o = 100 ppm		Turbidity NTU			TSS ppm			TS ppm		
c.d. ($mAcm^{-2}$)		10	20	30	10	20	30	10	20	30
Q (L/hr)	t (min)									
2	0	285	102	243	520	171	280	2060	2211	1980
	20	79.6	67.5	222	696	308	2040	2166	1748	3270
	120	59.3	61.3	120	456	432	2168	2066	1822	3438
4	0	285	102	215	520	994.5	845	2060	2524.5	2145
	20	84.4	55.6	121	324	364	1888	1874	1674	3168
	120	79.7	30.5	116	512	324	1820	2112	1454	3060
6	0	285	102	210	520	851.5	806	2030	2161.5	2046
	20	152	35.9	191	28	116	1616	1506	1496	2866
	120	107	32	149	112	88	1192	1612	1468	2442
C_o = 200 ppm		Turb101idity NTU			TSS ppm			TS ppm		
c.d. ($mAcm^{-2}$)		10	20	30	10	20	30	10	20	30
Q (L/hr)	t (min)									
2	0	101	120	297	520	864.5	793	2070	2194.5	2013
	20	47.1	15.1	250	72	96	1224	1322	1366	2454
	120	22.5	14	49.3	12	280	860	1587	1620	2110
4	0	81.5	102	138	520	792	806	1860	2013	2046
	20	38.94	98	22.7	88	530	308	1708	1860	1518
	120	29.1	17.2	8.16	36	482	208	1626	1972	1448
6	0	101.3	115	167	520	786.5	702	1680	1996.5	1782
	20	23.8	47.1	53.2	120	591	100	1530	1861	1360
	120	13.1	21.2	49.7	20	483	32	1400	1483	1252
C_o = 300 ppm		Turbidity NTU204			TSS ppm			TS ppm		
c.d. ($mAcm^{-2}$)		10	20	30	10	20	30	10	20	30
Q (L/hr)	t (min)									
2	0	101.3	83.3	204	942.5	747.5	812.5	2392.5	1897.5	2062.5
	20	119	35.3	53	548	476	308	2068	1676	1558
	120	110	21.8	34.2	460	1060	84	2030	2360	1324
4	0	101.3	237	217	1007.5	663	786.5	2557.5	1683	1996.5
	20	41.5	69	37.6	368	1212	120	1938	2452	120
	120	1705	35.4	25.6	612	1032	84	2132	2296	2095.5
6	0	101	41.5	258	962	825.5	825.5	2444	2095.5	1344
	20	18.41	36.3	45.6	420	1256	314.8	2420	2556	1564.8
	120	18	21	18.5	604	2263	56	2684	3496	1306

Appendix C

C.1. *Al test device*

Table C;1 Aluminum X-ray florescent analysis by Bruker AXS model D76187 Karisruhe. Germany

Name	Value	Z	Crystal Name	Line ID
Al	99.178 %	13	PET	Al KA1-HR-Tr
Si	0.302 %	14	PET	Si KA1-HR-Tr
S	0.060 %	16	PET	S KA1-HR-Tr
Cl	0.075 %	17	PET	Cl KA1-HR-Tr
K	0.043 %	19	LiF200	K KA1-HR-Tr
Ca	0.071 %	20	LiF200	Ca KA1-HR-Tr
Sc	79.711 PPM	21	LiF200	Sc KA1-HR-Tr
V	0.014 %	23	LiF200	V KA1-HR-Tr
Fe	0.204 %	26	LiF200	Fe KA1-HR-Tr
Cu	96.031 PPM	29	LiF200	Cu KA1-HR-Tr
Zn	74.302 PPM	30	LiF200	Zn KA1-HR-Tr
Ga	0.010 %	31	LiF200	Ga KA1-HR-Tr

X-Ray F

Appendix C

C.2 test devisees& the deionized water analysis ,crude oil

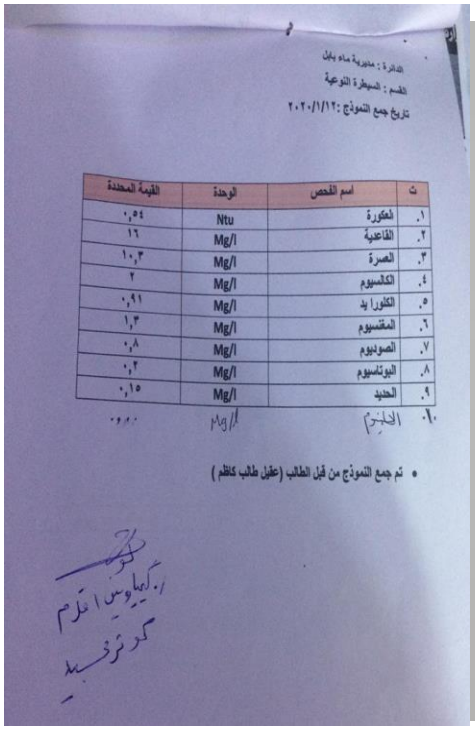

الدائرة : مديرية مياه بيان
القسم : السيطرة النوعية
تاريخ جمع النموذج: ٢٠٢٠/١/١٢

ت	اسم الفحص	الوحدة	القيمة المحددة
١.	العكورة	Ntu	٠,٥٤
٢.	القاعدية	Mg/l	١٦
٣.	الصرة	Mg/l	١٠,٣
٤.	الكالسيوم	Mg/l	٢
٥.	الكلورايد	Mg/l	٠,٩١
٦.	المغنسيوم	Mg/l	١,٣
٧.	الصوديوم	Mg/l	٠,٨
٨.	البوتاسيوم	Mg/l	٠,٢
٩.	الحديد	Mg/l	٠,١٥
١٠.	الملوحة	Mg/l	٠٠٠٠

• تم جمع النموذج من قبل الطالب (عقيل طالب كاظم)

Component List Component List of Crude Oil Sample

COMPONENT	Wt. %
Ethane	0.020
Propane	0.200
i-Butane	0.126
n-Butane	0.596
i-Pentane	1.916
unknown	0.781
n-Pentane	0.823
2-Methylbutene-2	0.026
2,2-Dimethylbutane	0.010
Cyclopentane	0.051
2,3-Dimethylbutane	0.084
2-Methylpentane	0.350
4-Methyl-c-pentene-2	0.085
3-Methylpentane	0.415
n-Hexane	0.956
2,2-Dimethylpentane	0.008
Methylcyclopentane	0.188
2,4-Dimethylpentane	0.030
Benzene	0.064
Unidentified	0.005
Cyclohexane	0.129
2-Methylhexane	0.269
2,3-Dimethylpentane	0.125
1,1-Dimethylcyclopentane	0.017
3-Methylhexane	0.375
1t,3-Dimethylcyclopentane	0.052
1c,3-Dimethylcyclopentane	0.048
3-Ethylpentane	0.044
1t,2-Dimethylcyclopentane	0.099
n-Heptane	0.880

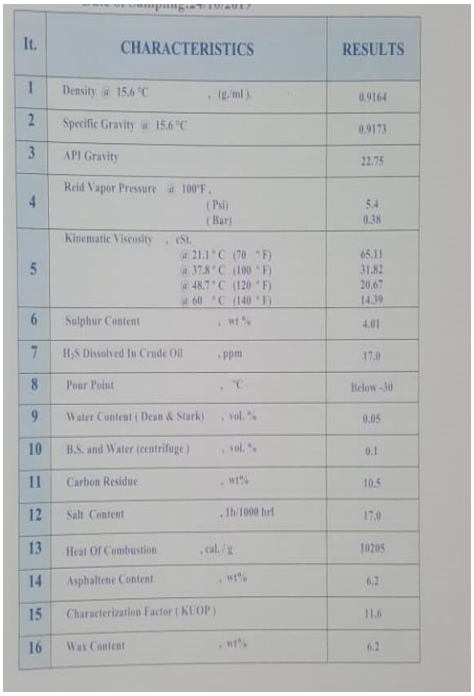

It.	CHARACTERISTICS	RESULTS
1	Density @ 15.6 °C , (g/ml).	0.9164
2	Specific Gravity @ 15.6 °C	0.9173
3	API Gravity	22.75
4	Reid Vapor Pressure @ 100°F , (Psi) (Bar)	5.4 0.38
5	Kinematic Viscosity , cSt. @ 21.1 °C (70 °F) @ 37.8 °C (100 °F) @ 48.7 °C (120 °F) @ 60 °C (140 °F)	65.11 31.82 20.67 14.39
6	Sulphur Content , wt %	4.01
7	H_2S Dissolved In Crude Oil , ppm	17.0
8	Pour Point , °C	Below -30
9	Water Content (Dean & Stark) , vol. %	0.05
10	B.S. and Water (centrifuge) , vol. %	0.1
11	Carbon Residue , wt%	10.5
12	Salt Content , lb/1000 brl	17.0
13	Heat Of Combustion , cal. / g	10205
14	Asphaltene Content , wt%	6.2
15	Characterization Factor (KUOP)	11.6
16	Wax Content , wt%	6.2

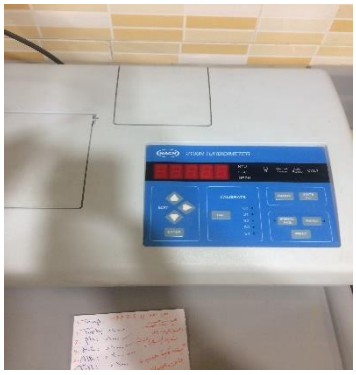

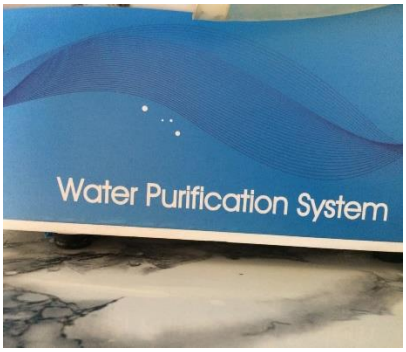

Appendix D

D. *Zeta potential analyzer*

Zeta potential analyzer by Water Research Center / Ministry of Science and Technology / Baghdad.

Table (D.1). Zeta potential of O/W emulsion droplets and Al-Al Electrodes as a function of initial O/W concentration.

Initial O/W Concentration (ppm)	Time (min)	
	0	120
	Zeta potential (mV)	
100	-35.32	-21.1
200	-39.73	27.98
300	-66.41	32.32

Table (D.2). Zeta potential of O/W emulsion droplets and Al-C. felt Electrodes as a functionof initial O/W concentration

Initial Crude Oil Concentration (ppm)	Time (min)	
	0	120
	Zeta potential (mV)	
100	-35.37	-11.18
200	-39.73	-17.47
300	-70	-19.04

Appendix E

E.1. *Emulsion drop size analysis*

Table E;1 . Emulsion drop size analysis by zeta plus (Brookhaven instrument Model 750 blue, USA)

Brookhaven Instruments

DLS
Graph

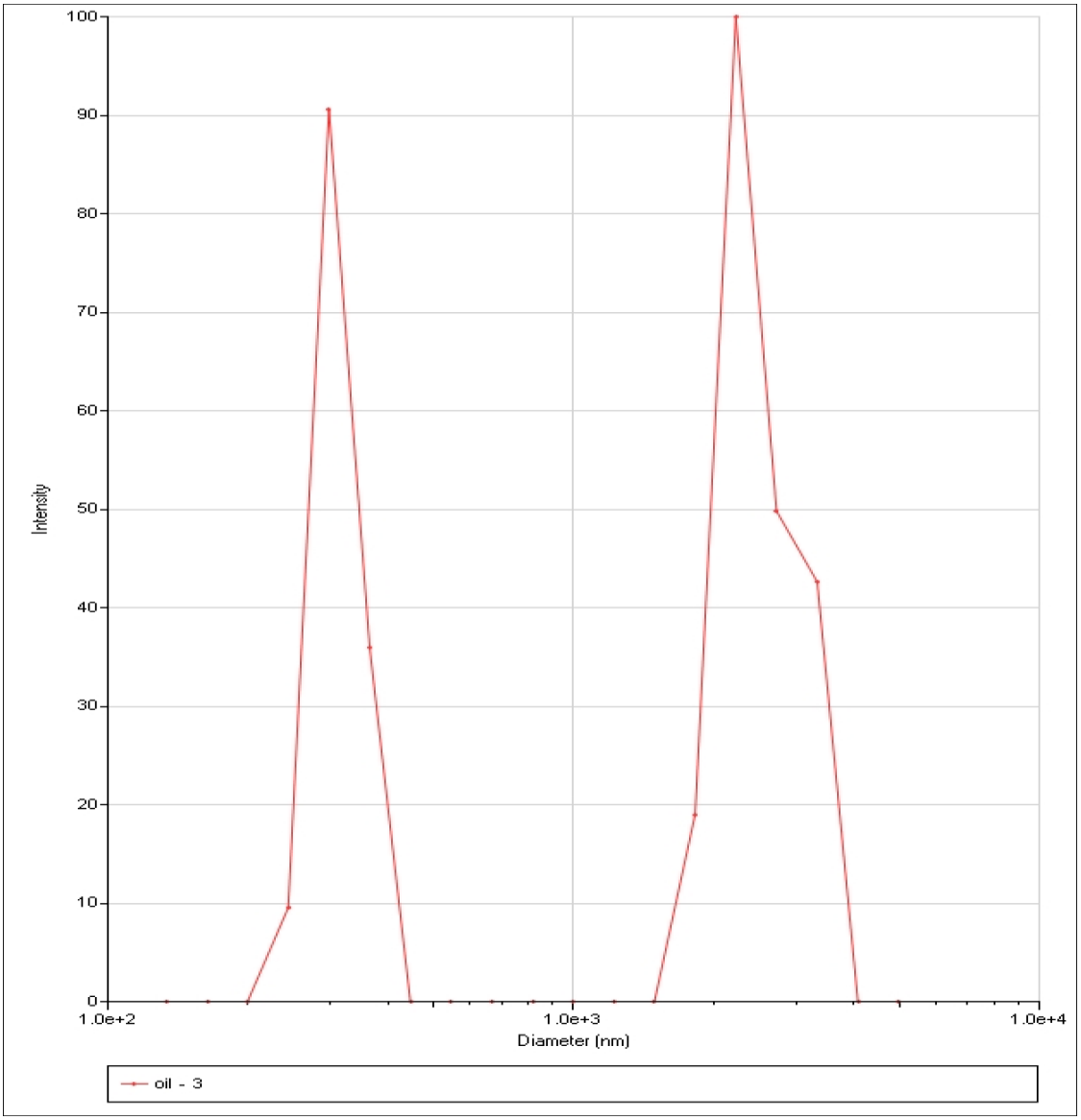

Printed: 19/01/2021 Particle Solutions v. 2.5 (scientific group company) 1 of 1

Table E;2 . Emulsion drop size analysis by zeta plus (Brookhaven instrument Model 750 blue, USA)

d (nm)	G(d)	C(d)
2.03e+2	0.00	0.00
2.39e+2	0.00	0.00
2.81e+2	0.00	0.00
3.31e+2	0.00	0.00
3.89e+2	87.65	31.84
4.57e+2	100.00	68.16
5.38e+2	87.65	100.00
6.32e+2	0.00	100.00
7.44e+2	0.00	100.00
8.74e+2	0.00	100.00
1.03e+3	0.00	100.00
1.21e+3	0.00	100.00
1.42e+3	0.00	100.00
1.67e+3	0.00	100.00
1.97e+3	0.00	100.00
2.31e+3	0.00	100.00
2.72e+3	0.00	100.00
3.20e+3	0.00	100.00
3.76e+3	0.00	100.00

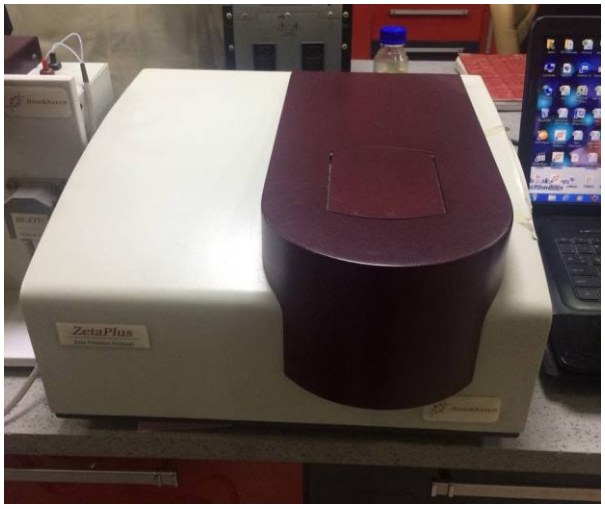

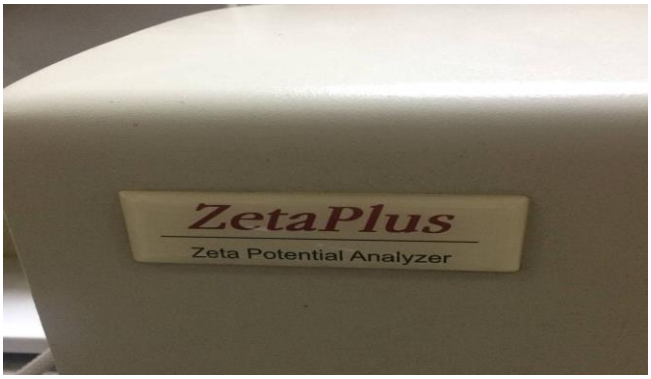

الملخص

يتناول هذا البحث تنقية وإزالة استحلاب مخلفات المياه الزيتية البترولية (O / W مستحلب) الناتجة من مصافي البترول باستخدام تقنيات التخثير الكهربائي / التعويم الكهربائي (EC / EF) . تم إنشاء نظام تدفق ديناميكي باستخدام تصميم مطوّر لمفاعل كهروكيميائي مدمج مصنوع من (زجاج بيرسبكس) يحتوي على لوحين عموديين متوازيين كأقطاب كهربائية .تم استخدام تقنية كلفانوستاتيكية لنوعين من الأقطاب الكهربائية ، Al-Alو Al-Carbon felt لتحقيق المعالجة الهجينة (EC /EF) في مفاعل واحد .تم تحضير مستحلب مخلفات مياه المصافي مختبرياًعن طريق خلط النفط الخام بتركيز(0.2.0.1 و 0.3 جرام) لكل لتر ماء منزوع الأيونات و أضيف 0.05 جرام / لتر كبريتات لوريل الصوديوم كعامل مثبت للأستحلاب بالاضافة الى ملح كلوريد الصوديوم بتركيز 1.5 جم / لتر لزيادة التوصيل الكهربائي .التخثير الكهربائي ينتج أيونات (Al^{3+}) ثلاثية التكافؤء عن طريق تآكل اقطاب الأنودات المضحية (المستهلكة)، وإطلاق مواد المخثرالضبابية النشطة في المحلول .علاوة على ذلك ، يؤدي إطلاق فقاعات غاز H_2 المتناهية الصغر عند قطب الكاثود إلى رفع المواد الضبابية المتخثرة (flocs) إلى السطح العلوي للمحلول .أجريت جميع التجارب في عملية مستمرة لمدة ساعتين مع مجموعة متنوعة من ظروف التشغيل ، بما في ذلك تركيز O W /الأولي ، وكثافة التيار ، ومعدل التدفق الحجمي ، ونوع الكاثود .أوضحت النتائج أنه بالنسبة لتركيز المستحلب O / W الابتدائي بمقدار 100 ppm وكثافة تيار 30 مللي أمبير / سم ^{2} مع معدل تدفق مختلف للمحلول يبلغ 2 ، 4 و 6 لتر / ساعة ، كانت كفاءة إزالة COD ،69.4 و 55.4 و 45.9٪ للأقطاب .Al-Al و 83 و 77.8 و 73.73٪ لاقطاب الالمنيوم –كاربون فيلد على التوالي .قللت هذه المعايير من تعكر المياه العادمة ، كما تمت دراسة الاستهلاك النوعي للطاقة الكهربائية (SEEC) وكفاءة التيار (CE) لعملية إزالة الاستحلاب و. قدرت تكلفة التشغيل الإجمالية للعملية بـ 1.5255 و 0.65383 دولار أمريكي / متر مكعب من مخلفات المياه الزيتية البترولية لمعالجة للأقطاب الكهربائية Al-Al و Al-Carbon ، على التوالي.

جمهورية العراق
وزارة التعليم العالي والبحث العلمي
جامعة بابل- كلية الهندسة
قسم الهندسة الكيمياوية

إزالة إستحلاب مخلفات مياه المصافي النفطية المصنعه بإستخدام تقنية التخثير/التعويم الكهروكيمياوي

رسالة مقدمة الى
كلية الهندسة في جامعة بابل وهي جزء من متطلبات نيل الماجستير في الهندسة الكهروكيمياوية

من قبل

عقيل طالب كاظم

بكالوريوس هندسة كيمياويه 1991

إشراف
أ.م. علاء نور غانم الموسوي

شباط 2022

رجب 1443